Geometric and probabilistic descriptions of chaotic phase space transport

Shane Ross

Dept. of Engineering Science and Mechanics, Virginia Tech

www.shaneross.com

In collaboration with P. Grover, C. Senatore, P. Tallapragada, P. Kumar, S. Naik, M. Gheisarieha, A. BozorgMagham, D. Schmale, F. Lekien, M. Stremler

NJIT Applied Mathematics Colloquium,

Department of Mathematics, February 10, 2012

MultiSTEPS: MultiScale Transport in Environmental & Physiological Systems, www.multisteps.esm.vt.edu

Motivation: application to real data

- Many systems defined from data or large-scale simulations
  — experimental measurements, observations
- e.g., from fluid dynamics, biology, social sciences

- Data-based, aperiodic, finite-time, finite resolution
  — in general, no fixed points, periodic orbits, or other invariant sets (or their stable and unstable manifolds) to organize phase space

Motivation: application to real data

- Perhaps can find appropriate analogs to the objects; adapt previous results to this setting
- Try some numerical explorations; see what merit furthers study

Chaotic phase space transport via lobe dynamics

- Suppose our dynamical system is a discrete map[1]

$$f : \mathcal{M} \longrightarrow \mathcal{M},$$

  e.g., $f = \phi_t^{t+T}$, flow map of time-periodic **vector field** and $\mathcal{M}$ is a differentiable, orientable, two-dimensional manifold e.g., $\mathbb{R}^2$, S^2

- To understand the transport of points under the f, consider **invariant manifolds of unstable fixed points**
  - Let $p_i, i = 1, ..., N_p$, denote saddle-type hyperbolic fixed points of f.

[1] Following Rom-Kedar and Wiggins [1990]

Partition phase space into regions

- Natural way to partition phase space
  - Pieces of $W^u(p_i)$ and $W^s(p_i)$ partition $\mathcal{M}$.

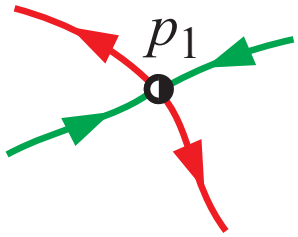

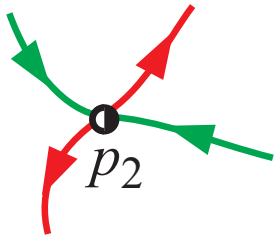

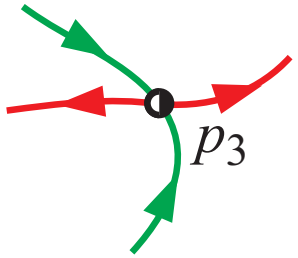

Unstable and stable manifolds in **red** and **green**, resp.

Partition phase space into regions

- Intersection of unstable and stable manifolds define **boundaries**.

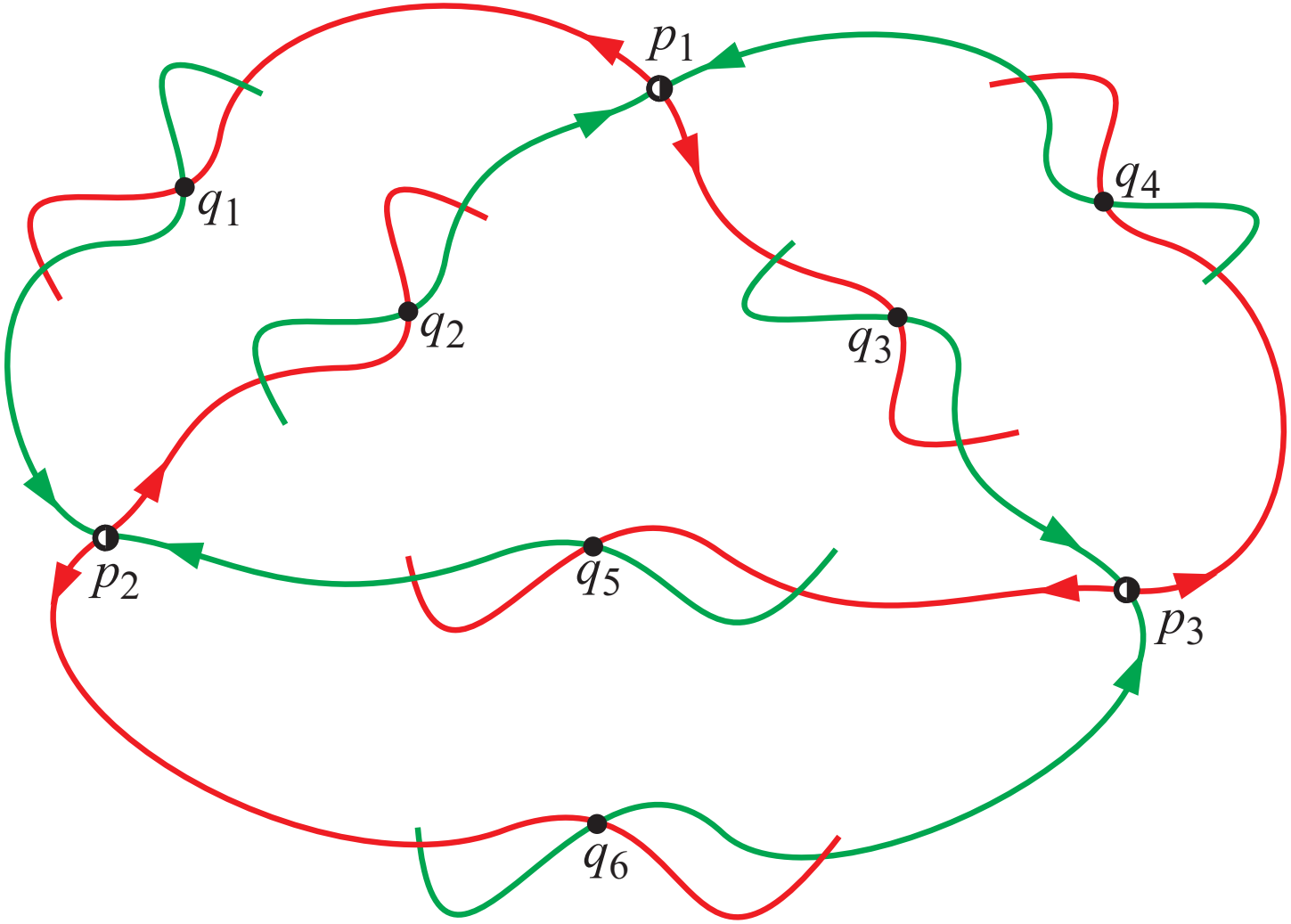

Partition phase space into regions

- These boundaries divide the phase space into **regions**

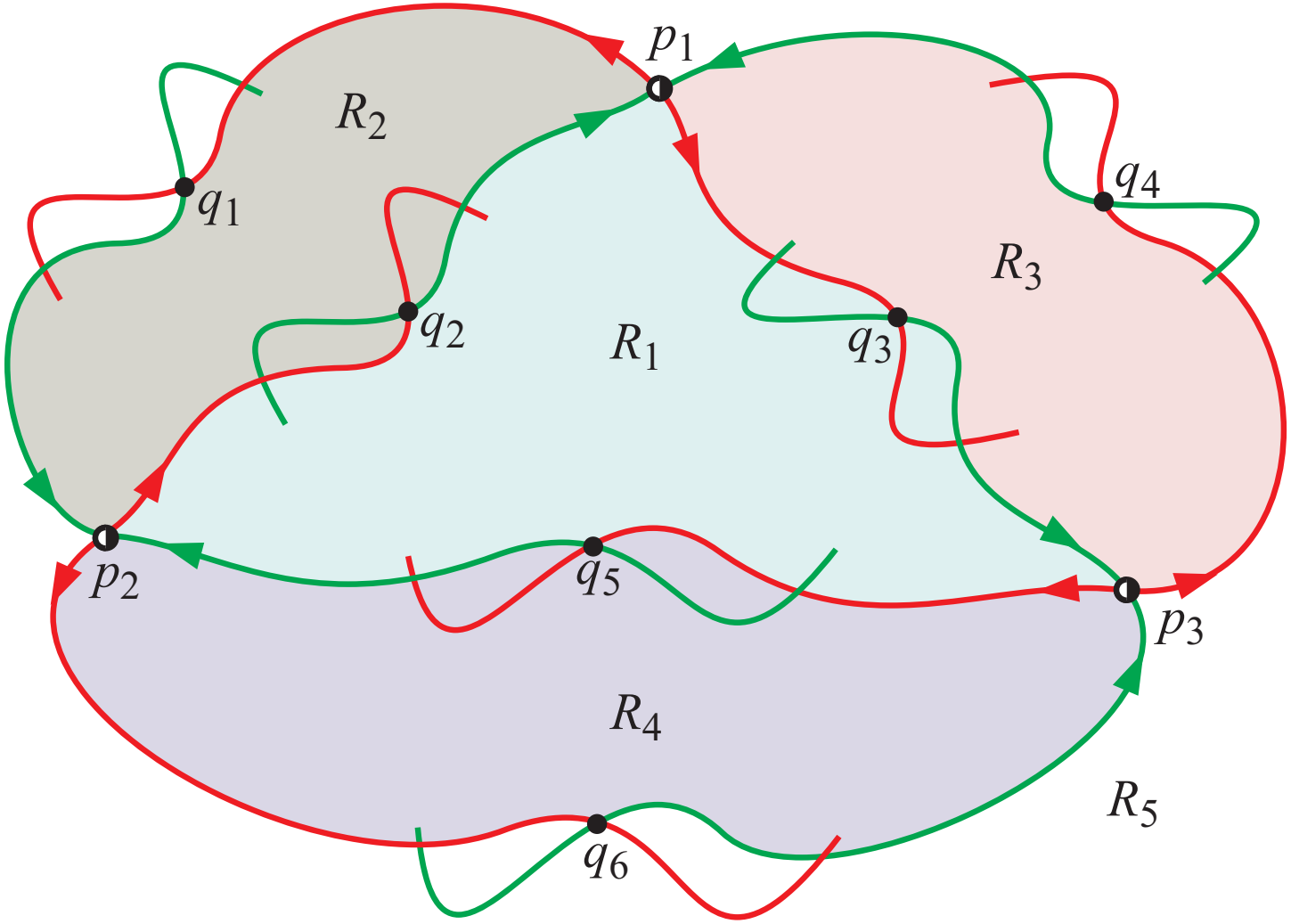

Label mobile subregions: ‘atoms’ of transport

- Can label mobile subregions based on their past and future whereabouts under one iterate of the map, e.g., $(\ldots, R_4, R_4, R_1, [R_1], R_2, \ldots)$

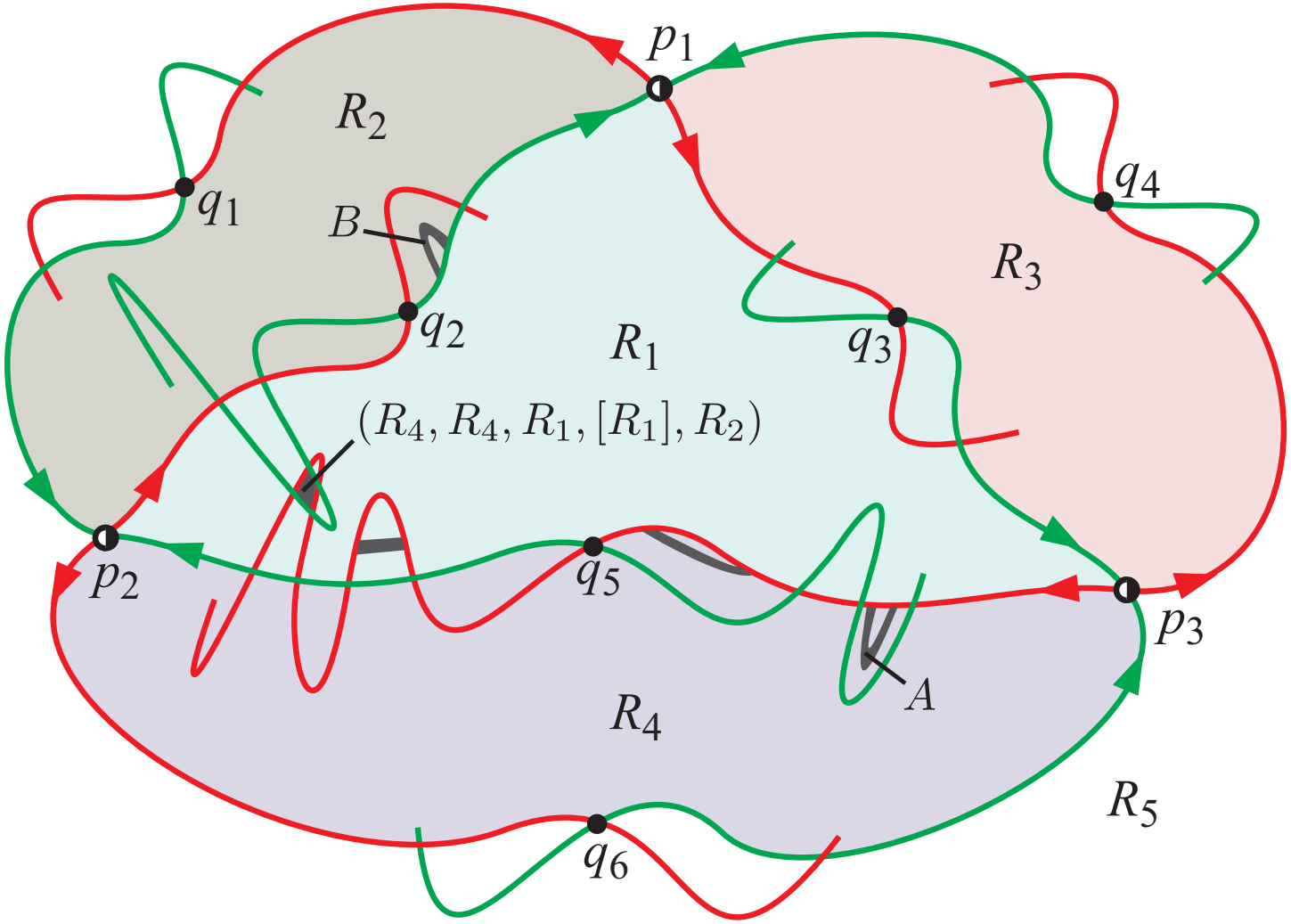

Lobe dynamics: transport across a boundary

- $W^u[f^{-1}(q), q] \bigcup W^s[f^{-1}(q), q]$ forms boundary of two lobes; one in R_1, labeled $L_{1,2}(1)$, or equivalently $([R_1], R_2)$, where $f(([R_1], R_2)) = (R_1, [R_2])$, etc. for $L_{2,1}(1)$

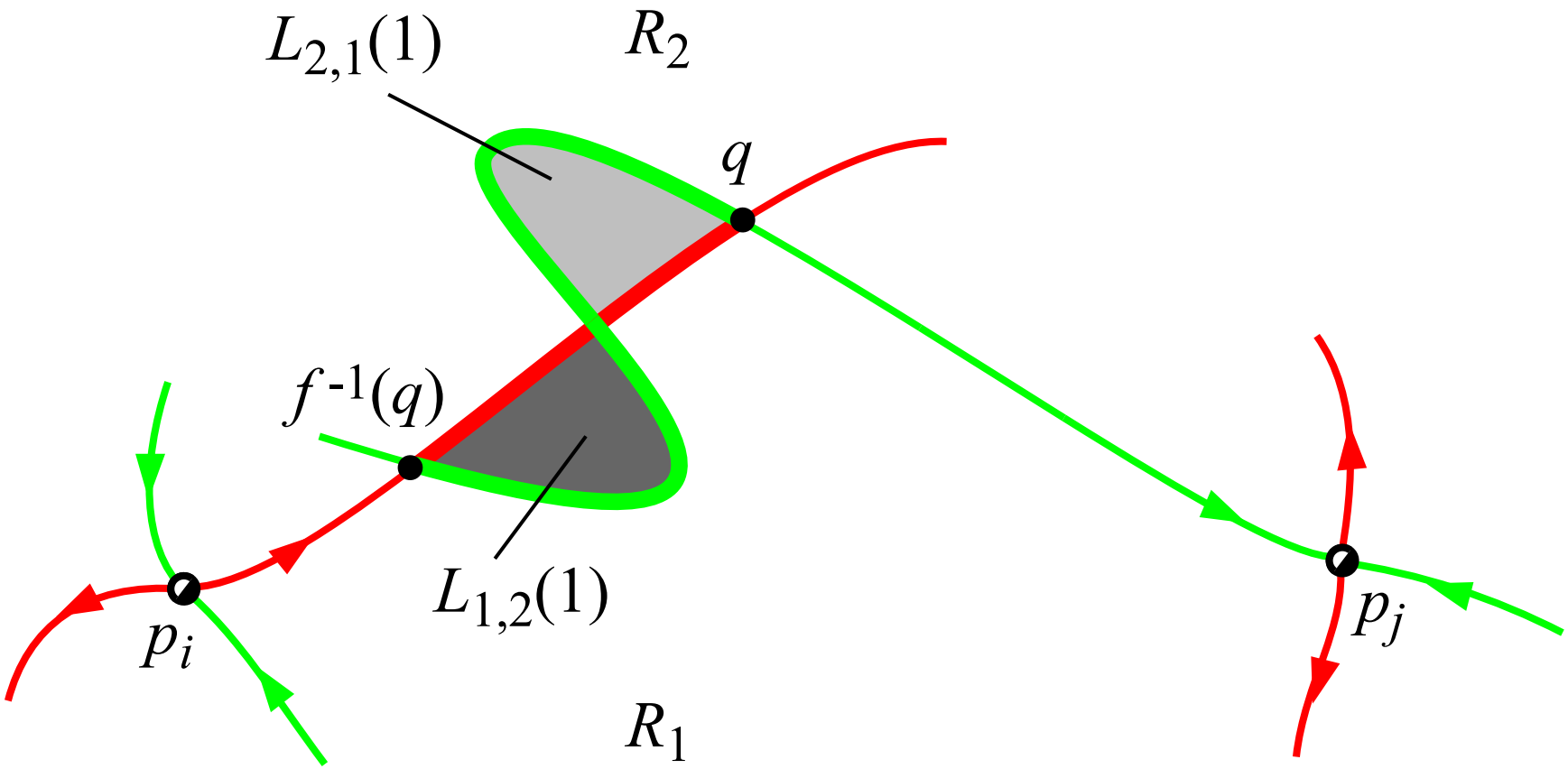

Lobe dynamics: transport across a boundary

- Under one iteration of f, **only points in** $L_{1,2}(1)$ can move from R_1 into R_2 by crossing their boundary, etc.
- The two lobes $L_{1,2}(1)$ and $L_{2,1}(1)$ are called a **turnstile**.

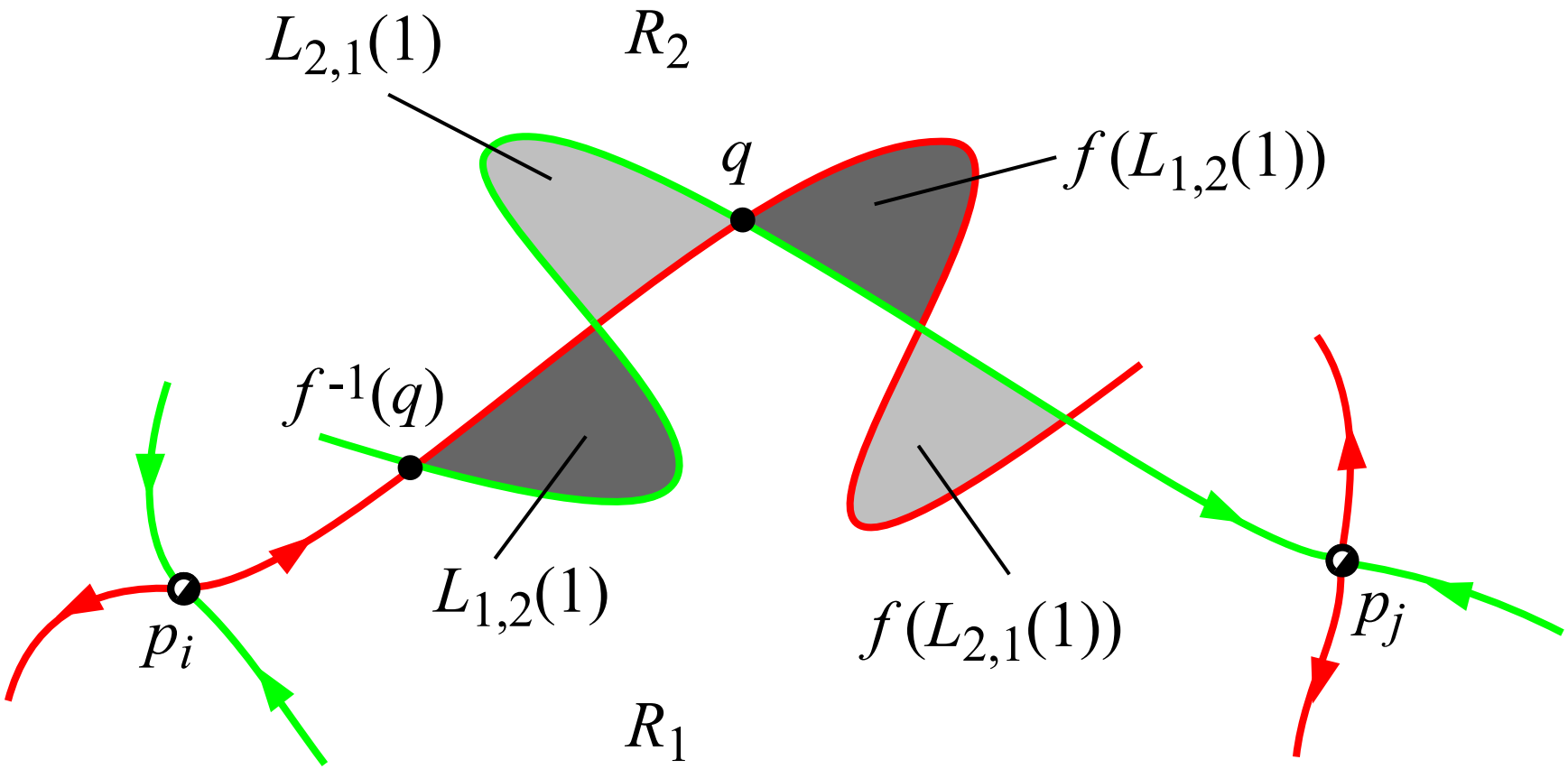

Lobe dynamics: transport across a boundary

- Essence of lobe dynamics: **dynamics associated with crossing a boundary is reduced to the dynamics of turnstile lobes associated with the boundary.**

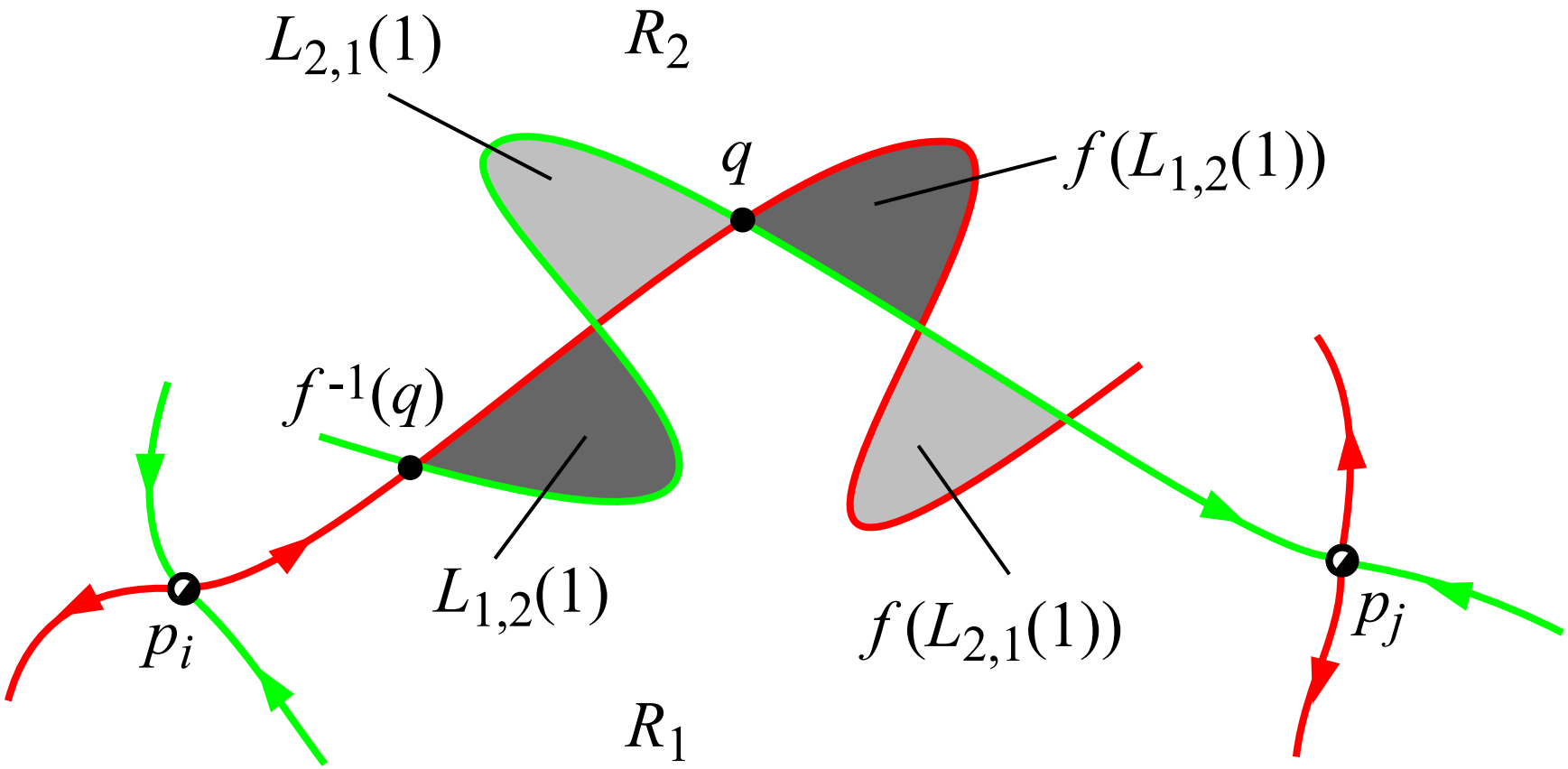

Identifying atoms of transport by itinerary

- In a complicated system, can still identify manifolds ...

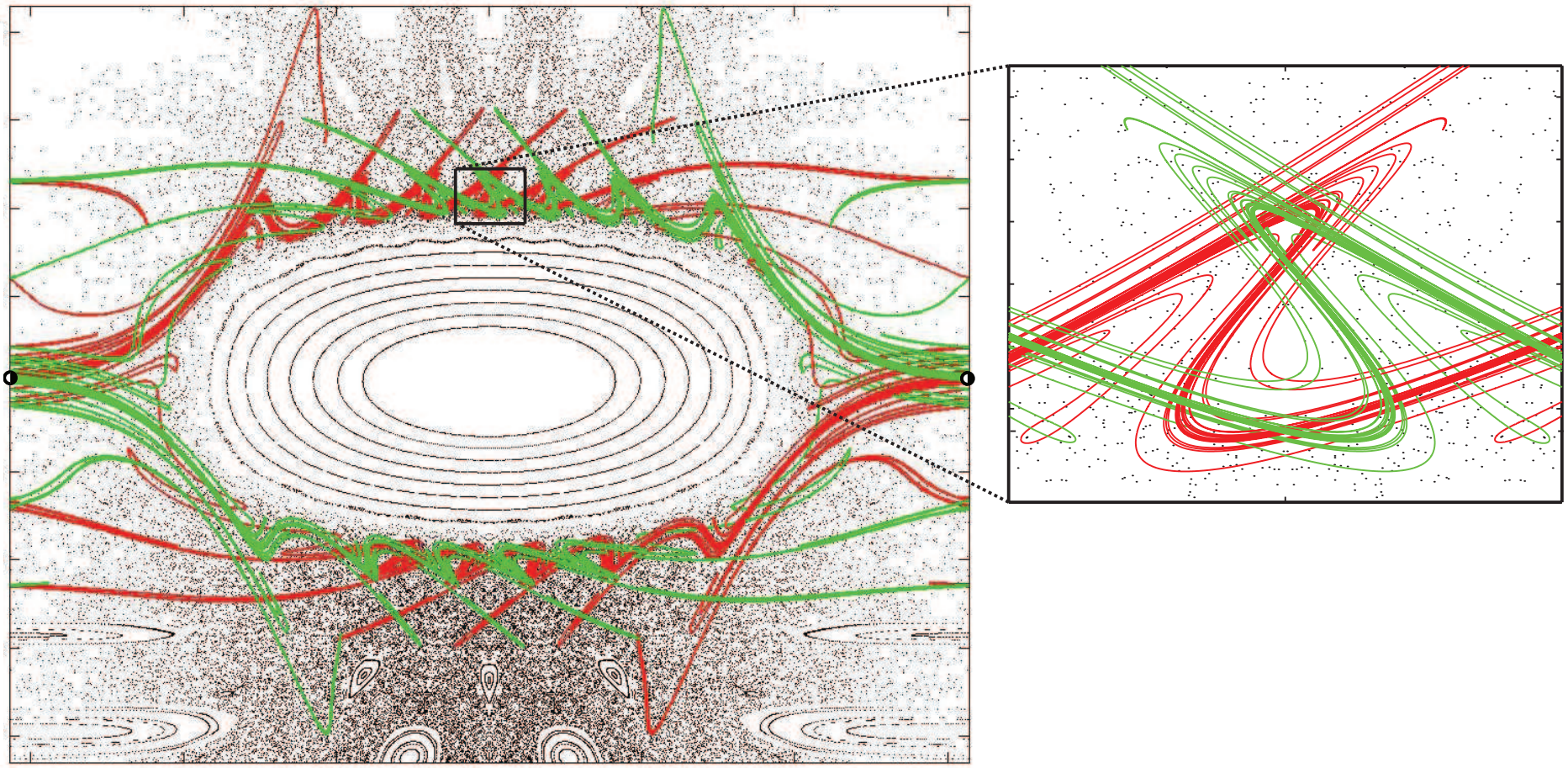

Unstable and stable manifolds in **red** and **green**, resp.

Identifying atoms of transport by itinerary

- ... and lobes

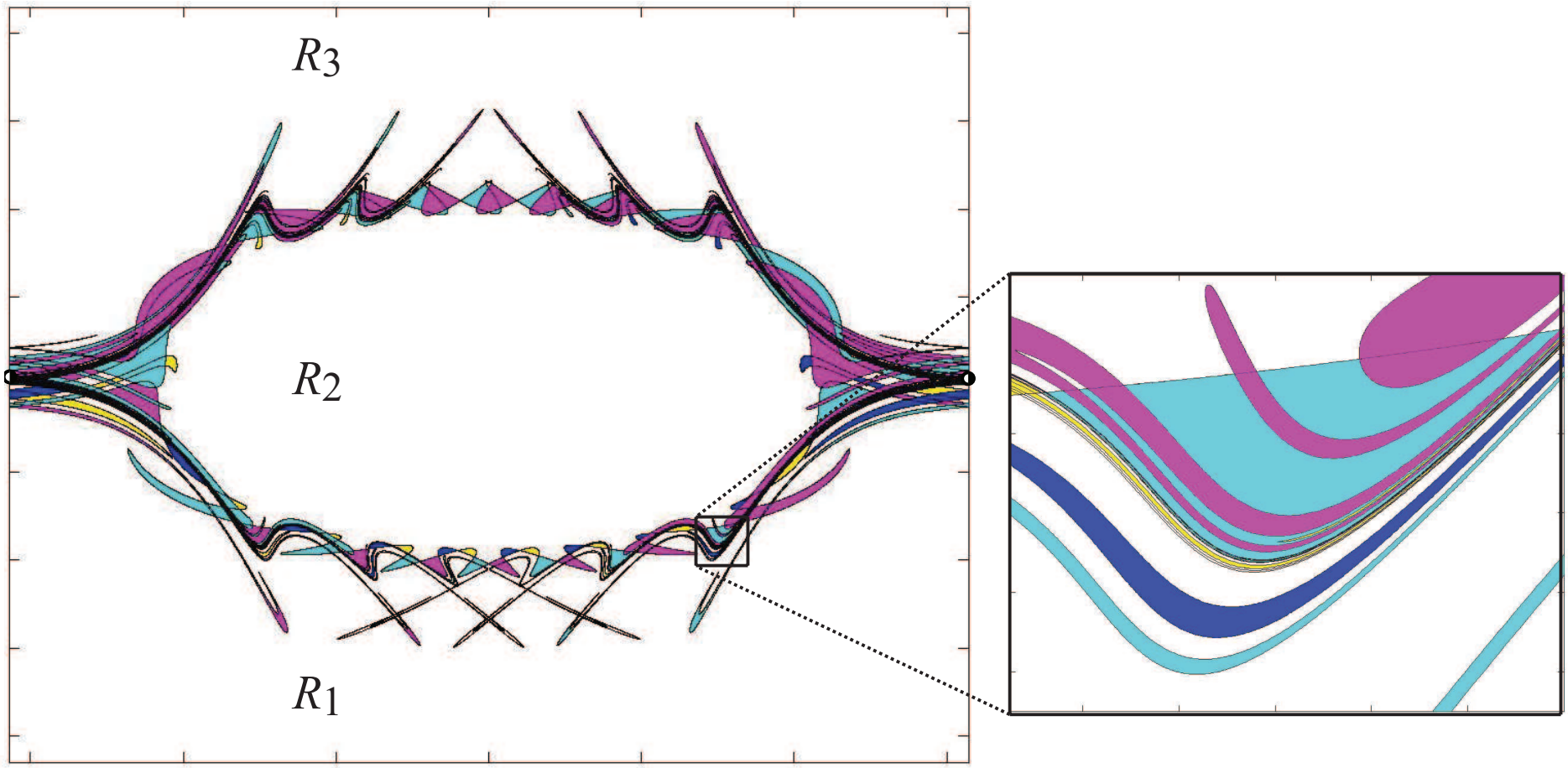

Significant amount of fine, filamentary structure.

Identifying atoms of transport by itinerary

- e.g., with three regions $\{R_1, R_2, R_3\}$, label lobe intersections accordingly.
  - Denote the intersection $(R_3, [R_2]) \bigcap ([R_2], R_1)$ by $(R_3, [R_2], R_1)$

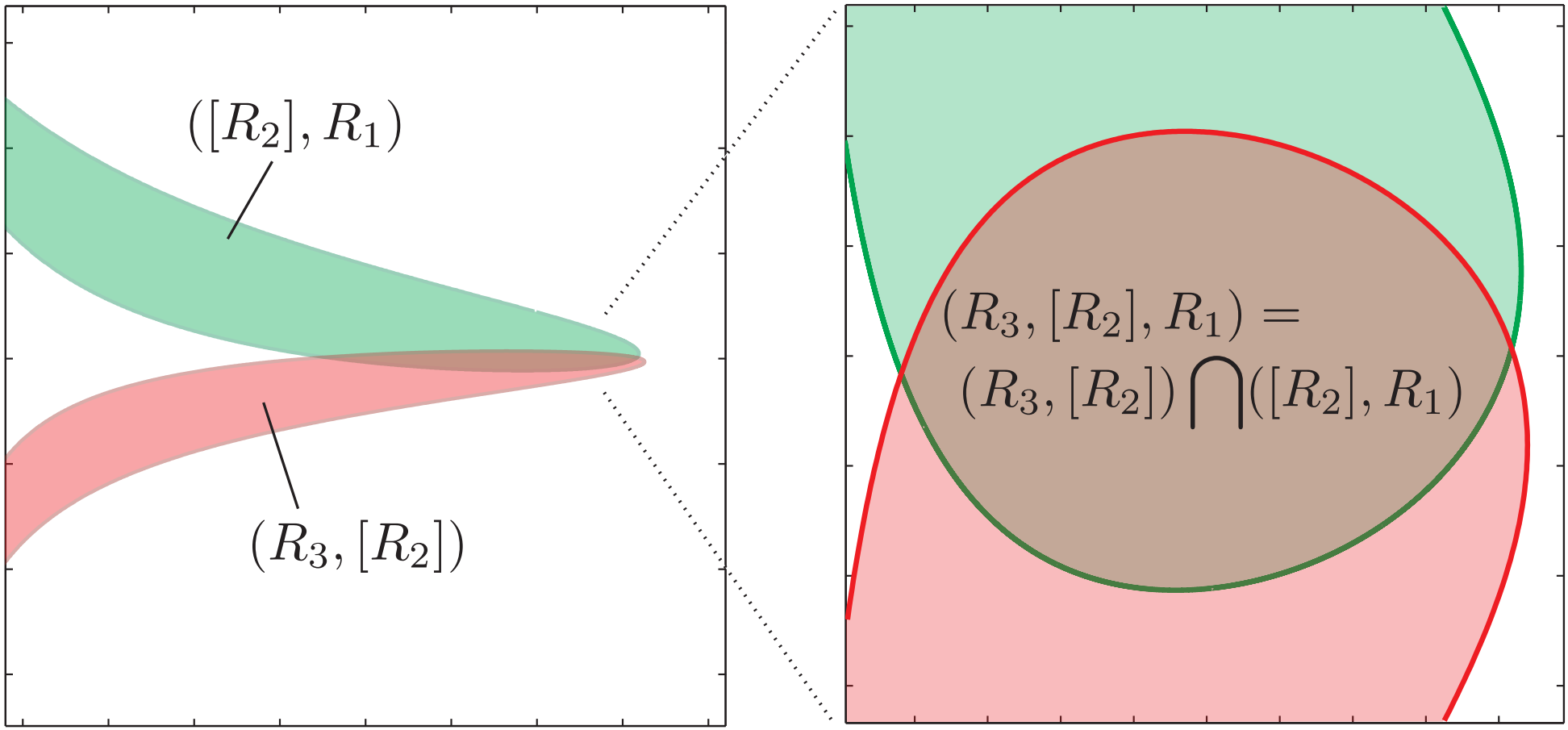

Identifying atoms of transport by itinerary

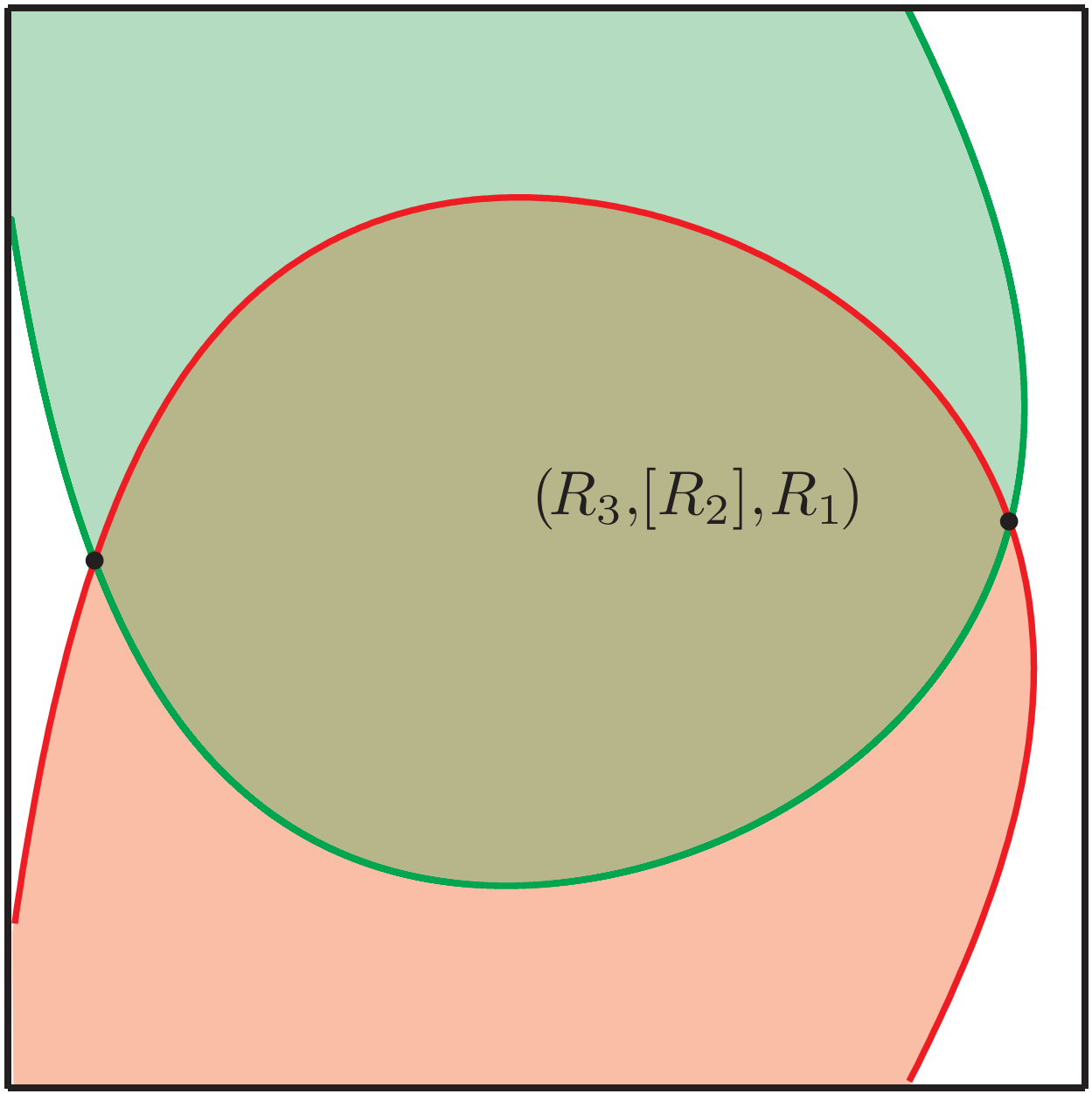

Longer itineraries...

Identifying atoms of transport by itinerary

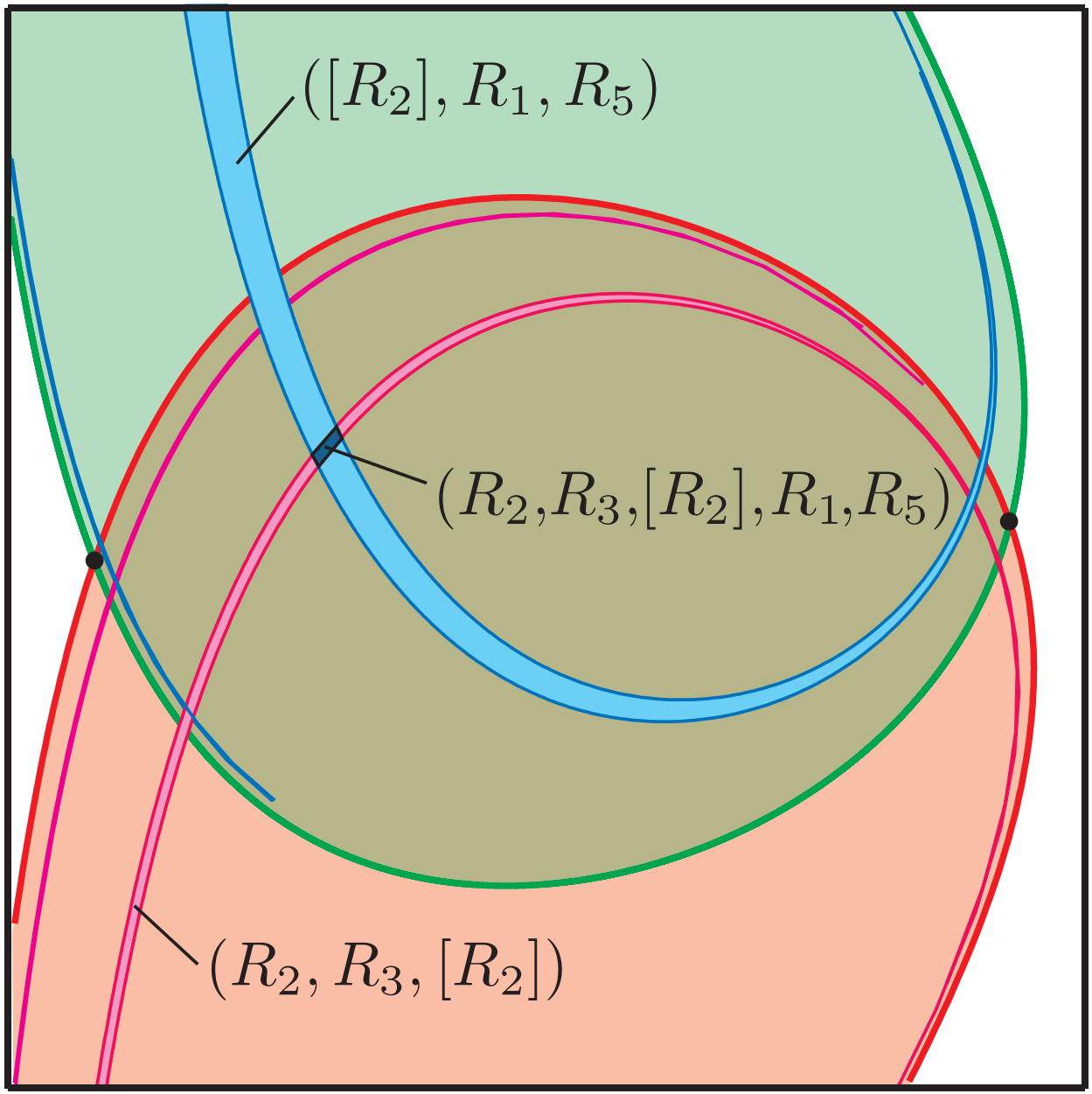

... correspond to smaller pieces of phase space; horseshoe dynamics, etc

Lobe dynamics intimately related to transport

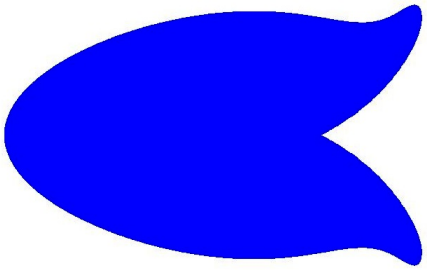

$n = 0$

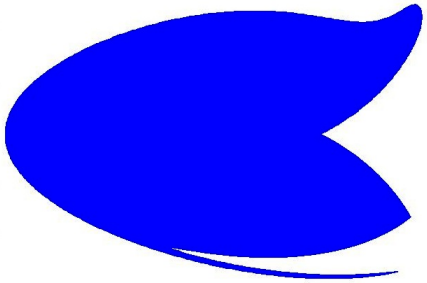

$n = 1$

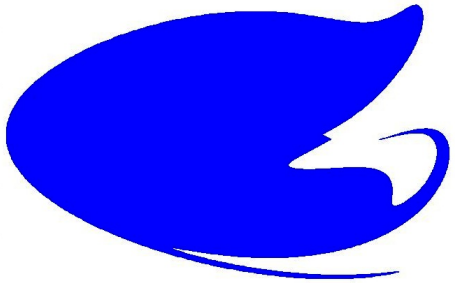

$n = 2$

$n = 3$

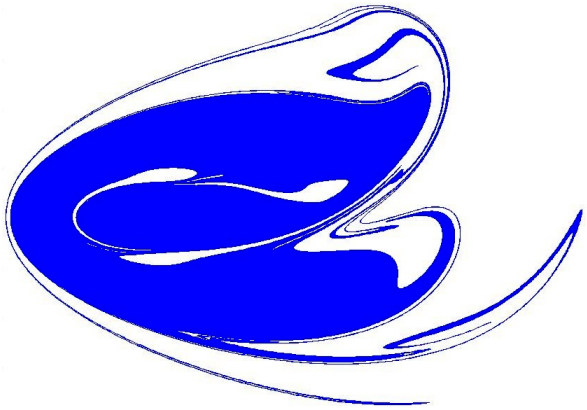

$n = 5$

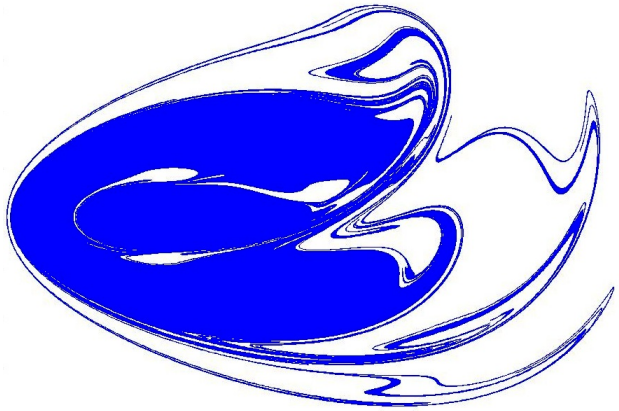

$n = 7$

Lobe Dynamics: example

- Restricted 3-body problem: chaotic sea has unstable fixed points.

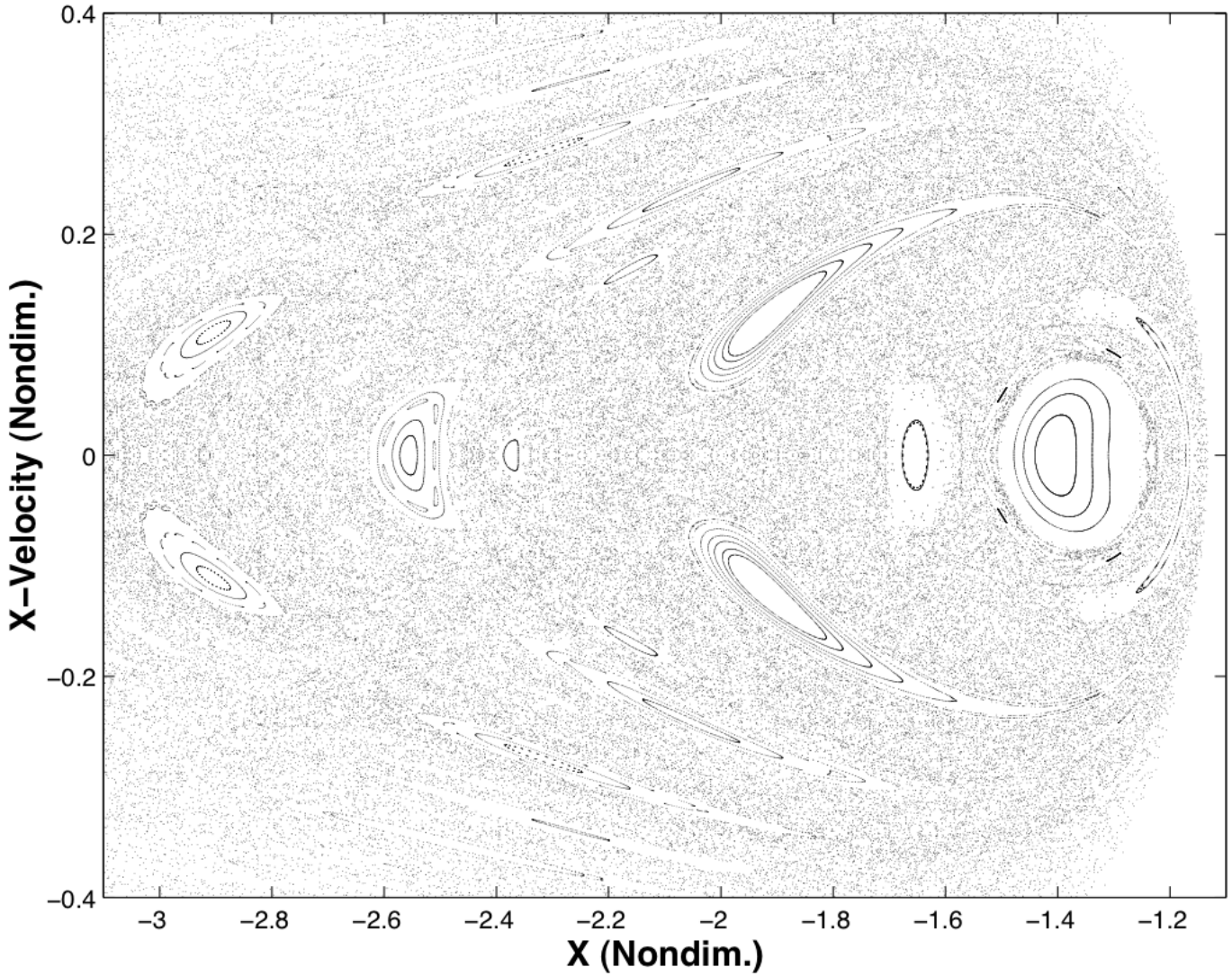

Compute a boundary

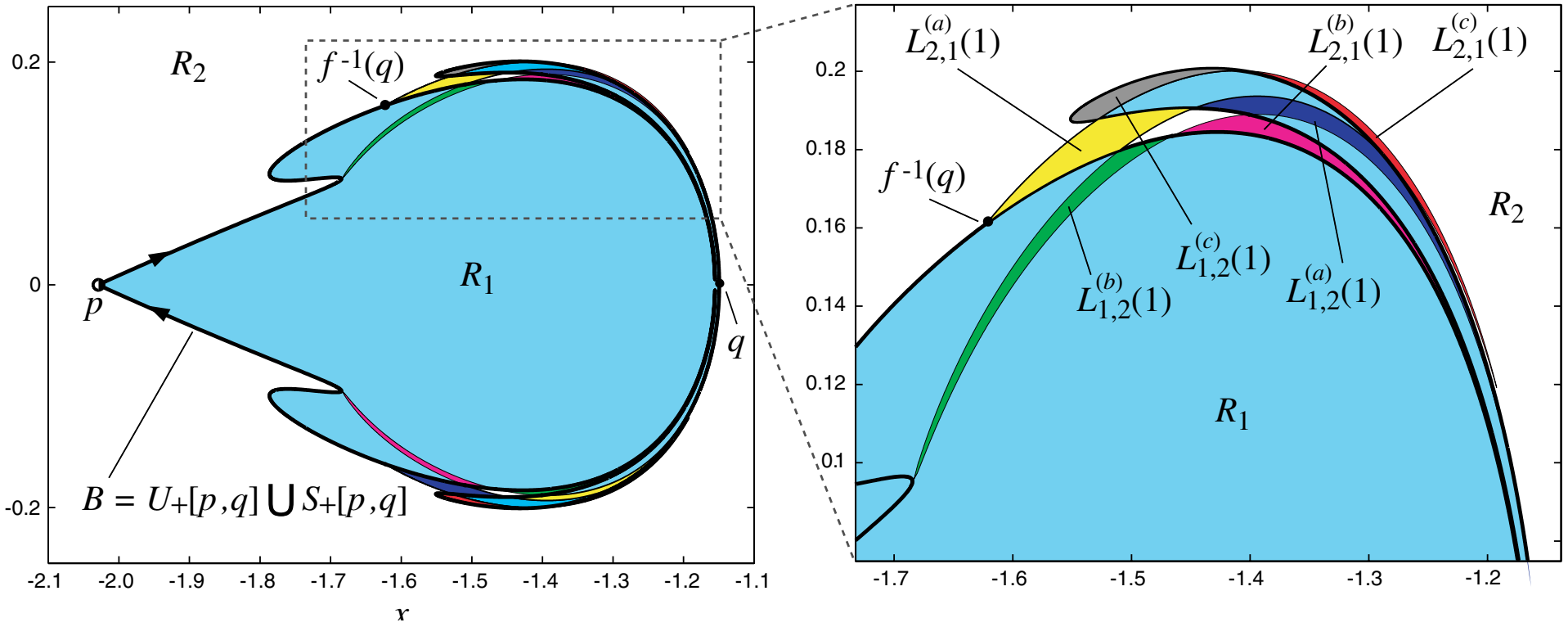

Transport between two regions

- The evolution of a lobe of species S_1 into R_2

Dellnitz, Junge, Lo, Marsden, Padberg, Preis, Ross, Thiere [2005] Physical Review Letters

Transport between two regions

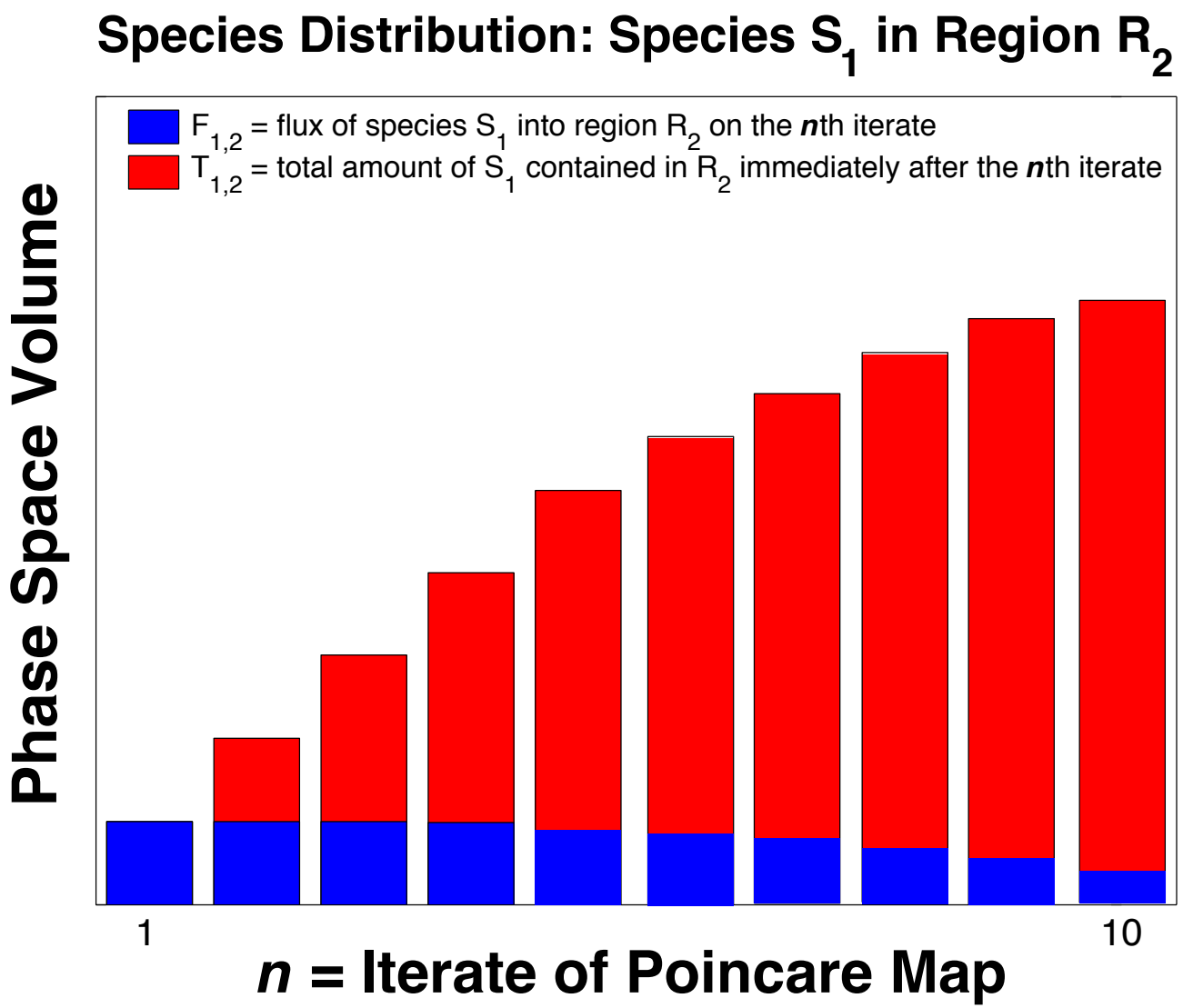

Lobe dynamics: fluid example

- Fluid example: time-periodic Stokes flow

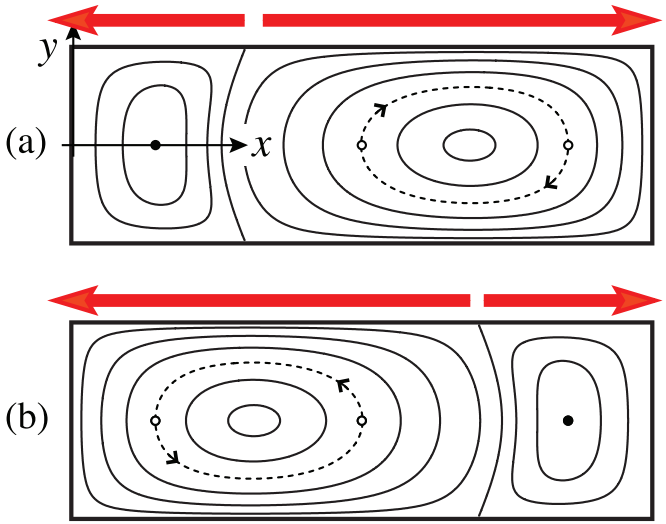

streamlines

tracer blob

Lid-driven cavity flow

- Model for microfluidic mixer
- System has parameter τ_f, which we treat as a bifurcation parameter — critical point $\tau_f^* = 1$; above and next few slides show $\tau_f > 1$

Lobe dynamics: fluid example

- Structure associated with saddles of Poincaré map

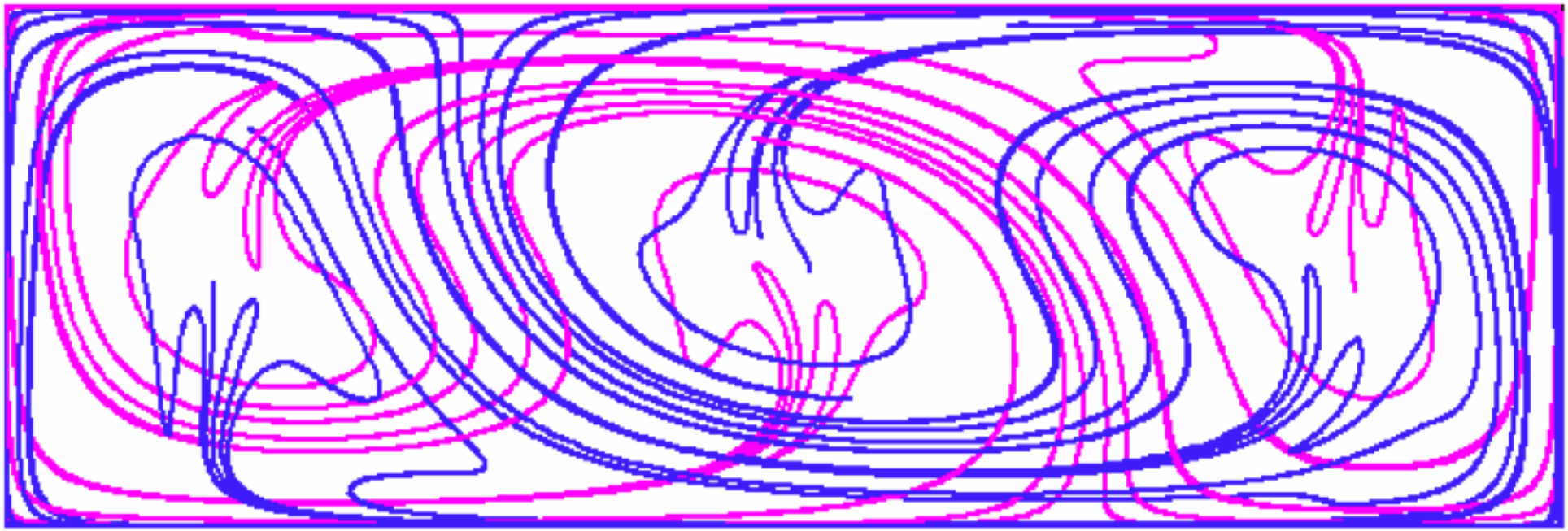

some invariant manifolds of saddles

Lobe dynamics: fluid example

- Can consider transport via **lobe dynamics**

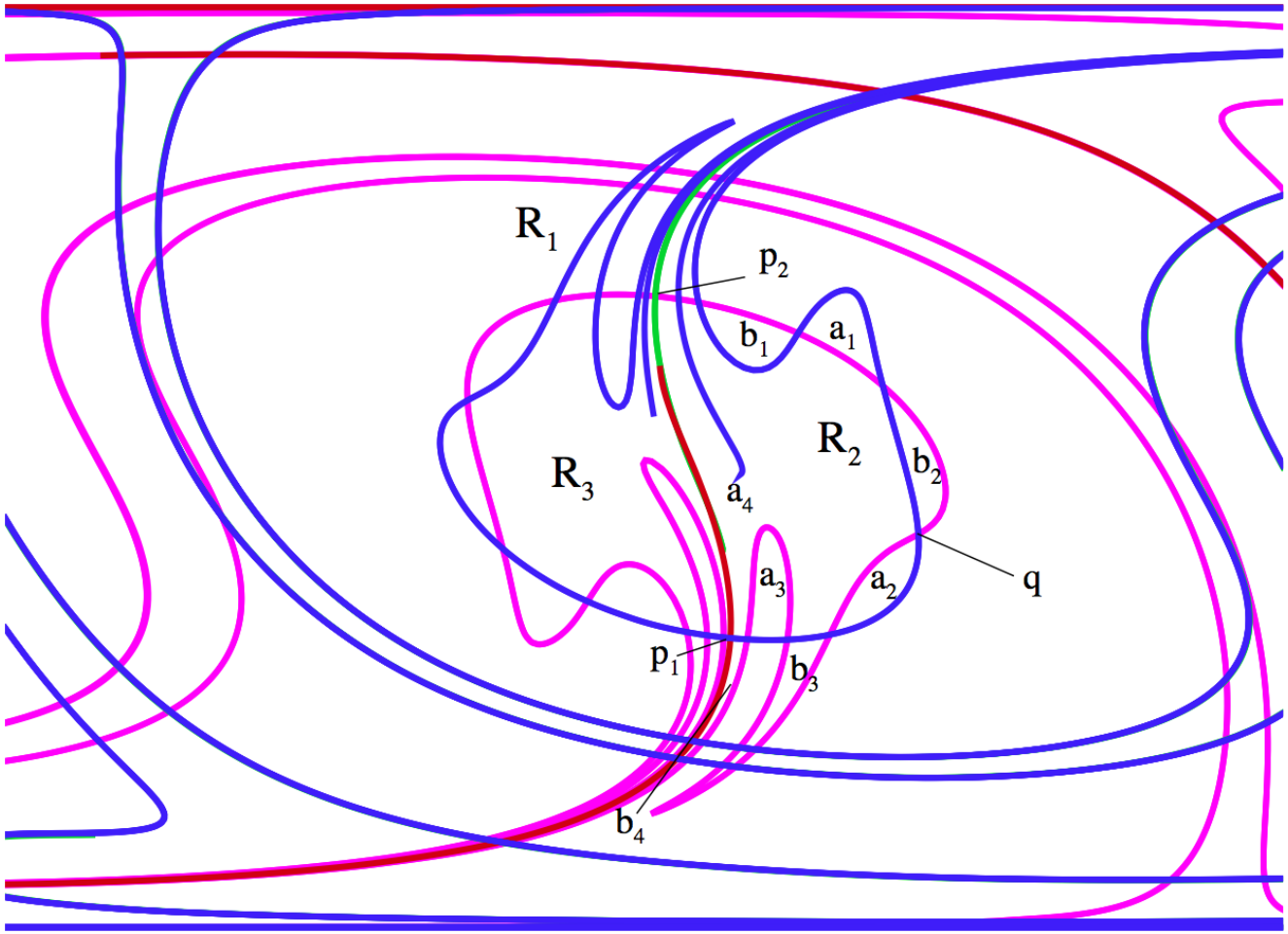

pips, regions and lobes labeled

Stable/unstable manifolds and lobes in fluids

material blob at $t = 0$

Stable/unstable manifolds and lobes in fluids

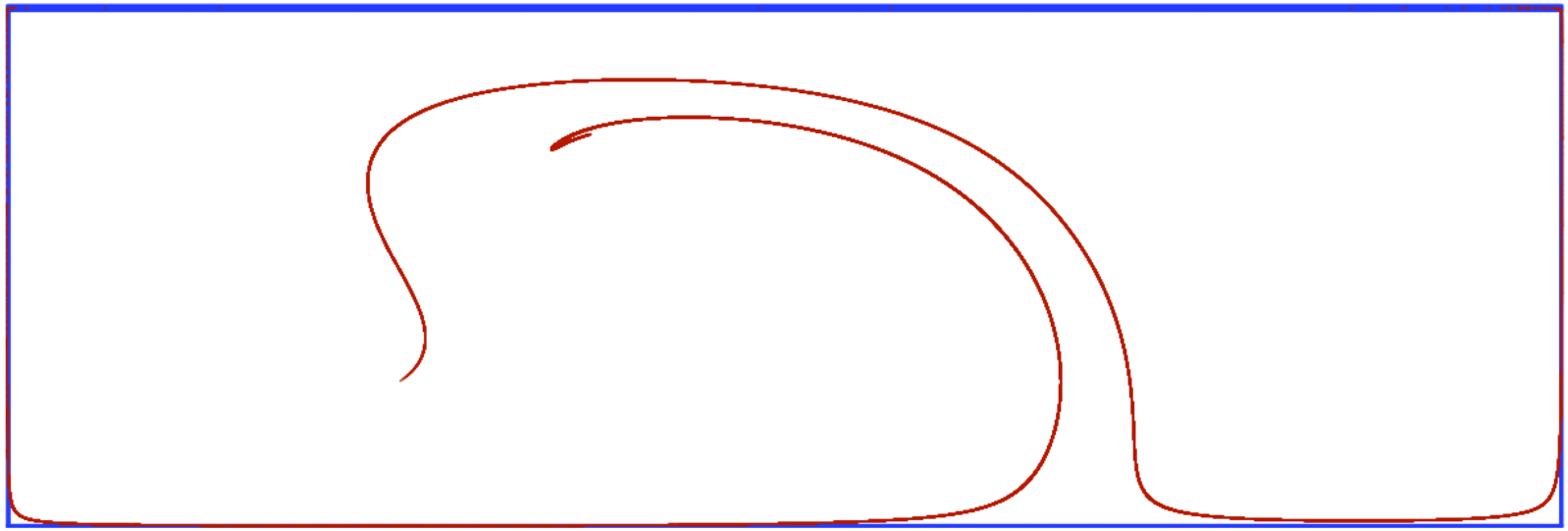

material blob at $t = 5$

Stable/unstable manifolds and lobes in fluids

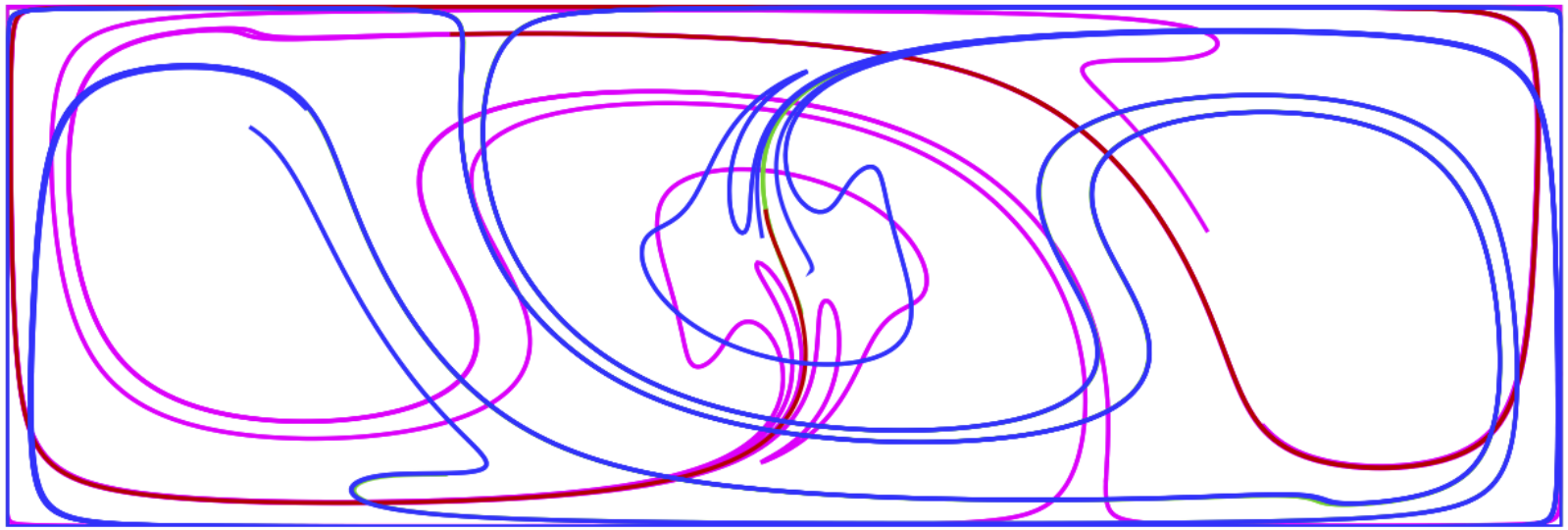

some invariant manifolds of saddles

Stable/unstable manifolds and lobes in fluids

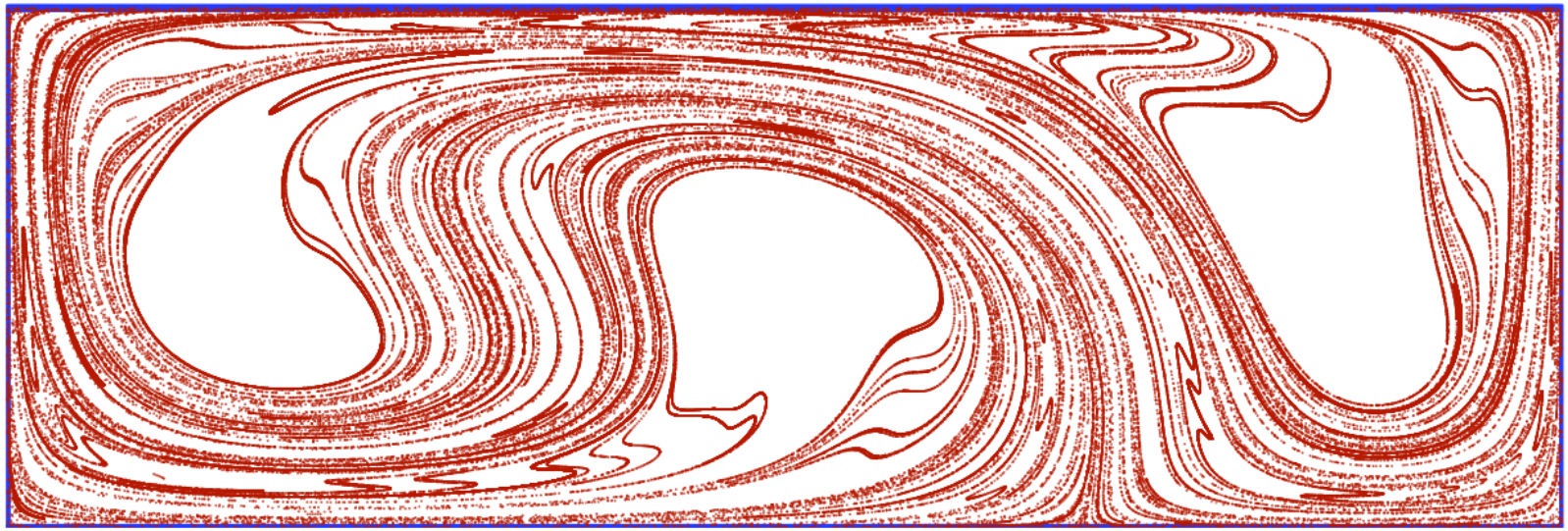

material blob at $t = 10$

Stable/unstable manifolds and lobes in fluids

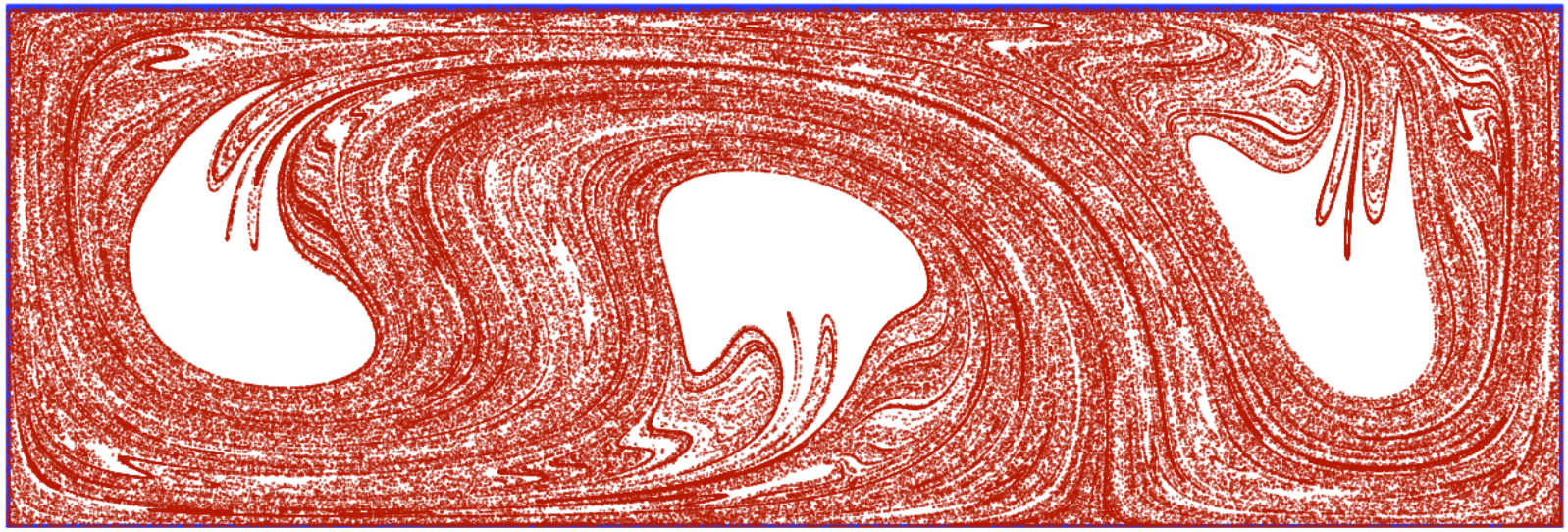

material blob at $t = 15$

Stable/unstable manifolds and lobes in fluids

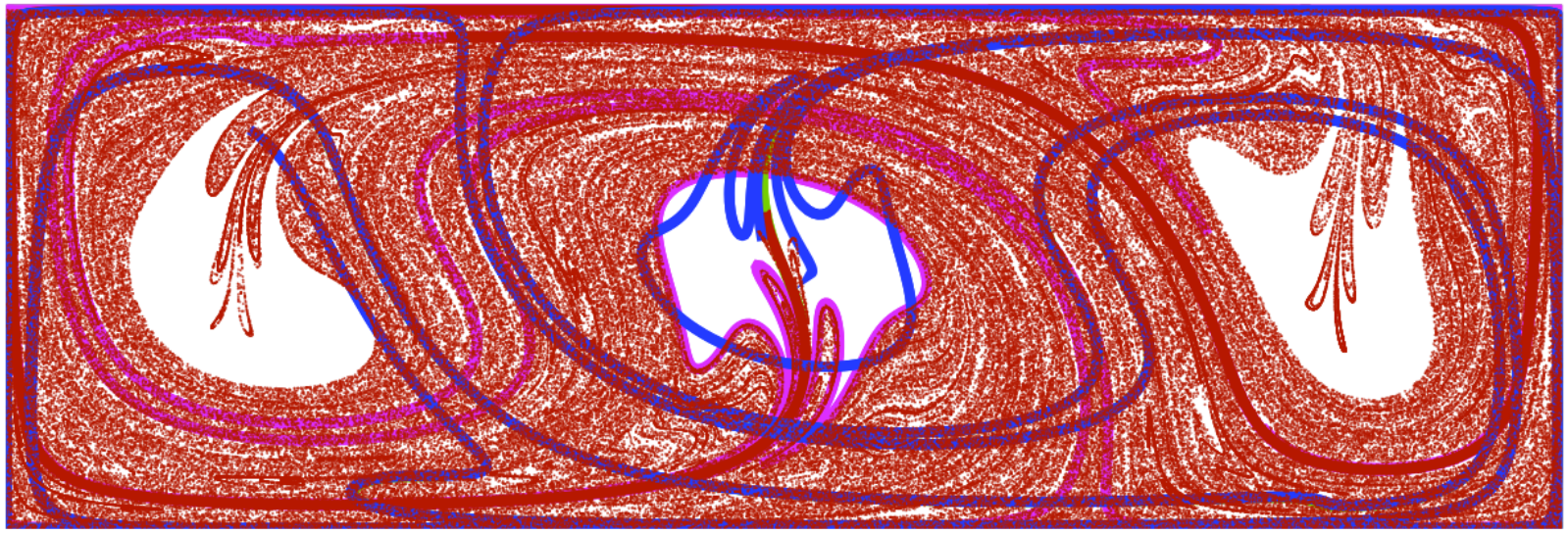

material blob and manifolds

Stable/unstable manifolds and lobes in fluids

material blob at $t = 20$

Stable/unstable manifolds and lobes in fluids

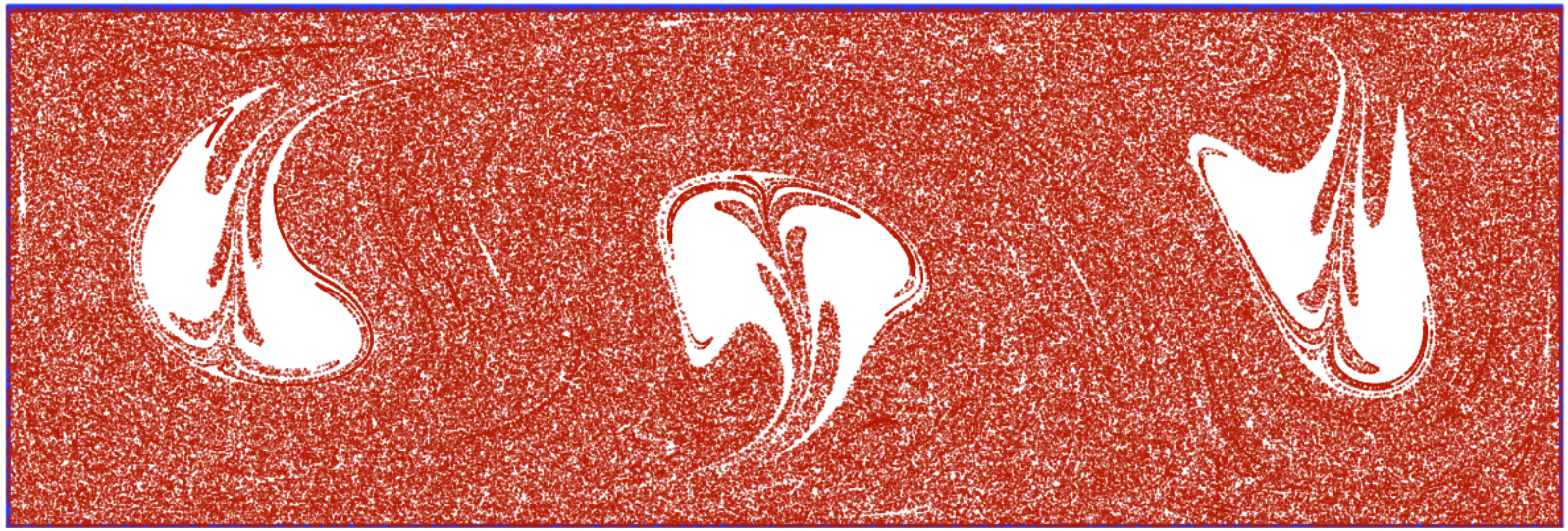

material blob at $t = 25$

Stable/unstable manifolds and lobes in fluids

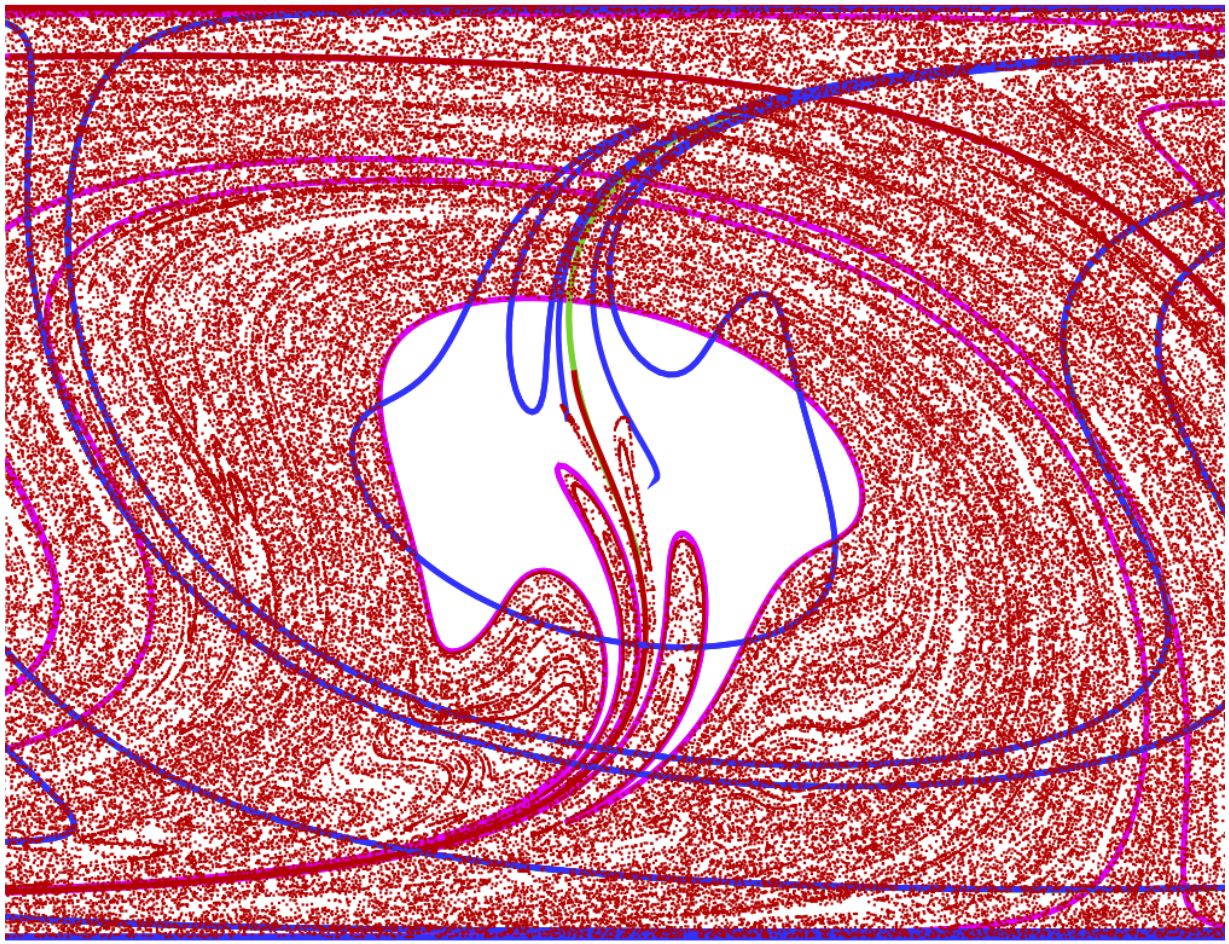

- Saddle manifolds and lobe dynamics provide template for motion

Stable/unstable manifolds and lobes in fluids

- Concentration variance; a measure of homogenization

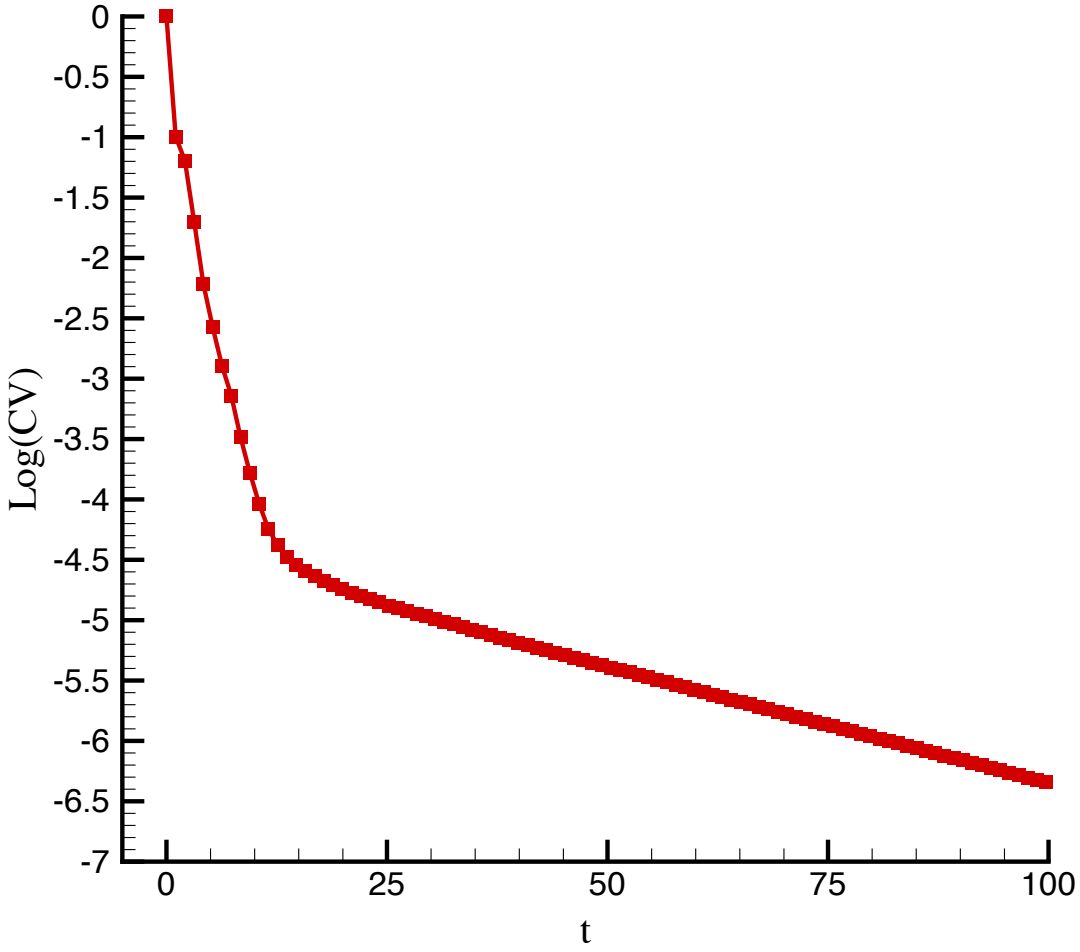

- Homogenization has two exponential rates: slower one related to lobes
- Fast rate due to braiding of 'ghost rods'

Stirring fluids with solid rods

turbulent mixing

spoon in coffee

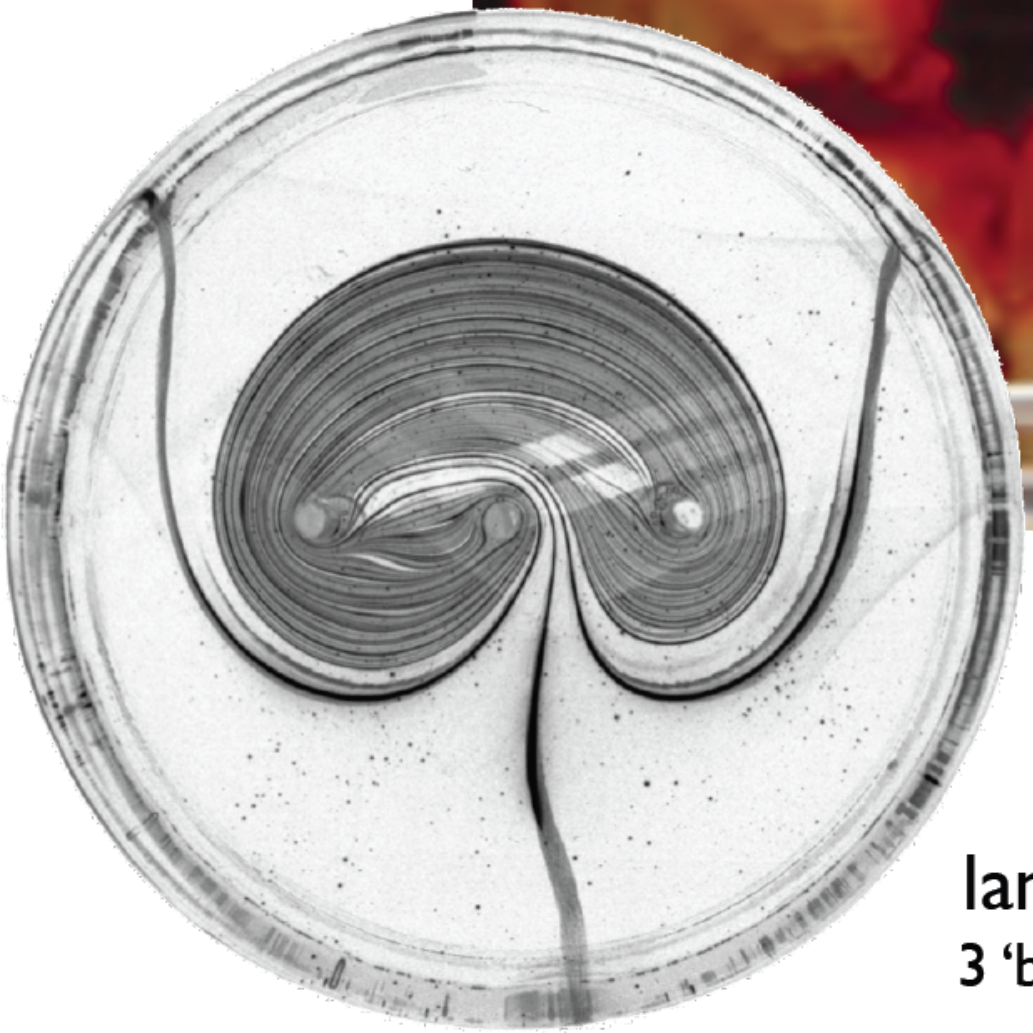

laminar mixing

3 ‘braiding’ rods in glycerin

Topological chaos through braiding of stirrers

- Topological chaos is 'built in' the flow due to the topology of boundary motions

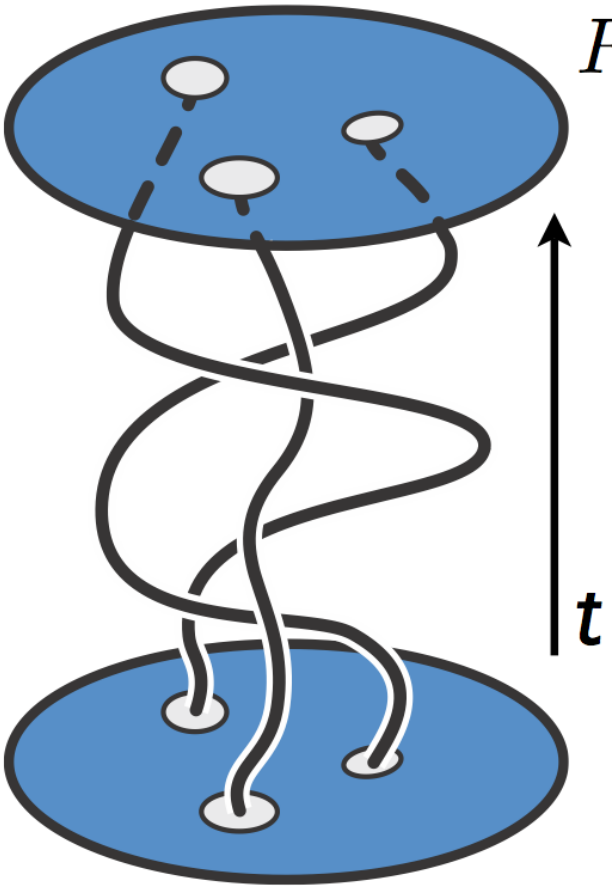

R_N : 2D fluid region with *N* stirring 'rods'

- stirrers move on periodic orbits
- stirrers = solid objects or *fluid particles*
- stirrer motions generate diffeomorphism

$$f : R_N \to R_N$$

- stirrer trajectories generate braids in 2+1 dimensional space-time

Thurston-Nielsen classification theorem

- Thurston (1988) Bull. Am. Math. Soc.
- A stirrer motion f is isotopic to a stirrer motion g of one of three types (i) finite order (f.o.): the nth iterate of g is the identity (ii) pseudo-Anosov (pA): g has dense orbits, (iii) reducible: g contains both f.o. and pA regions
- h_{TN} computed from 'braid word', e.g., $\sigma_{-1}\sigma_2$
- $\log(\lambda_{PF}(A))$ provides a **lower bound** on the true topological entropy
- i.e., non-trivial material lines grow like $\ell \sim \ell_0 \lambda^n$, where $\lambda \geq \lambda_{\mathrm{TN}}$

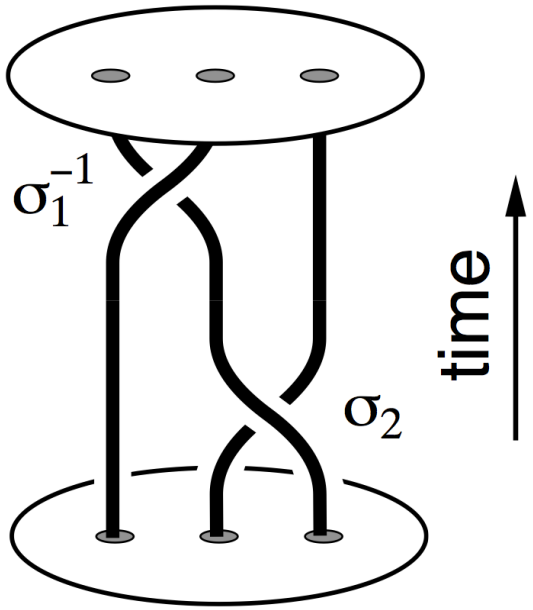

Topological chaos in a viscous fluid experiment

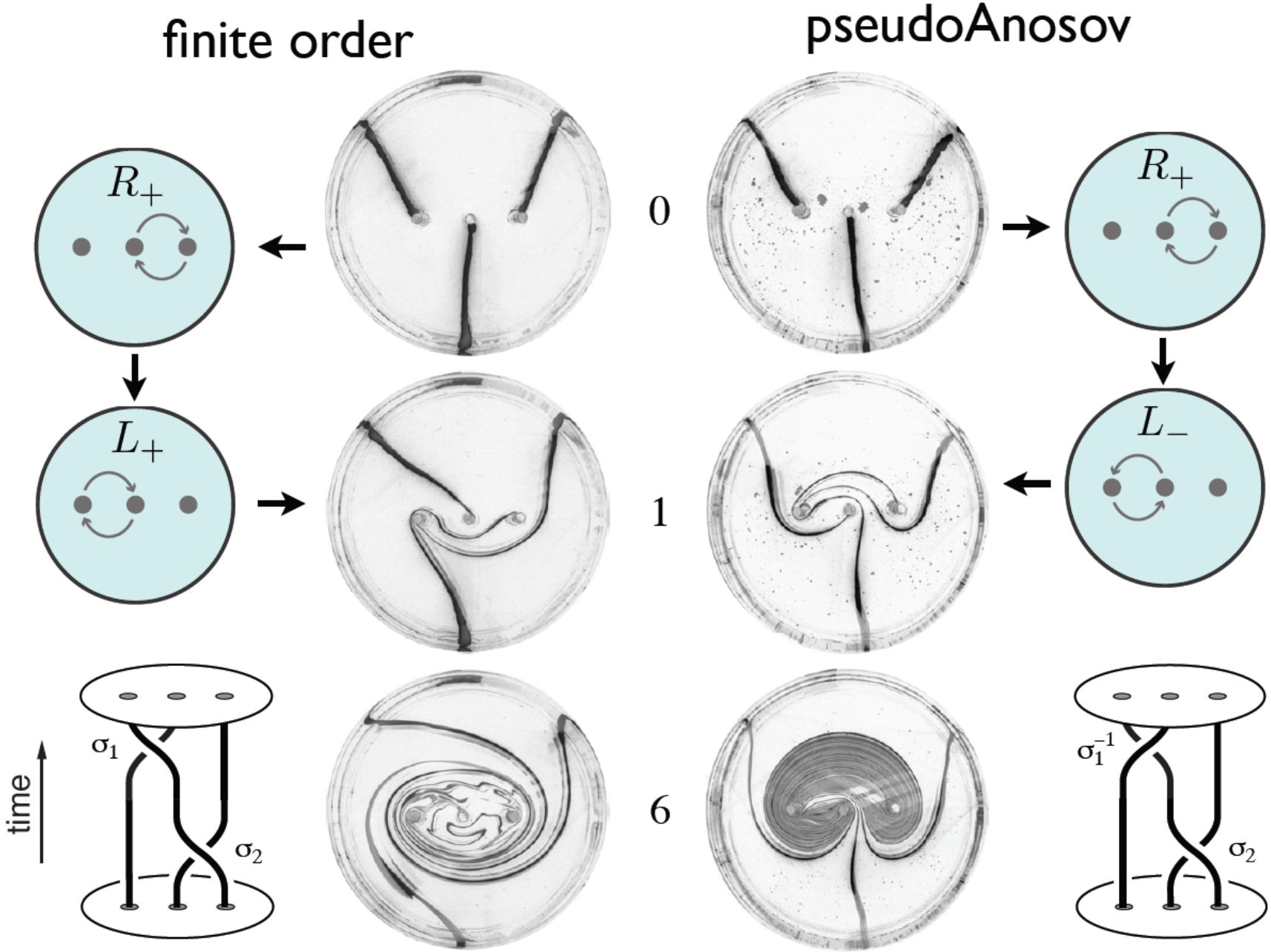

Identifying 'ghost rods': periodic points

tracer blob for $\tau_f > 1$

- For $\tau_f > 1$, groups of elliptic and saddle periodic points of period 3
  — streamlines around groups resemble fluid motion around a solid rod $\Rightarrow$
- At $\tau_f = 1$, points merge into parabolic points
- Below $\tau_f < 1$, periodic points vanish

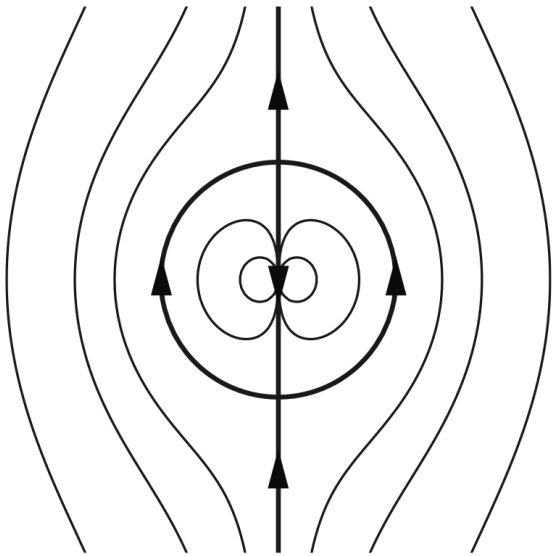

Identifying 'ghost rods': periodic points

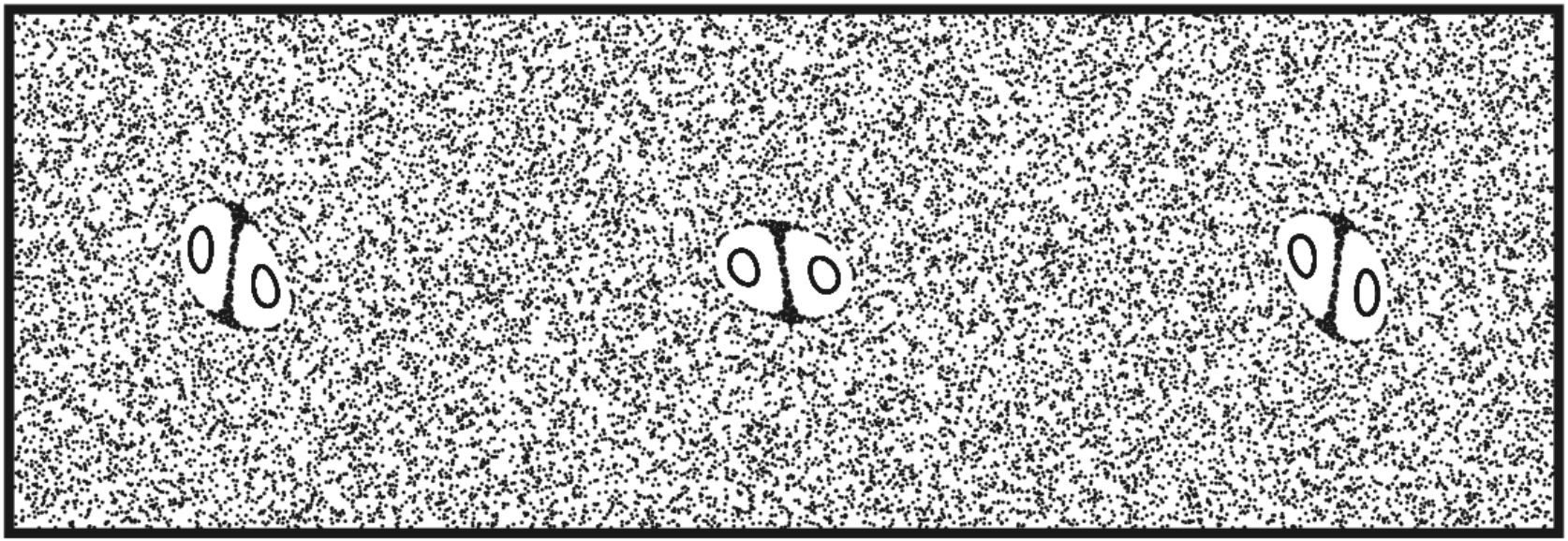

Poincaré section for $\tau_f > 1$

- For $\tau_f > 1$, groups of elliptic and saddle periodic points of period 3
  — streamlines around groups resemble fluid motion around a solid rod $\Rightarrow$
- At $\tau_f = 1$, points merge into parabolic points
- Below $\tau_f < 1$, periodic points vanish

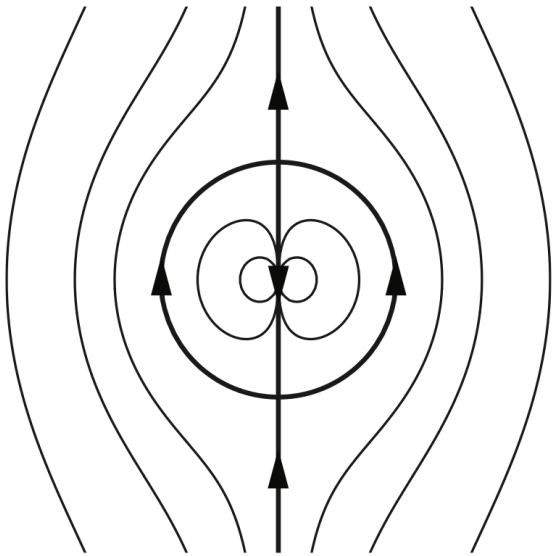

Identifying ‘ghost rods’: periodic points

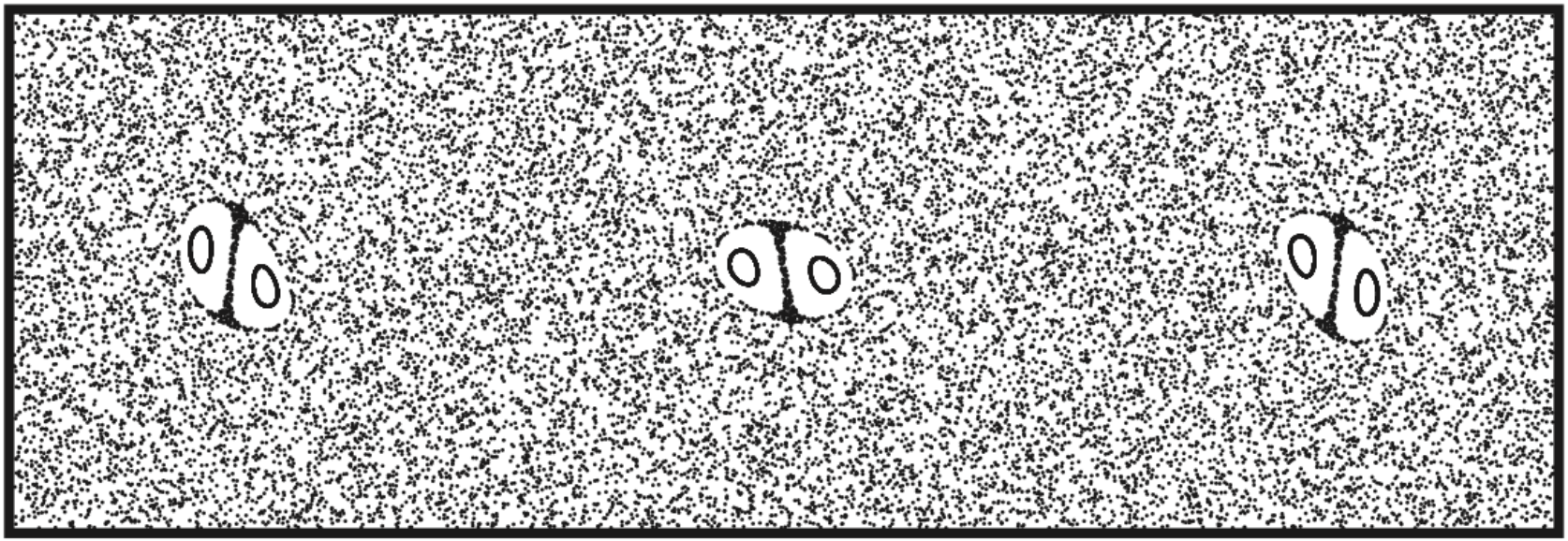

Poincaré section for $\tau_f > 1$

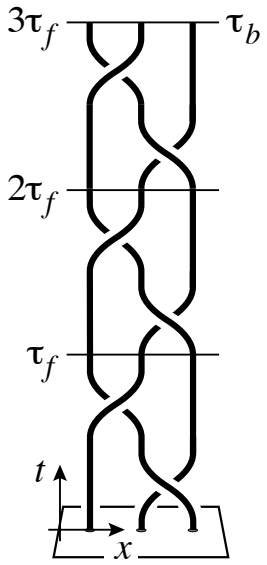

- Periodic points of period 3 $\Rightarrow$ act as ‘ghost rods’
- Their braid has $h_{\mathrm{TN}} = 0.96242$ from TNCT
- Actual $h_{\mathrm{flow}} \approx 0.964$
- $\Rightarrow$ h_{TN} is an excellent lower bound

Topological entropy continuity across critical point

- Consider $\tau_f < 1$

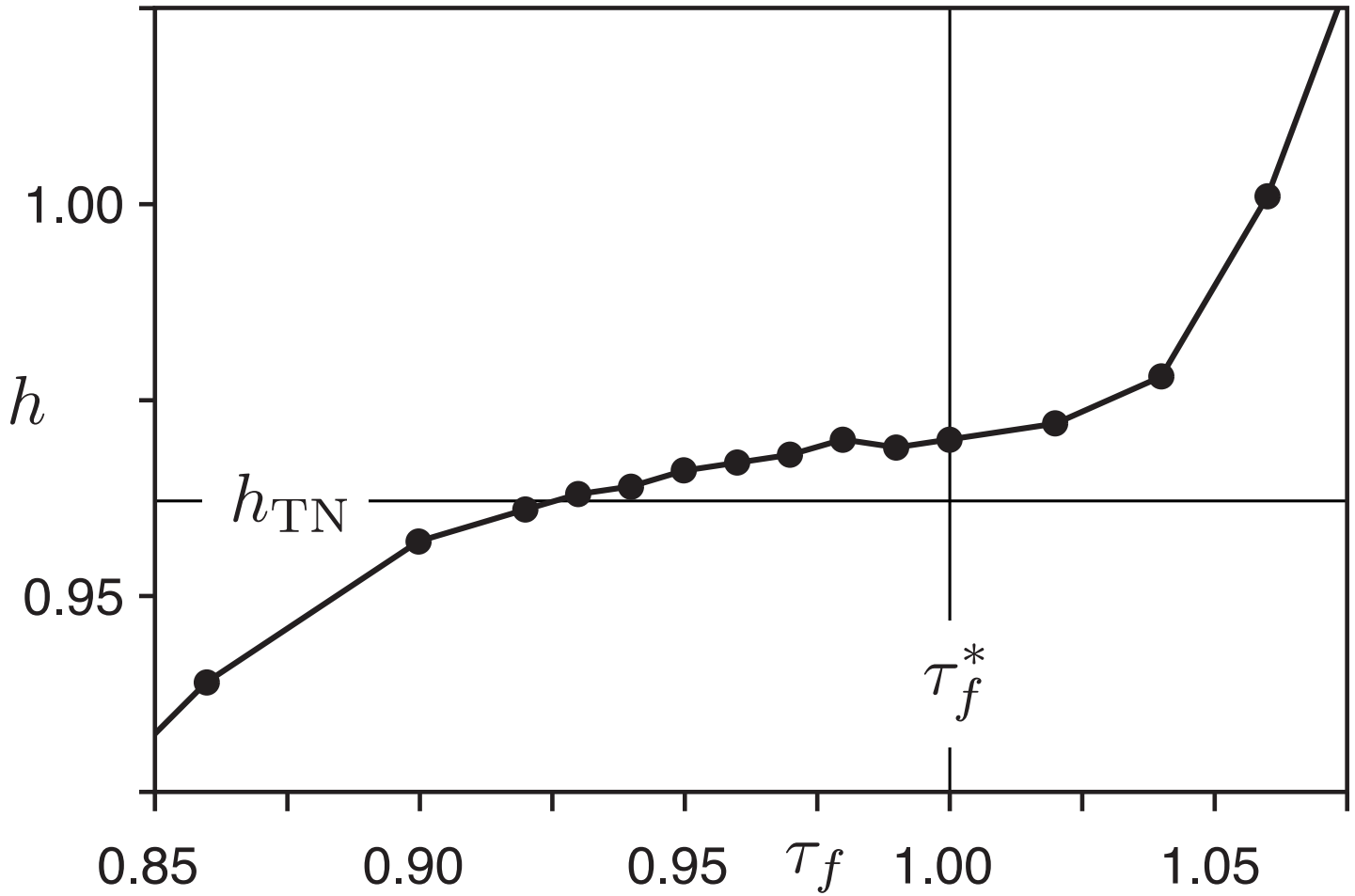

topological entropy as a function of τ_f

Identifying 'ghost rods'?

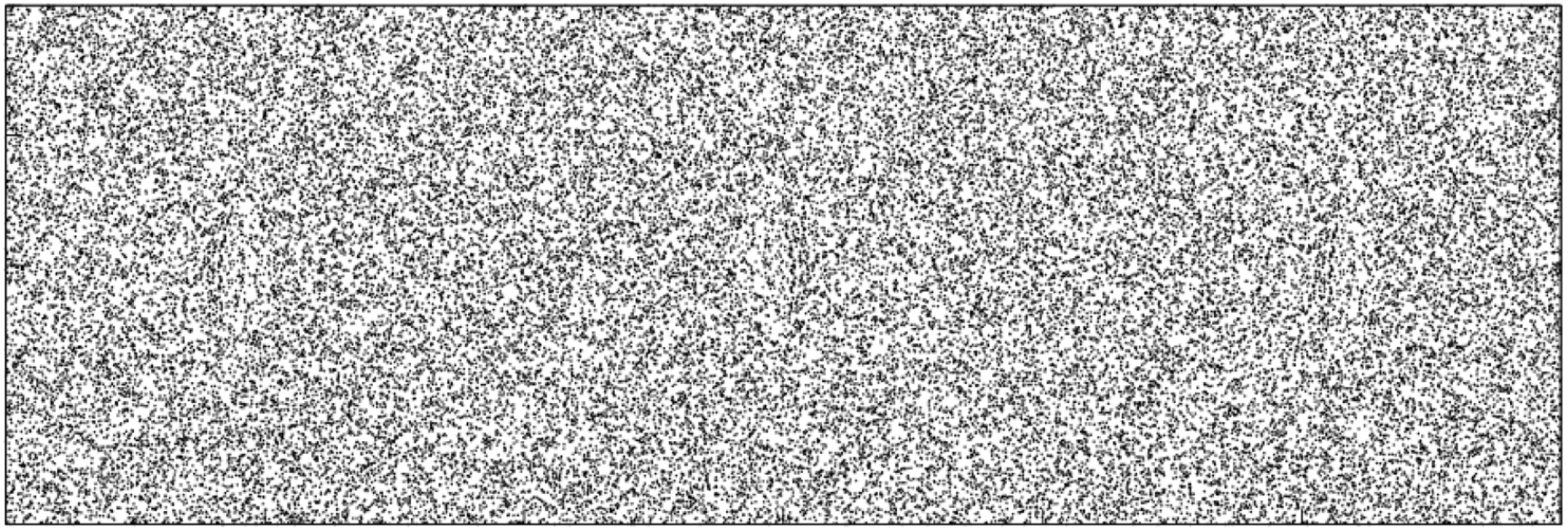

Poincaré section for $\tau_f < 1 \Rightarrow$ no obvious structure!

- Note the absence of any elliptical islands
- No periodic orbits of low period were found
- Is the phase space featureless?

Almost-invariant set (AIS) approach

- Take probabilistic point of view
- Partition phase space into **loosely coupled regions**

Almost-invariant sets $\approx$ regions with a long residence time[2]

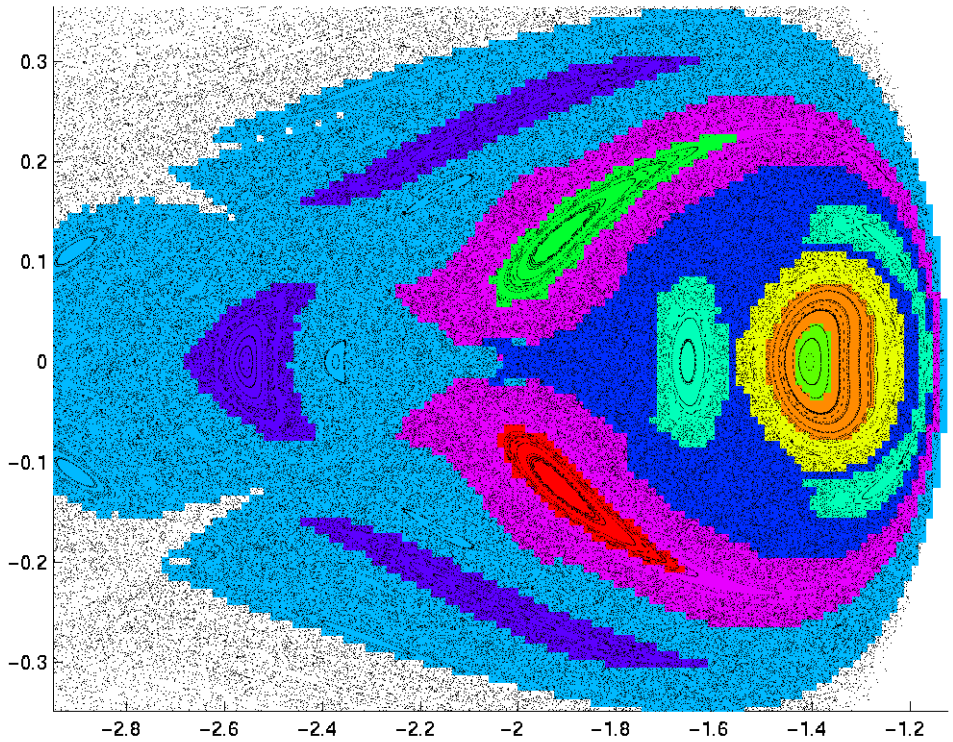

3-body problem phase space is divided into several invariant and almost-invariant sets.

[2]Dellnitz, Junge, Koon, Lekien, Lo, Marsden, Padberg, Preis, Ross, Thiere [2005] Int. J. Bif. Chaos

Almost-invariant set (AIS) approach

- Create box partition of phase space $\mathcal{B} = \{B_1, \ldots B_q\}$, with q large
- Consider a q-by-q **transition (Ulam) matrix**, P, for our deterministic dynamical system, where

$$P_{ij} = \frac{m(B_i \cap f^{-1}(B_j))}{m(B_i)},$$

the *transition probability* from B_i to B_j using, e.g., $f = \phi_t^{t+T}$, computed numerically

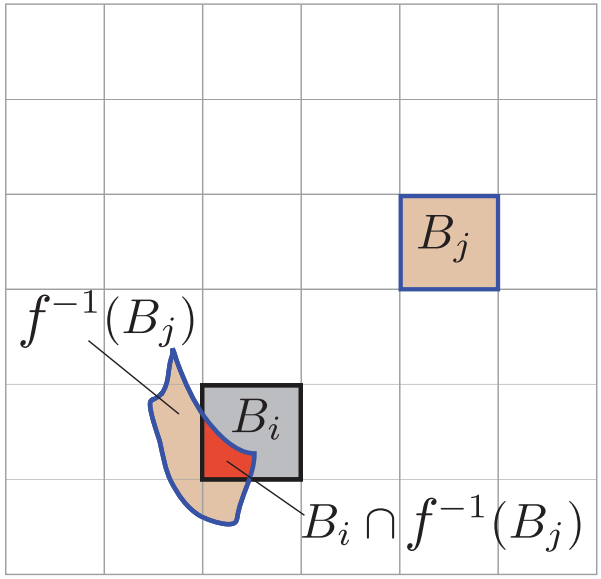

- P approximates our dynamical system via a finite state Markov chain.
- P approximates $\mathcal{P}$, Perron-Frobenius operator
  — which evolves densities, ν, ensembles of trajectories over one iterate of f, as $\mathcal{P}\nu$

Almost-invariant set (AIS) approach

- A set B is called almost invariant over the interval $[t, t+T]$ if

$$\rho(B) = \frac{m(B \cap f^{-1}(B))}{m(B)} \approx 1.$$

- Can maximize value of ρ over all possible combinations of sets $B \in \mathcal{B}$.

- In practice, AIS identified from spectrum of P or graph-partitioning

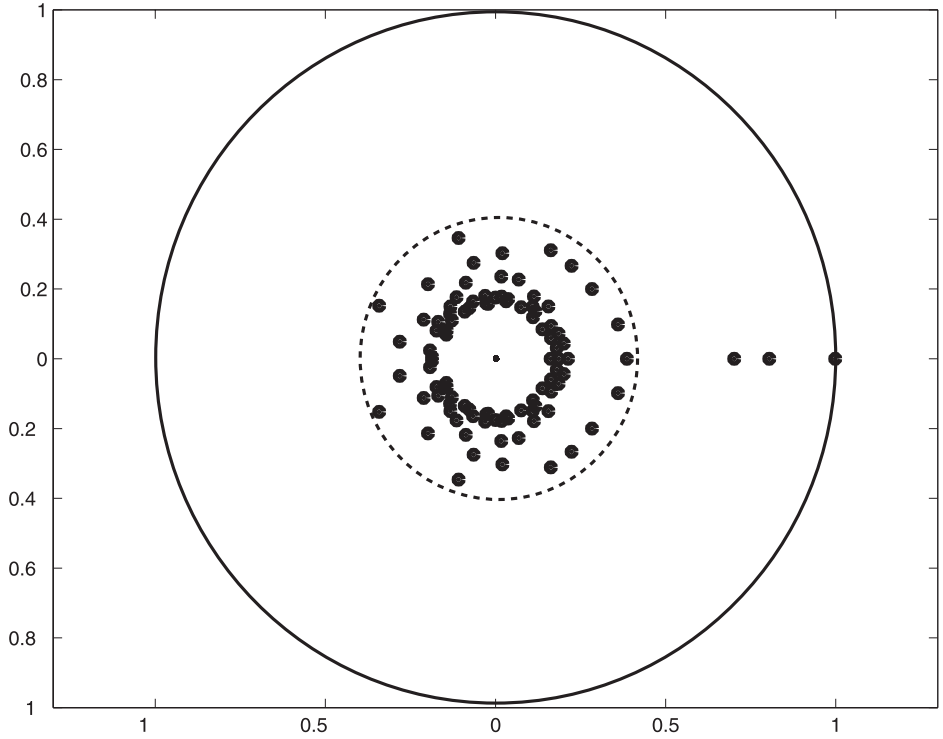

spectrum of P

Dellnitz, Froyland, Sertl [2000] Nonlinearity

Identifying AISs by spectrum of P

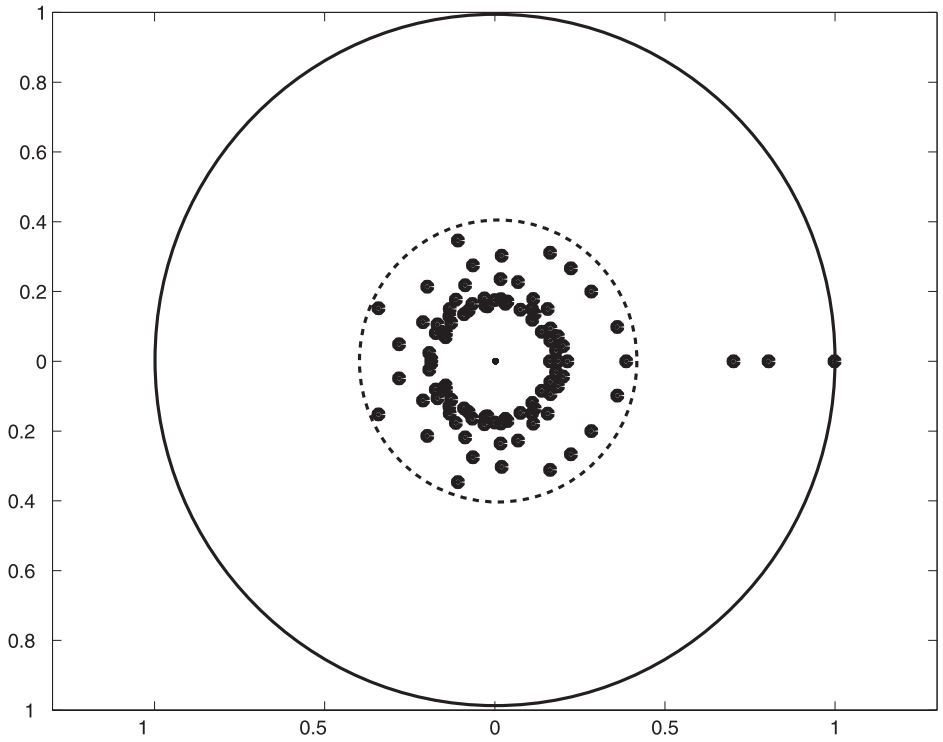

- Invariant densities are those fixed under P, $P\nu = \nu$, i.e., eigenvalue 1
- Essential spectrum lies within a disk of radius $r < 1$ which depends on the weakest expansion rate of the underlying system.
- The other real eigenvalues identify so-called almost-invariant sets

Dellnitz, Froyland, Sertl [2000] Nonlinearity

Identifying AISs by graph-partitioning

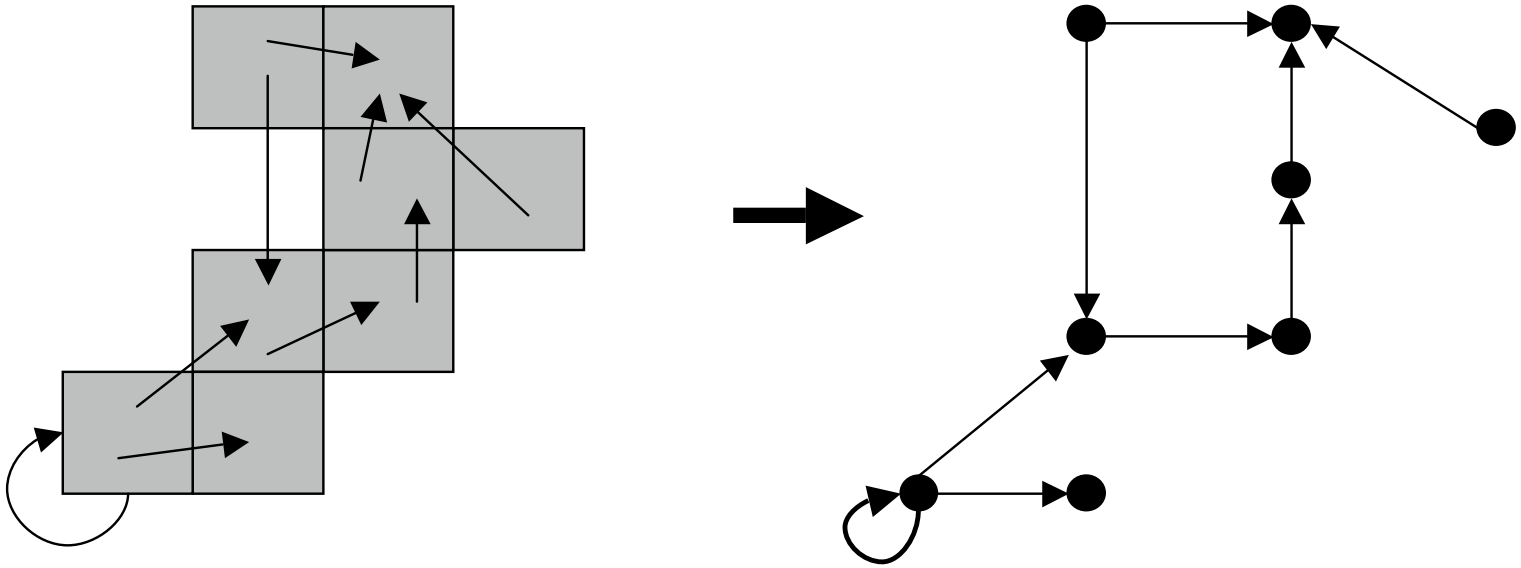

- P has graph representation where nodes correspond to boxes B_i and transitions between them are edges of a directed graph
- use graph partitioning methods to divide the nodes into an optimal number of parts such that each part is highly coupled within itself and only loosely coupled with other parts
- by doing so, we can obtain AISs and transport between them

Identifying 'ghost rods': almost-invariant sets

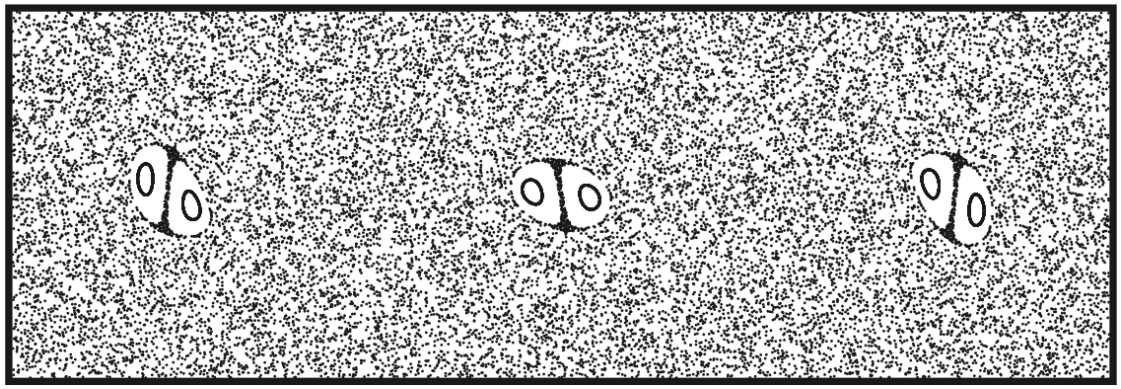

- Return to $\tau_f > 1$ case, where periodic points and manifolds exist
- Agreement between AIS boundaries and manifolds of periodic points
- Known previously[3] and applies to more general objects than periodic points, i.e. normally hyperbolic invariant manifolds (NHIMs)

[3] Dellnitz, Junge, Lo, Marsden, Padberg, Preis, Ross, Thiere [2005] Phys. Rev. Lett.; Dellnitz, Junge, Koon, Lekien, Lo, Marsden, Padberg, Preis, Ross, Thiere [2005] Int. J. Bif. Chaos

Identifying 'ghost rods': almost-invariant sets

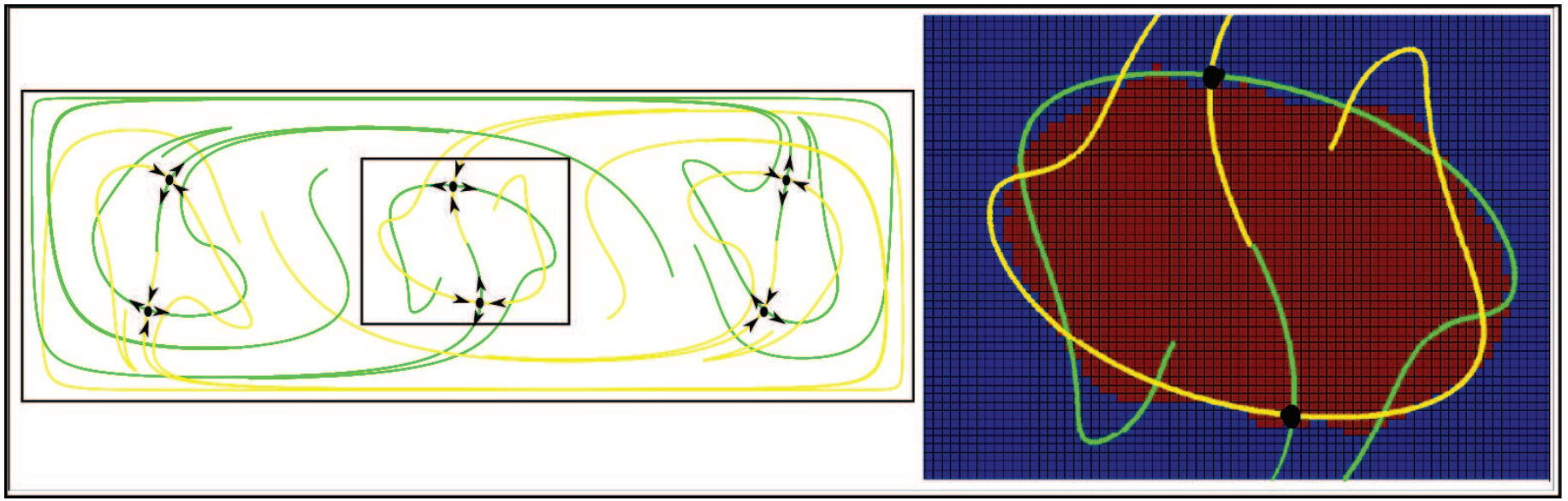

- Return to $\tau_f > 1$ case, where periodic points and manifolds exist
- Agreement between AIS boundaries and manifolds of periodic points
- Known previously[4] and applies to more general objects than periodic points, i.e. normally hyperbolic invariant manifolds (NHIMs)

[4]Dellnitz, Junge, Lo, Marsden, Padberg, Preis, Ross, Thiere [2005] Phys. Rev. Lett.; Dellnitz, Junge, Koon, Lekien, Lo, Marsden, Padberg, Preis, Ross, Thiere [2005] Int. J. Bif. Chaos

Identifying 'ghost rods': almost-invariant sets

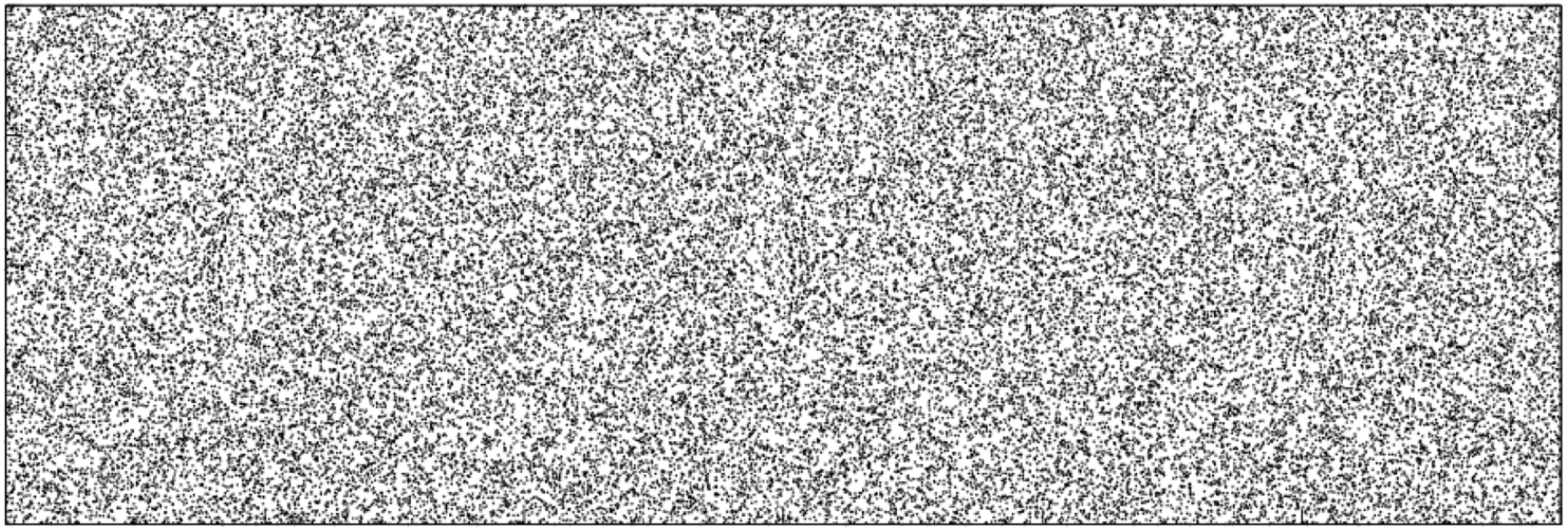

Poincaré section for $\tau_f < 1 \Rightarrow$ no obvious structure!

- Return to $\tau_f < 1$ case, where no periodic orbits of low period known
- Is the phase space featureless?

- Consider transition matrix $P_t^{t+\tau_f}$ induced by Poincaré map $\phi_t^{t+\tau_f}$

Identifying ‘ghost rods’: almost-invariant sets

Top eigenvectors for $\tau_f = 0.99$ reveal hierarchy of phase space structures

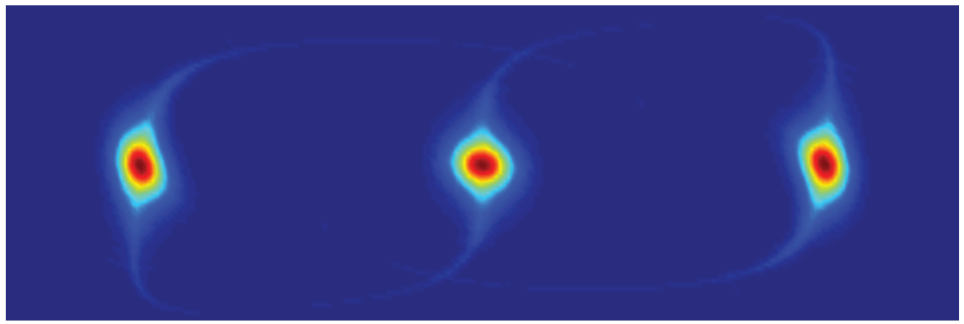

ν_2

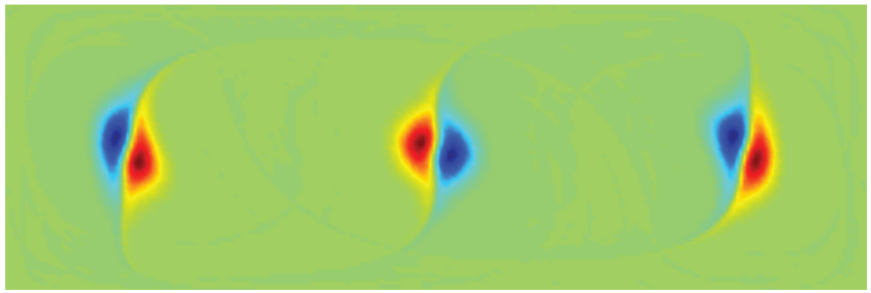

ν_3

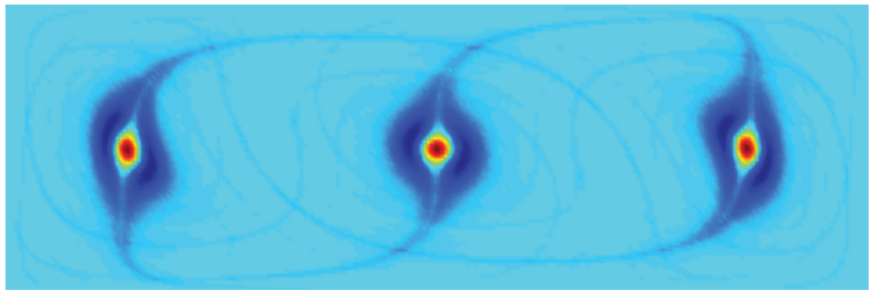

ν_4

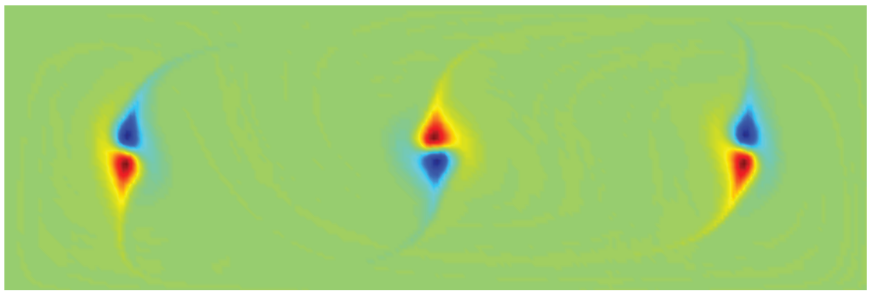

ν_5

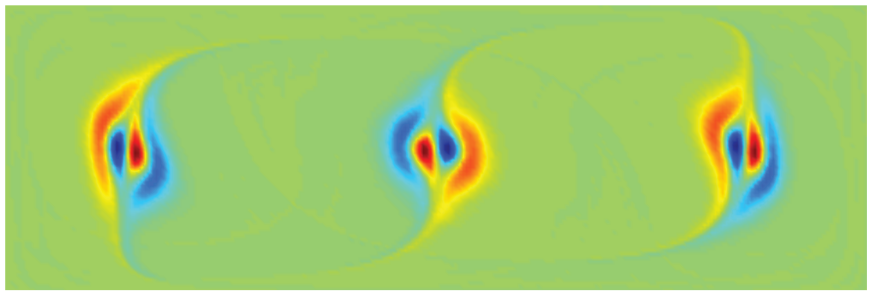

ν_6

Identifying ‘ghost rods’: almost-cyclic sets

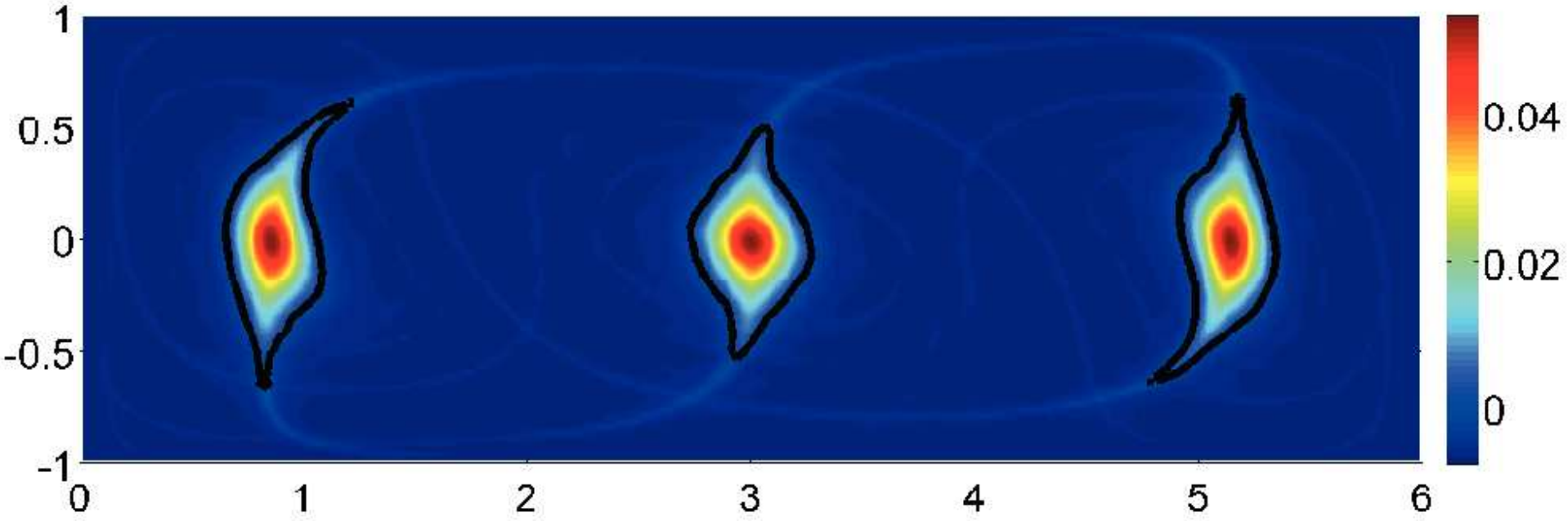

The zero contour (black) is the boundary between the two almost-invariant sets.

- Three-component AIS made of 3 almost-cyclic sets (ACSs) of period 3
- ACSs effectively replace compact region bounded by saddle manifolds
- Also: we see a **dynamical remnant of the global ‘stable and unstable manifolds’ of the saddle points**, despite no saddle points

Identifying ‘ghost rods’: almost-cyclic sets

Almost-cyclic sets stirring the surrounding fluid like ‘ghost rods’
— **works even when periodic orbits are absent!**

Movie shown is second eigenvector for $P_t^{t+\tau_f}$ for $t \in [0, \tau_f)$

Identifying ‘ghost rods’: almost-cyclic sets

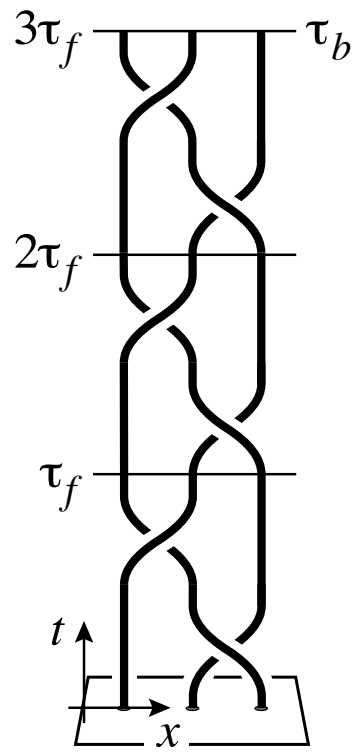

Braid of ACSs gives lower bound of entropy via Thurston-Nielsen

— One only needs approximately cyclic blobs of fluid

— Even though the theorems require exactly periodic points!

— Stremler, Ross, Grover, Kumar [2011] Phys. Rev. Lett.

Topological entropy vs. bifurcation parameter

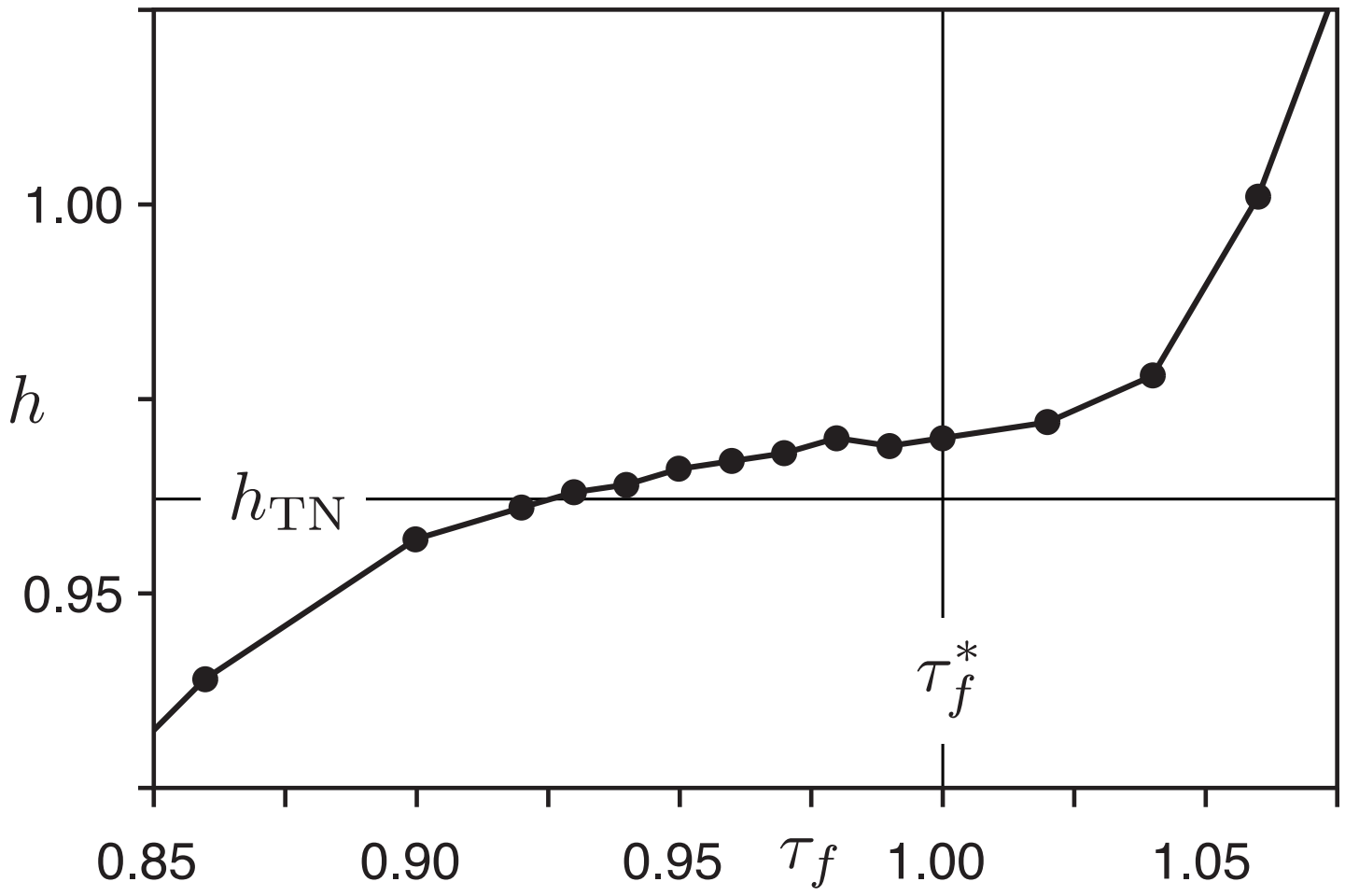

topological entropy as a function of τ_f

- h_{TN} shown for ACS braid on 3 strands

Eigenvalues/eigenvectors vs. bifurcation parameter

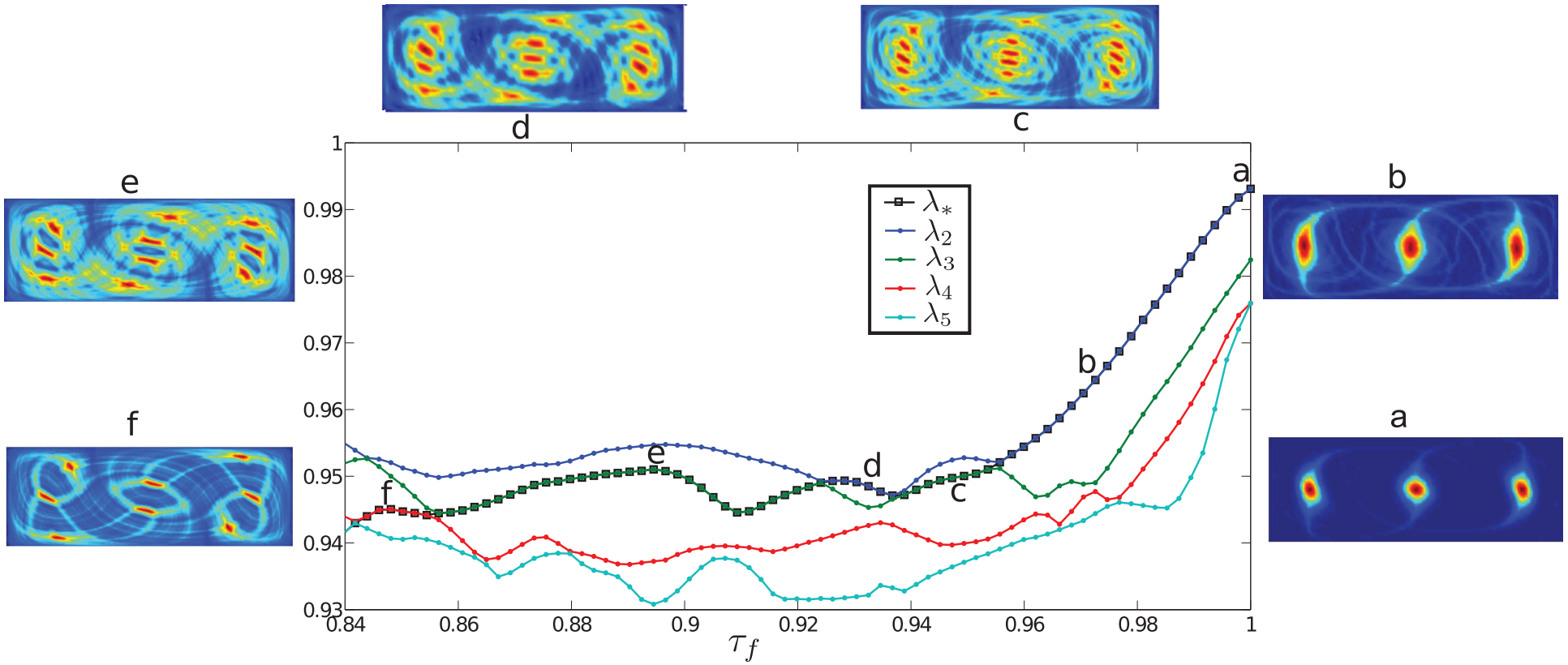

Movie shows change in eigenvector along branch marked with '–□–' above (a to f), as τ_f decreases $\Rightarrow$

Bifurcation of ACSs

For example, braid on 13 strands for $\tau_f = 0.92$

Movie shown is second eigenvector for $P_t^{t+\tau_f}$ for $t \in [0, \tau_f)$

Thurson-Nielsen for this braid provides lower bound on topological entropy

Sequence of ACS braids bounds entropy

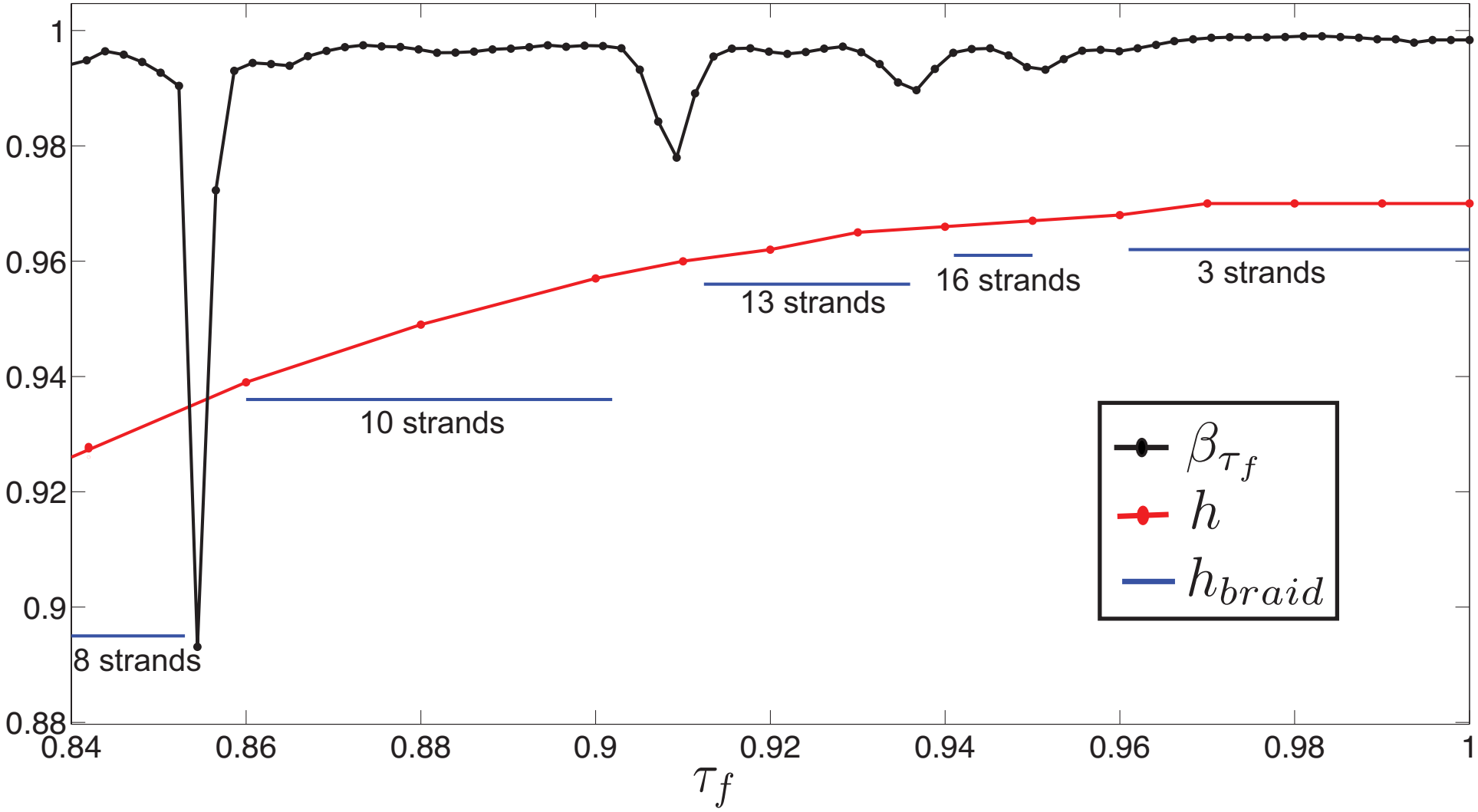

For various braids of ACSs, the calculated entropy is given, bounding from below the true topological entropy over the range where the braid exists

Chaotic transport: aperiodic, finite-time setting

- Data-driven, finite-time, aperiodic setting
  — e.g., non-autonomous ODEs for fluid flow
- How do we get at transport?
- Recall the flow, $x \mapsto \phi_t^{t+T}(x)$, where $\phi : \mathbb{R}^n \to \mathbb{R}^n$

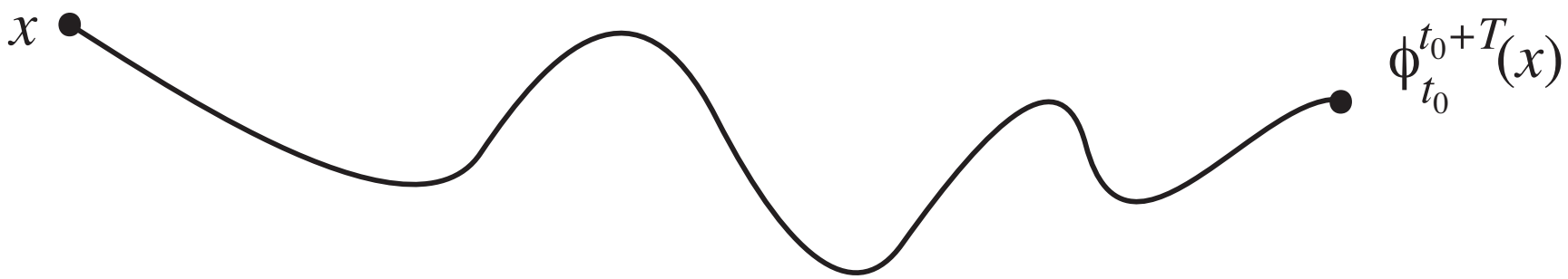

Identify regions of high sensitivity of initial conditions

- Small initial perturbations $\delta x(t)$ grow like

$$\begin{aligned}\delta x(t+T) &= \phi_t^{t+T}(x+\delta x(t)) - \phi_t^{t+T}(x) \\ &= \frac{d\phi_t^{t+T}(x)}{dx}\delta x(t) + O(||\delta x(t)||^2)\end{aligned}$$

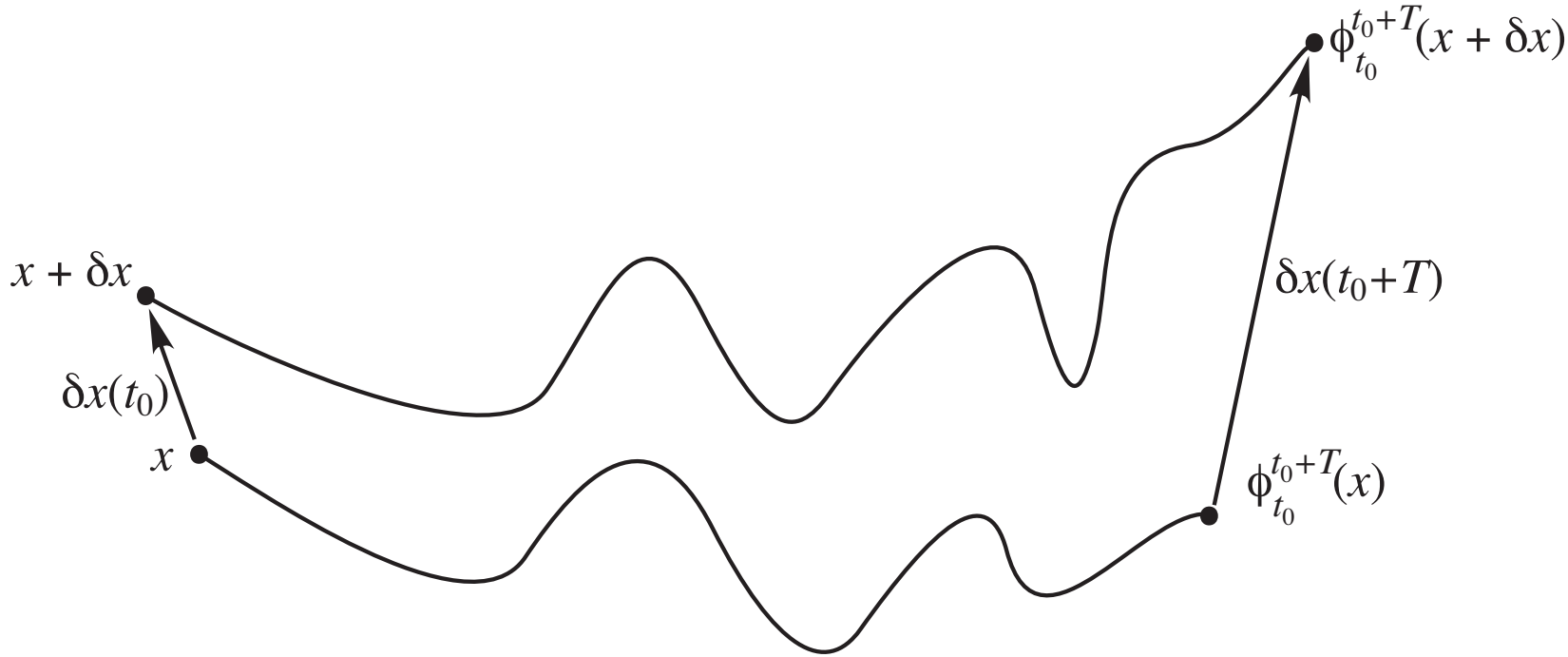

Identify regions of high sensitivity of initial conditions

- Small initial perturbations $\delta x(t)$ grow like

$$\begin{aligned}\delta x(t+T) &= \phi_t^{t+T}(x+\delta x(t)) - \phi_t^{t+T}(x) \\ &= \frac{d\phi_t^{t+T}(x)}{dx}\delta x(t) + O(||\delta x(t)||^2)\end{aligned}$$

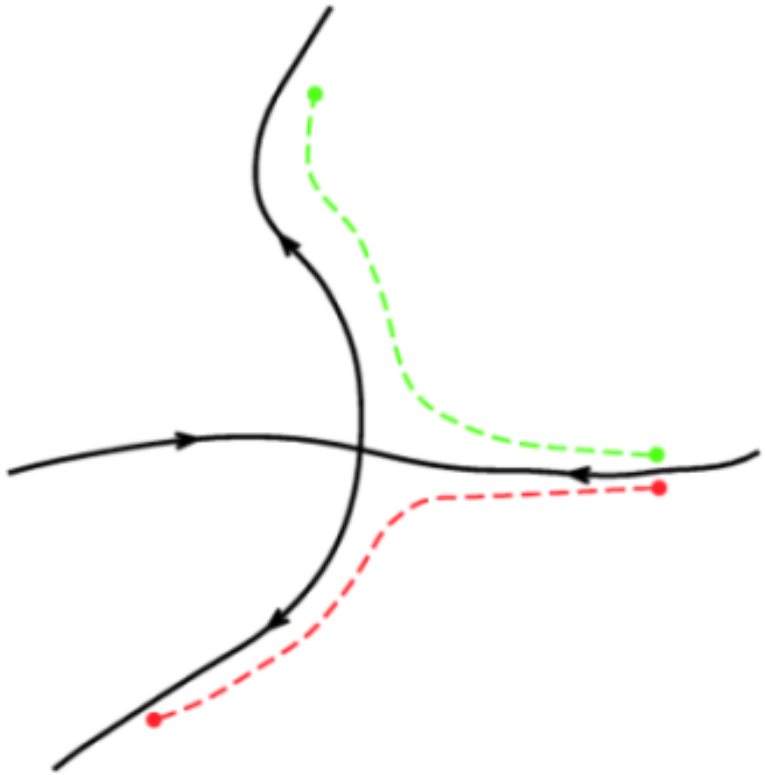

Invariant manifold analogs: FTLE-LCS approach

- The finite-time Lyapunov exponent (FTLE),

$$\sigma_t^T(x) = \frac{1}{|T|} \log \left\| \frac{d\phi_t^{t+T}(x)}{dx} \right\|$$

measures the maximum stretching rate over the interval T of trajectories starting near the point x at time t

- Ridges of σ_t^T are candidate hyperbolic codim-1 surfaces; finite-time analogs of stable/unstable manifolds; 'Lagrangian coherent structures'[5]

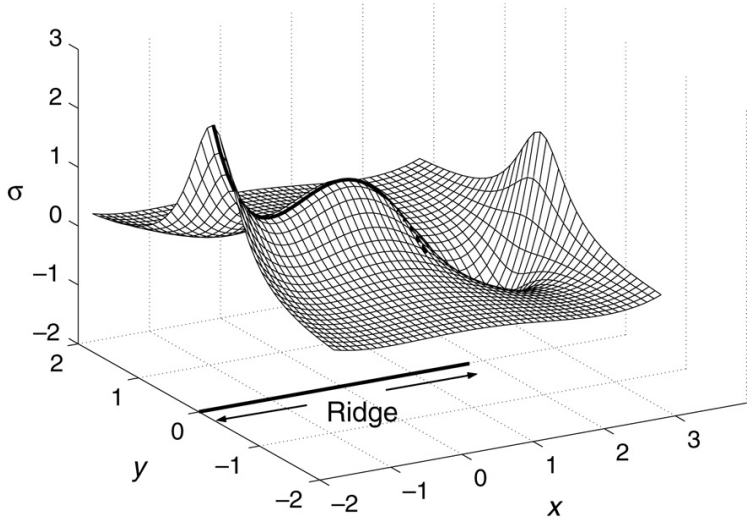

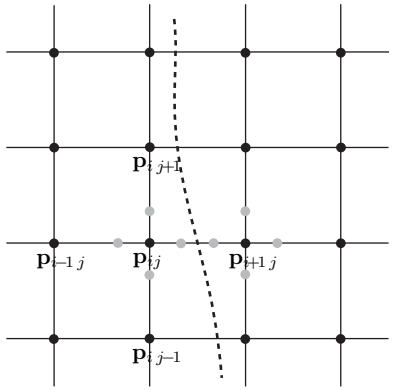

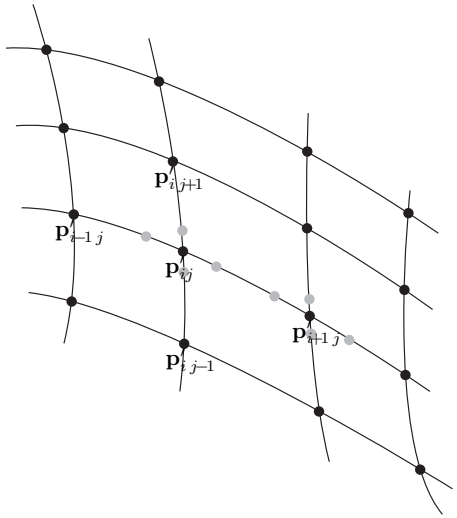

[5] cf. Bowman, 1999; Haller & Yuan, 2000; Haller, 2001; Shadden, Lekien, Marsden, 2005

Invariant manifold analogs: FTLE-LCS approach

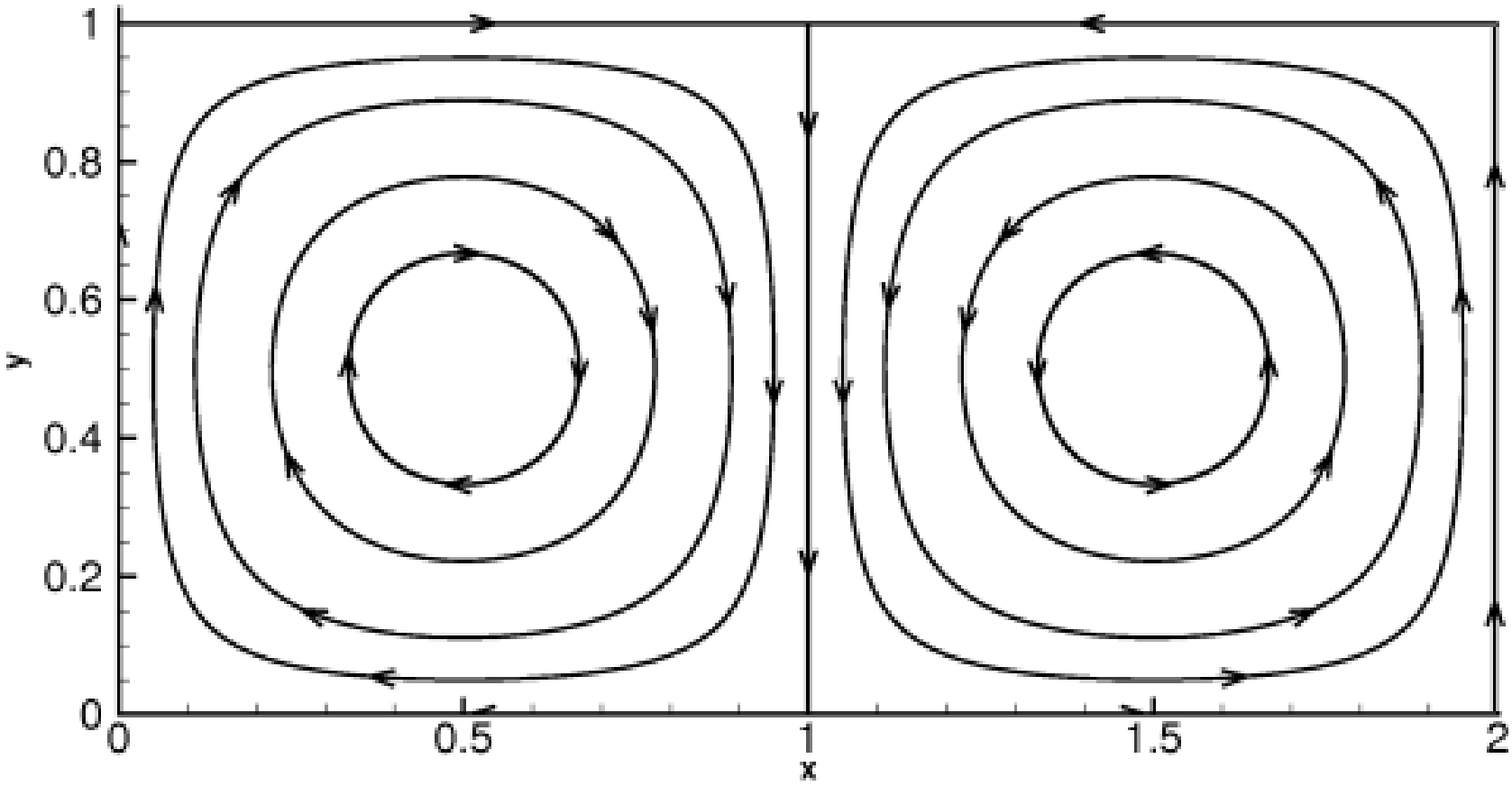

Autonomous double-gyre flow

Invariant manifold analogs: FTLE-LCS approach

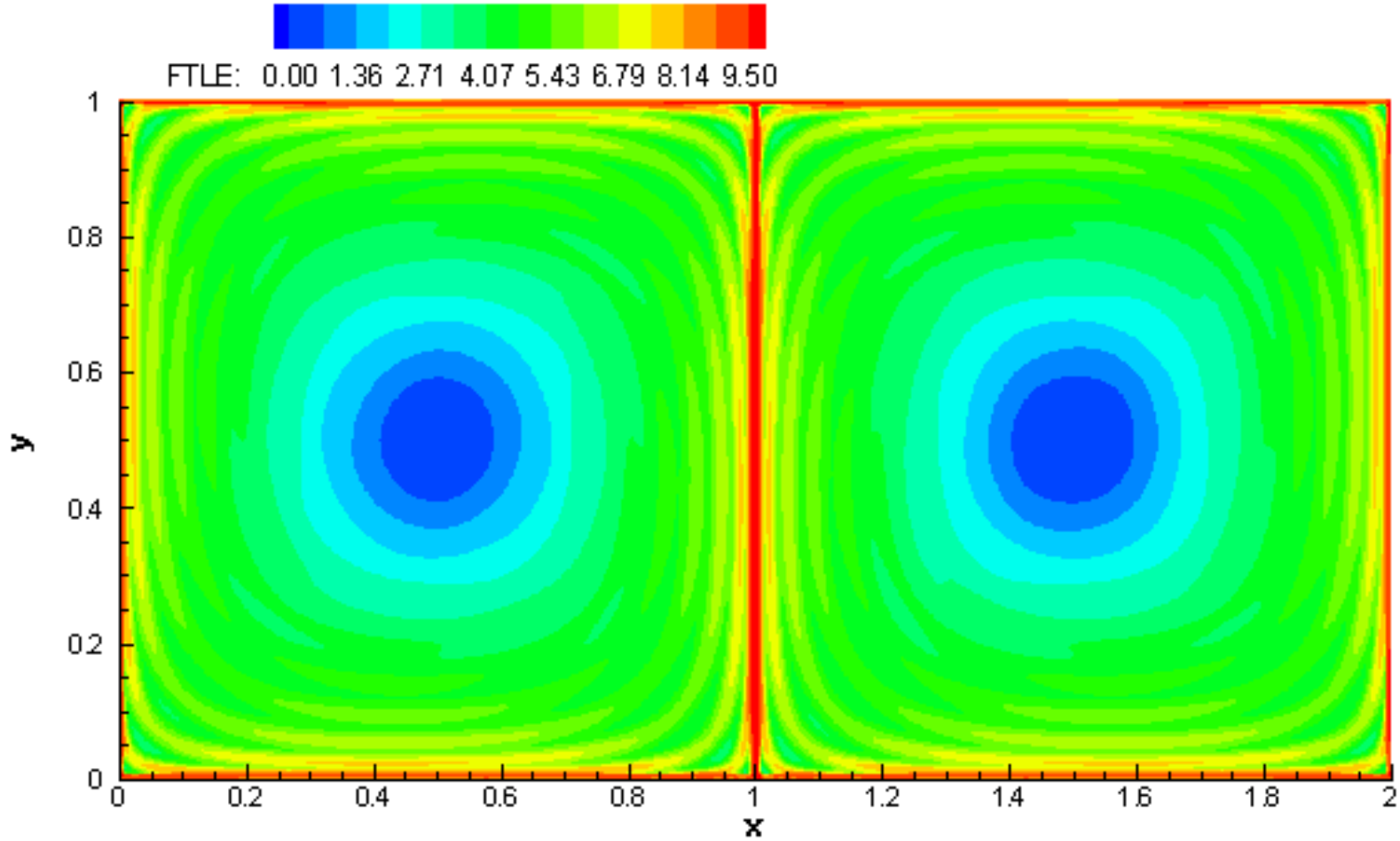

Invariant manifold analogs: FTLE-LCS approach

Use your intuition about ridges, a mountain ridge

Invariant manifold analogs: FTLE-LCS approach

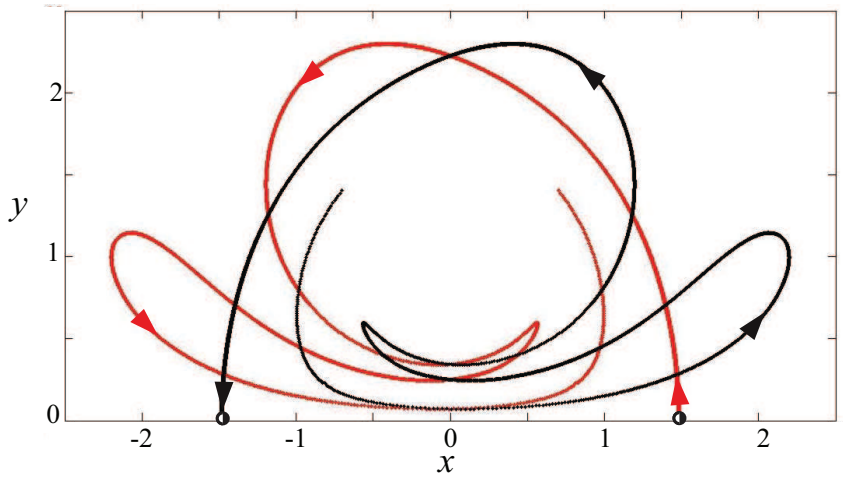

Invariant manifolds

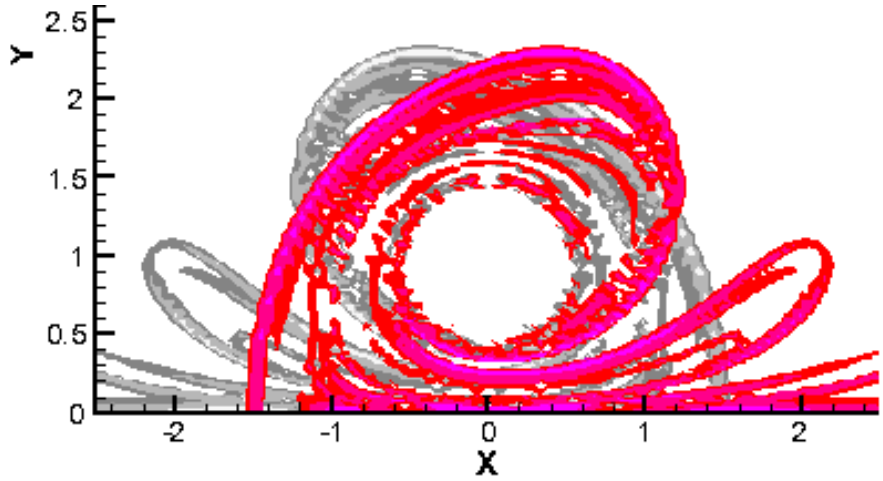

LCS

Time-periodic oscillating vortex pair flow

Invariant manifold analogs: FTLE-LCS approach

- We can define the FTLE for Riemannian manifolds[3]

$$\sigma_t^T(x) = \frac{1}{|T|} \ln \left\| \mathrm{D}\phi_t^{t+T} \right\| \doteq \frac{1}{|T|} \log \left(\max_{\mathrm{y} \neq 0} \frac{\left\| \mathrm{D}\phi_t^{t+T}(\mathrm{y}) \right\|}{\|\mathrm{y}\|} \right)$$

with y a small perturbation in the tangent space at x.

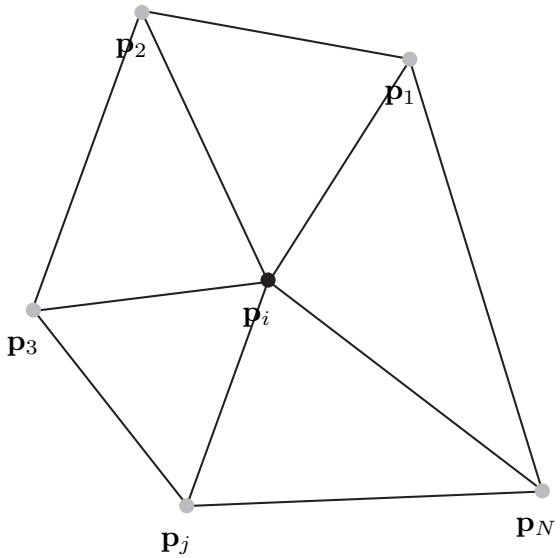

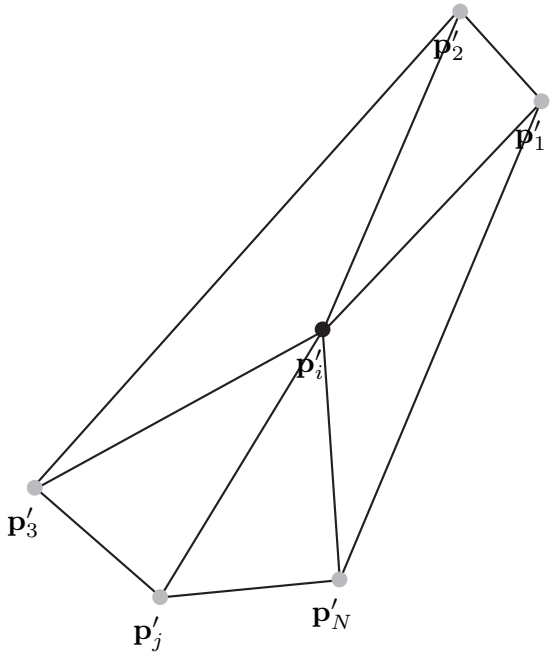

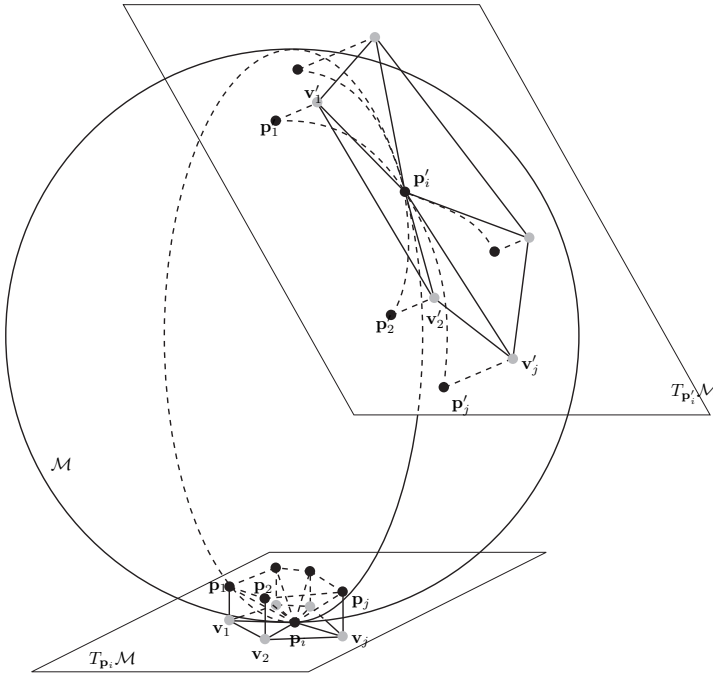

[3] Lekien & Ross [2010] Chaos

Transport barriers on Riemannian manifolds

- Ridges correspond to dynamical barriers[3] or Lagrangian coherent structures (LCS): repelling surfaces for $T > 0$, attracting for $T < 0$

cylinder Moebius strip

Each frame has a different initial time t

[3] Lekien & Ross [2010] Chaos

Atmospheric flows: Antarctic polar vortex

ozone data

Atmospheric flows: Antarctic polar vortex

ozone data + LCSs (red = repelling, blue = attracting)

Atmospheric flows: Antarctic polar vortex

air masses on either side of a repelling LCS

Atmospheric flows: continental U.S.

LCSs: orange = repelling, blue = attracting

Atmospheric flows and lobe dynamics

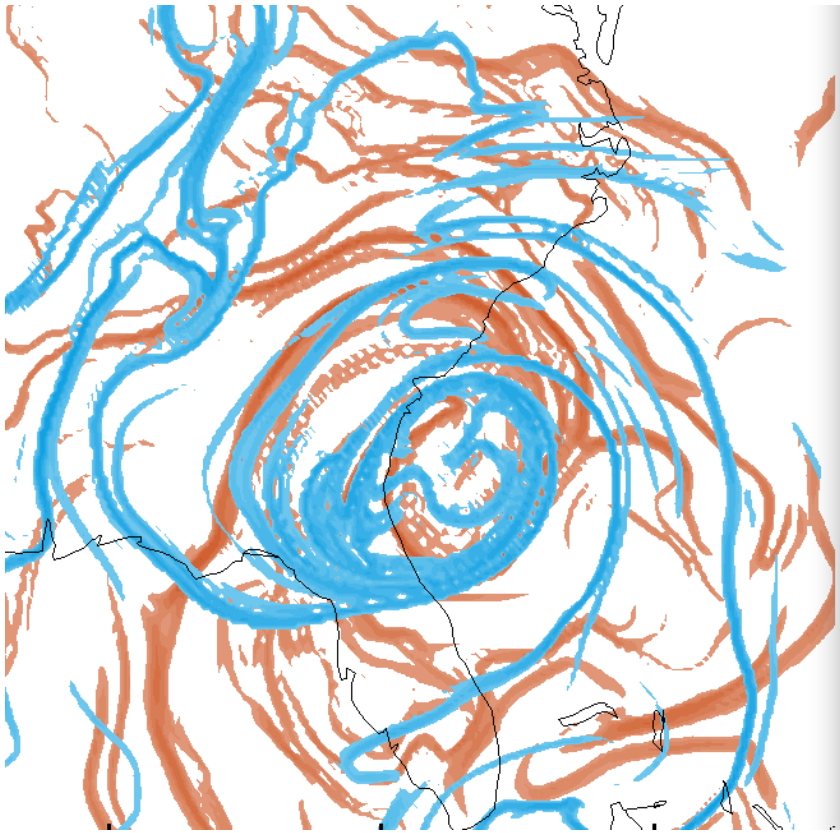

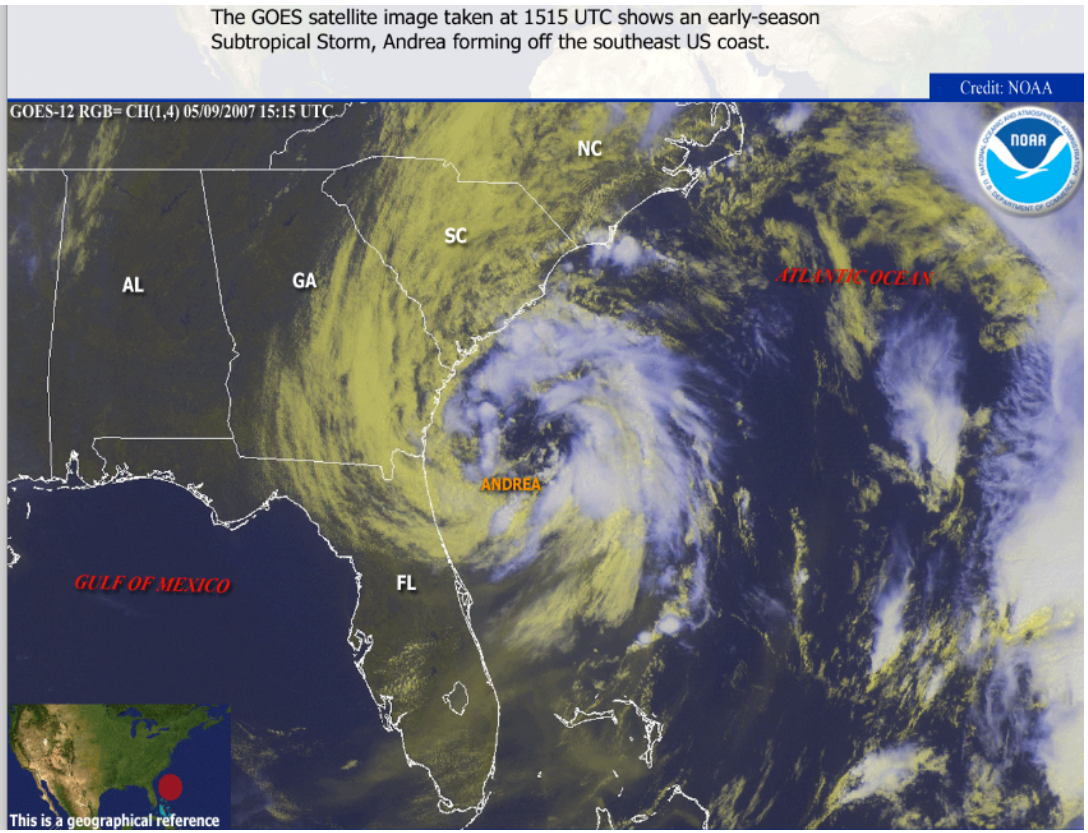

orange = repelling LCSs, blue = attracting LCSs

satellite

Andrea, first storm of 2007 hurricane season

cf. Sapsis & Haller [2009], Du Toit & Marsden [2010], Lekien & Ross [2010], Ross & Tallapragada [2011]

Atmospheric flows and lobe dynamics

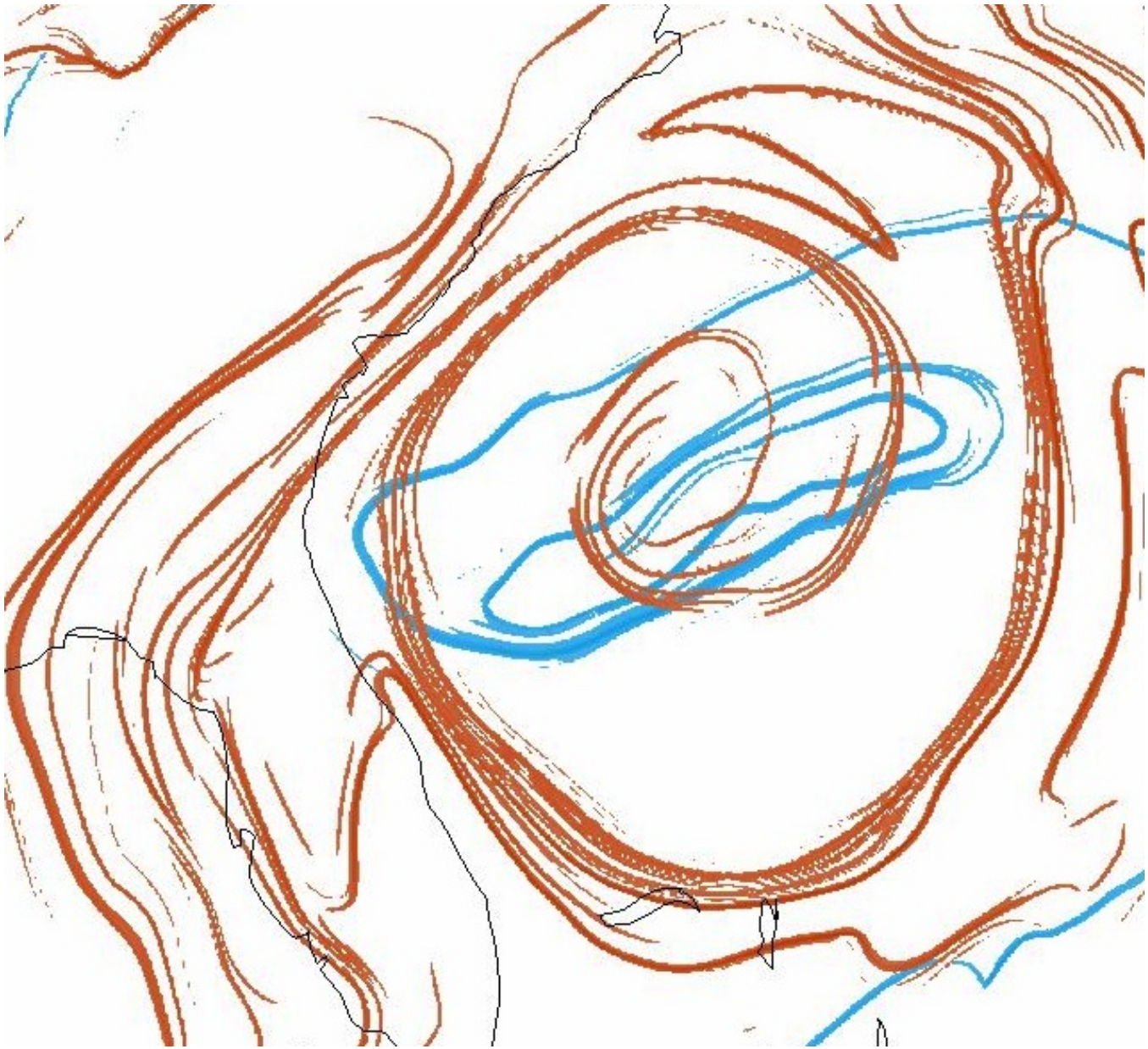

Andrea at one snapshot; LCS shown (orange = repelling, blue = attracting)

Atmospheric flows and lobe dynamics

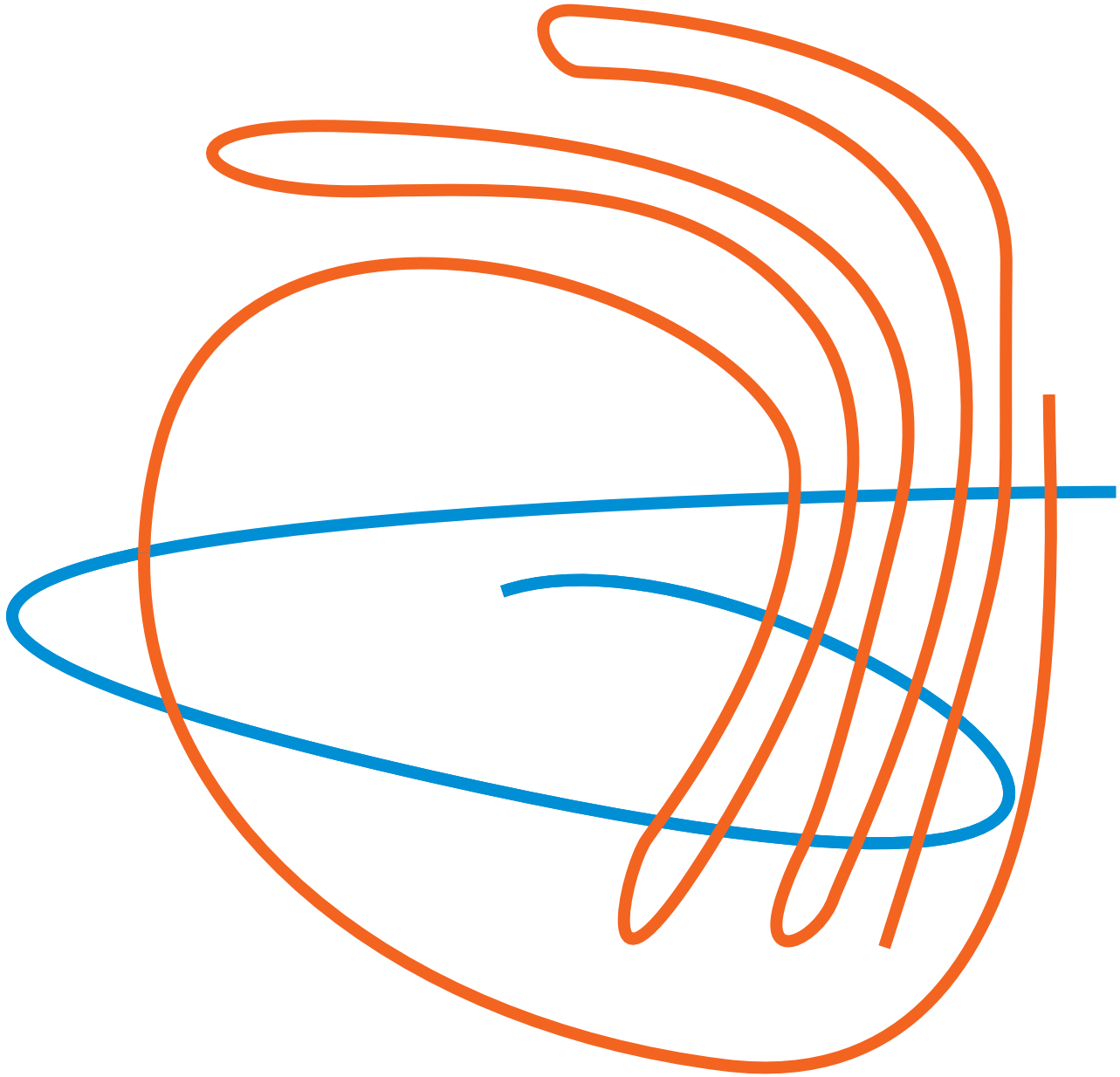

orange = repelling (stable manifold), blue = attracting (unstable manifold)

Atmospheric flows and lobe dynamics

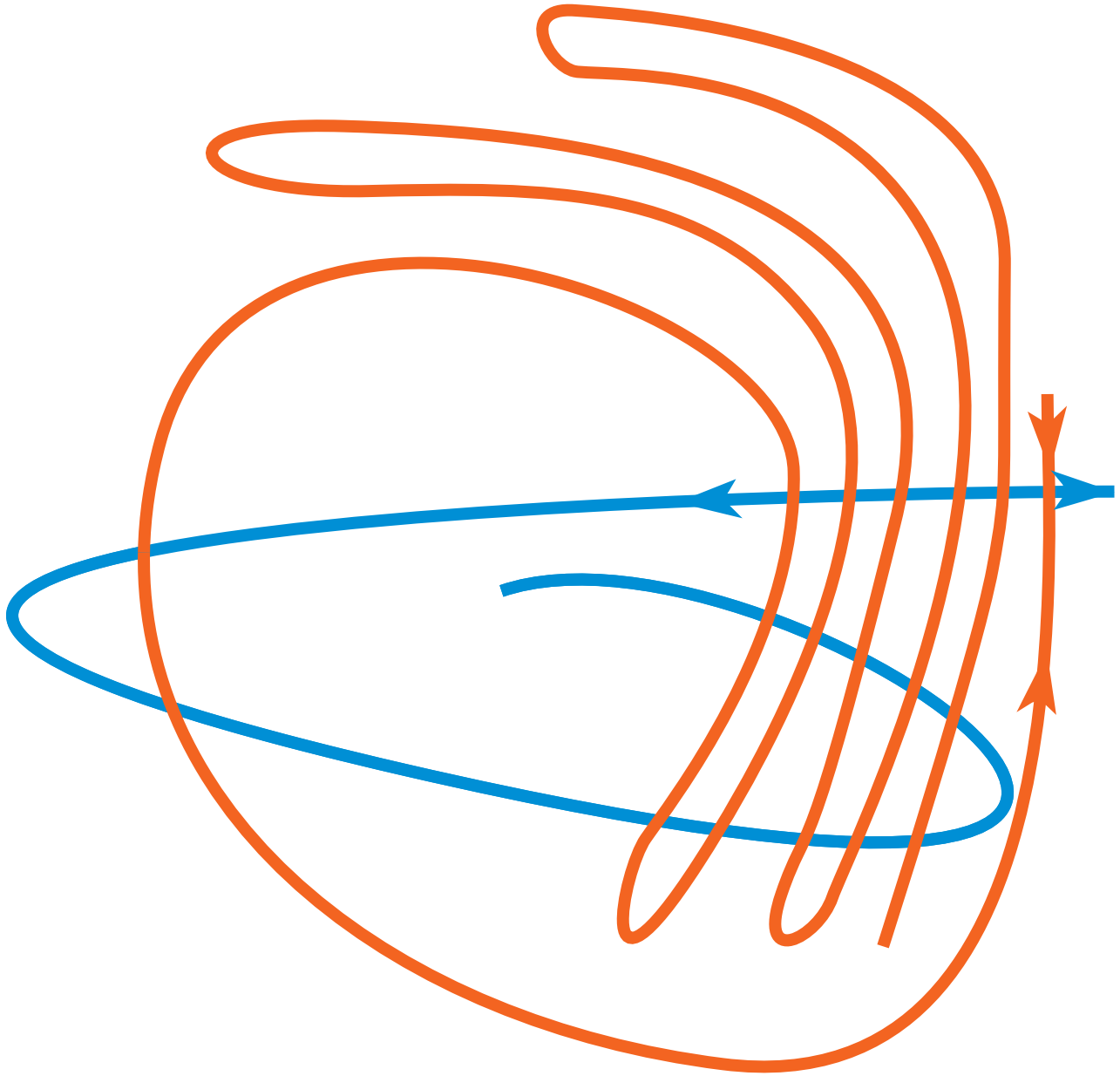

orange = repelling (stable manifold), blue = attracting (unstable manifold)

Atmospheric flows and lobe dynamics

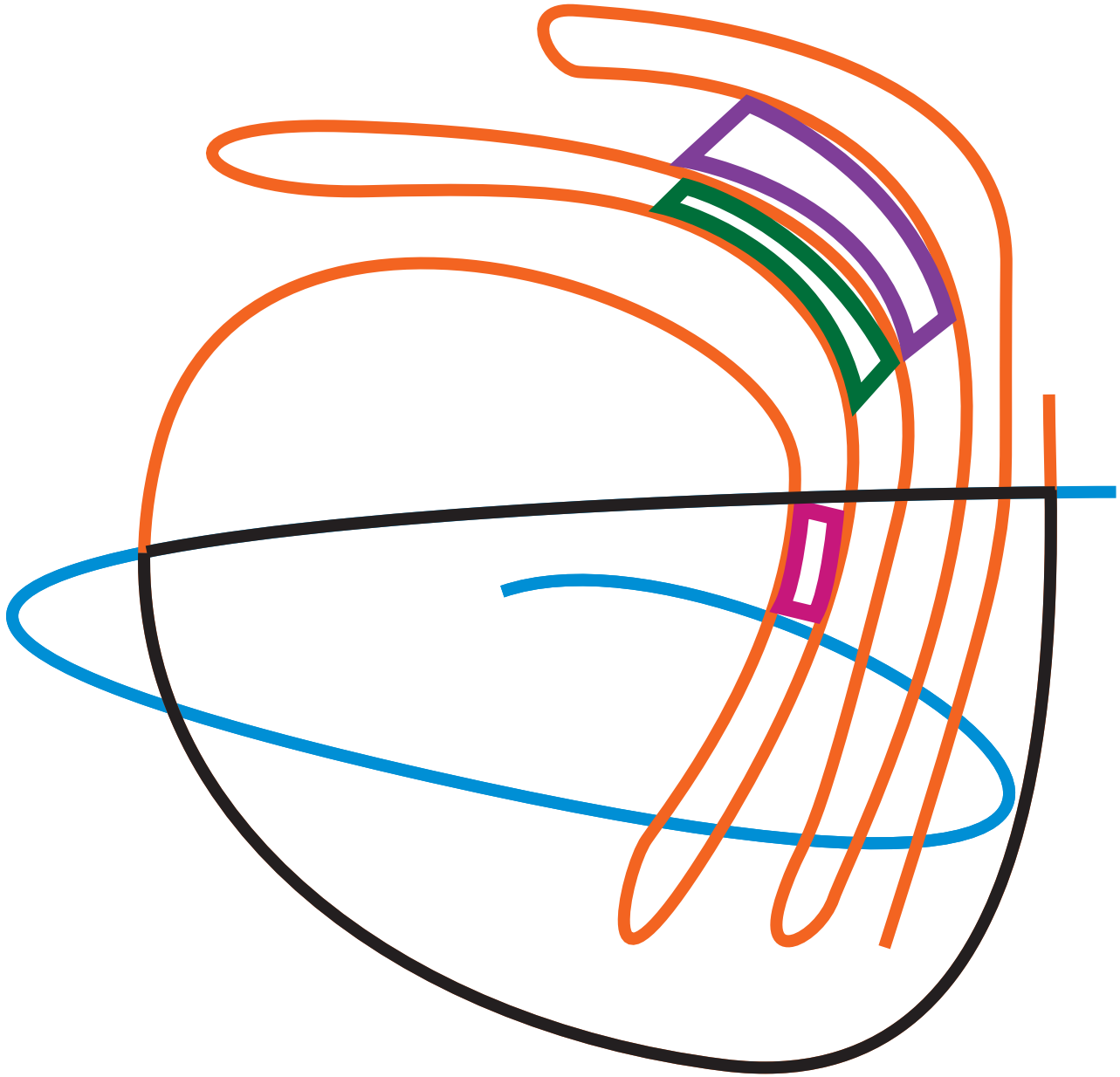

Portions of lobes colored; magenta = outgoing, green = incoming, purple = stays out

Atmospheric flows and lobe dynamics

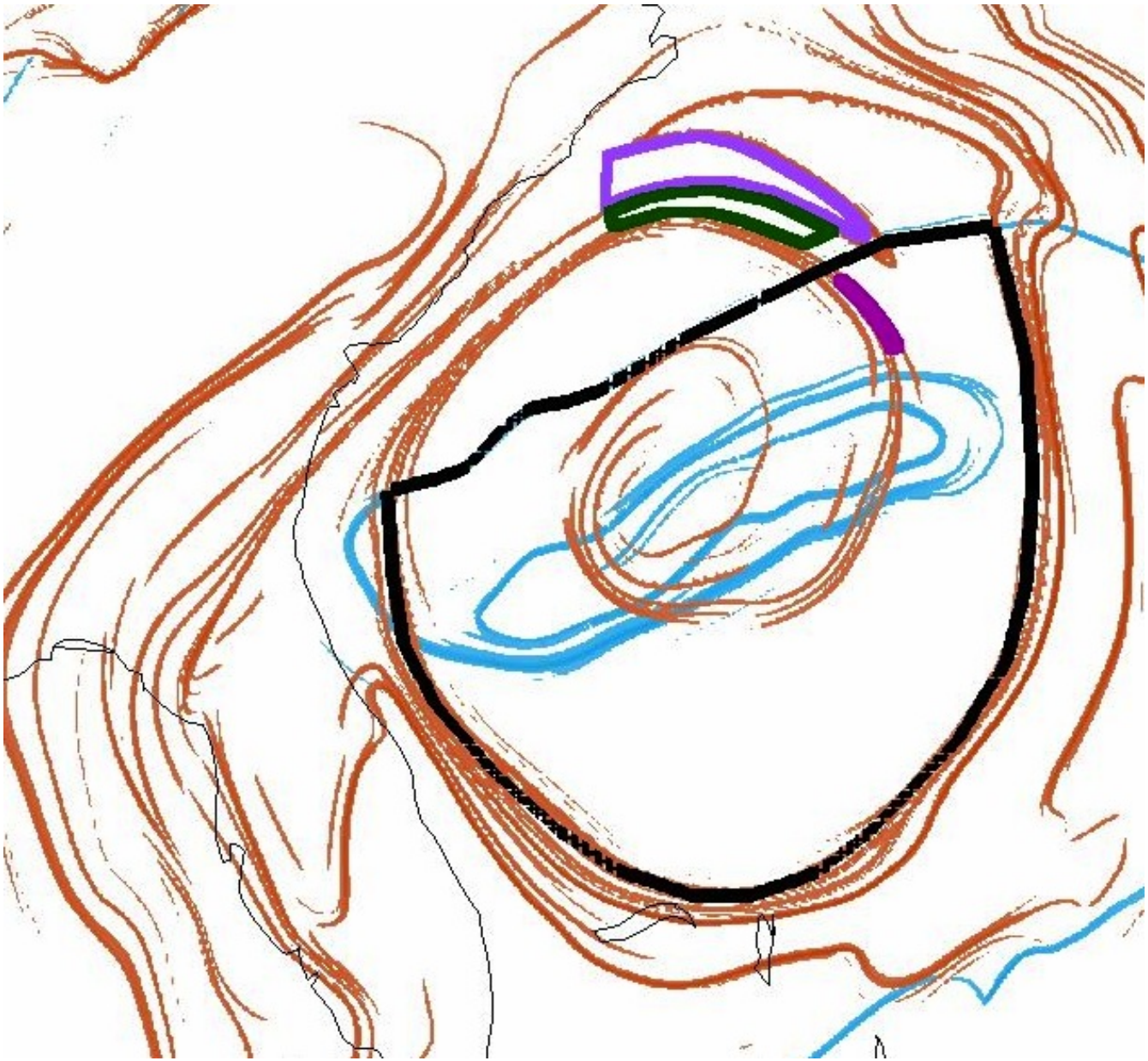

Portions of lobes colored; magenta = outgoing, green = incoming, purple = stays out

Atmospheric flows and lobe dynamics

Sets behave as lobe dynamics dictates

Atmospheric transport network relevant for aeroecology

Skeleton of large-scale horizontal transport

relevant for large-scale spatiotemporal patterns of important biota e.g., plant pathogens

orange = repelling LCSs, blue = attracting LCSs

Tallapragada, Schmale, Ross [2011] Chaos

2D curtain-like structures bounding air masses

2D curtain-like structures bounding air masses

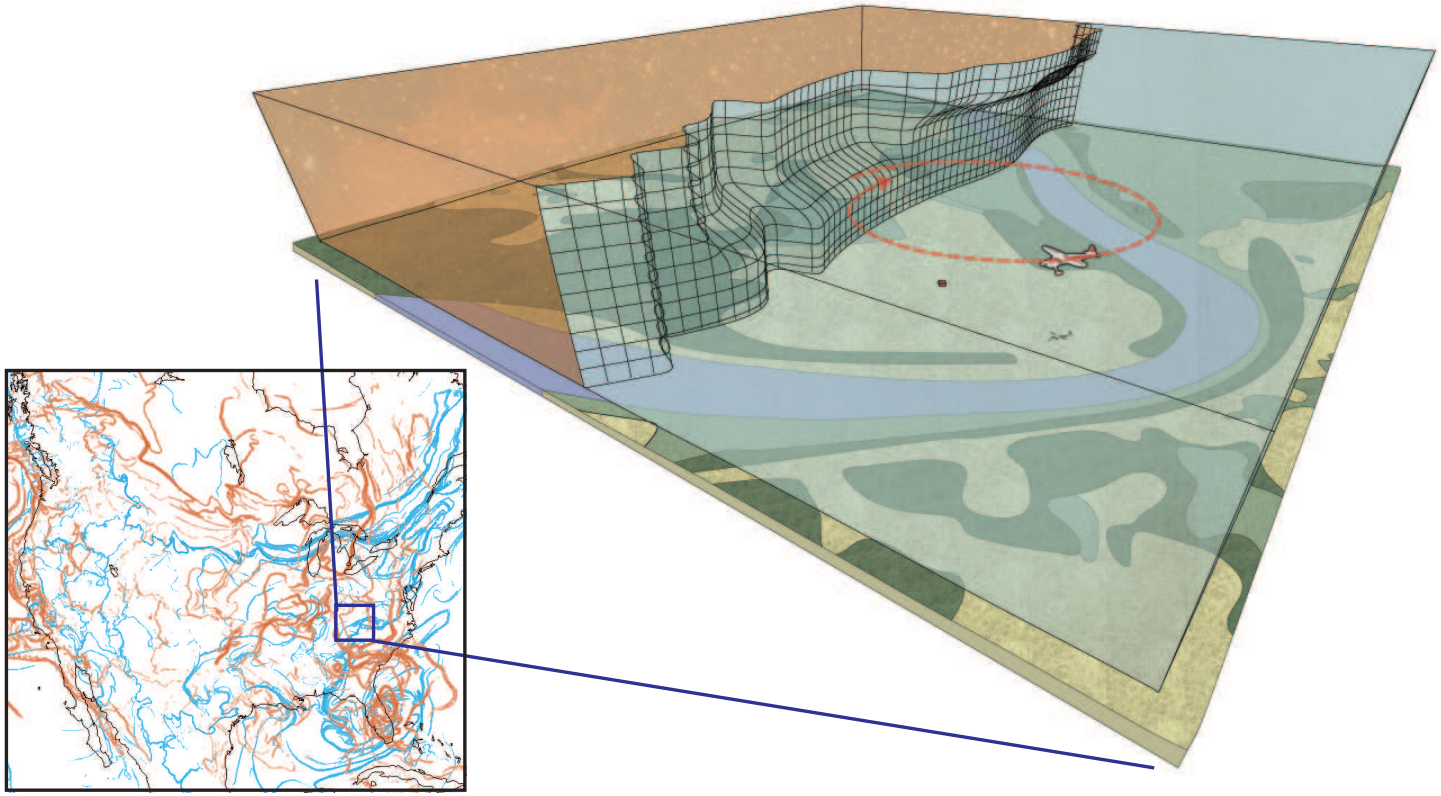

Pathogen transport: filament bounded by LCS

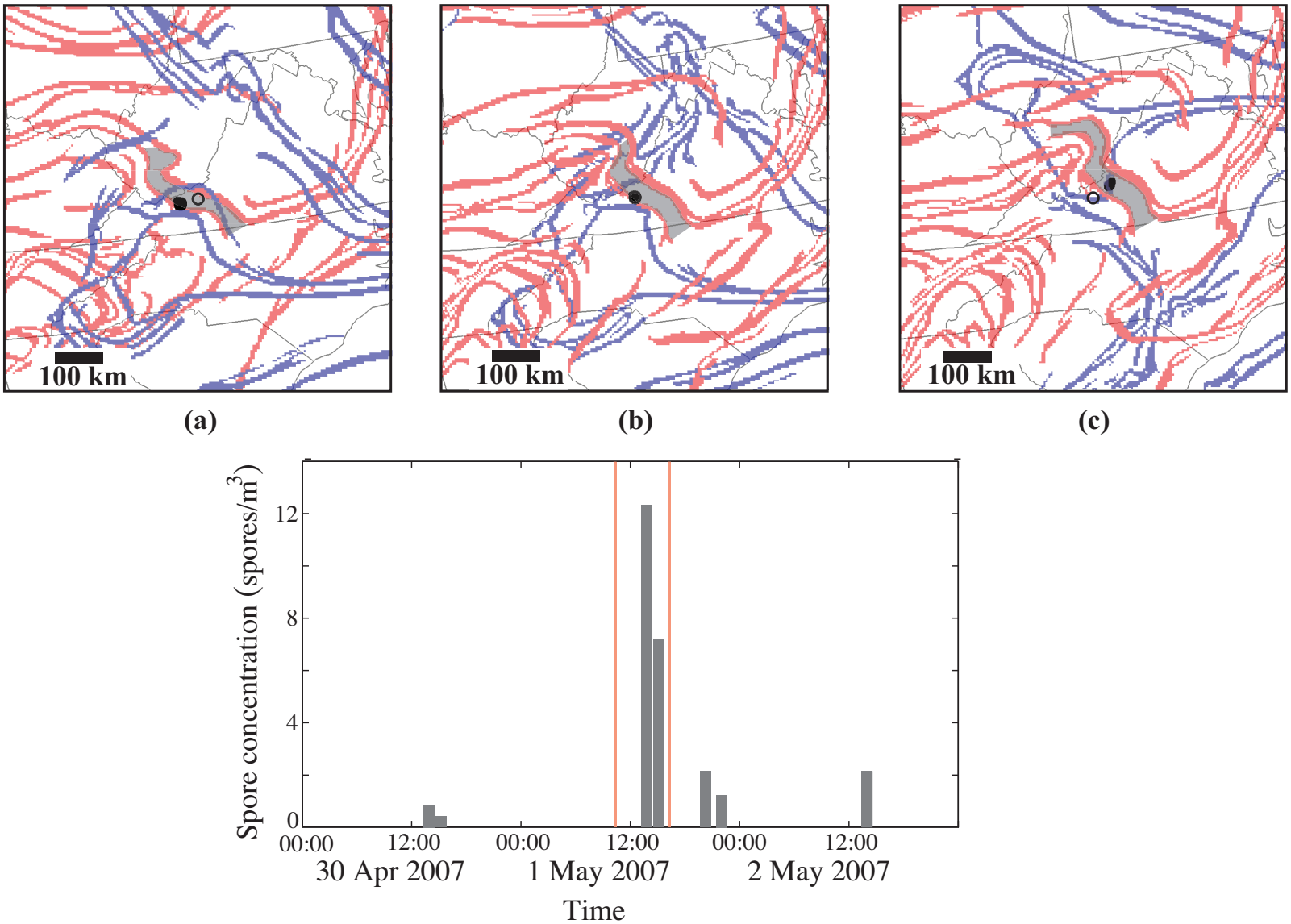

12:00 UTC 1 May 2007 15:00 UTC 1 May 2007 18:00 UTC 1 May 2007

Pathogen transport: filament bounded by LCS

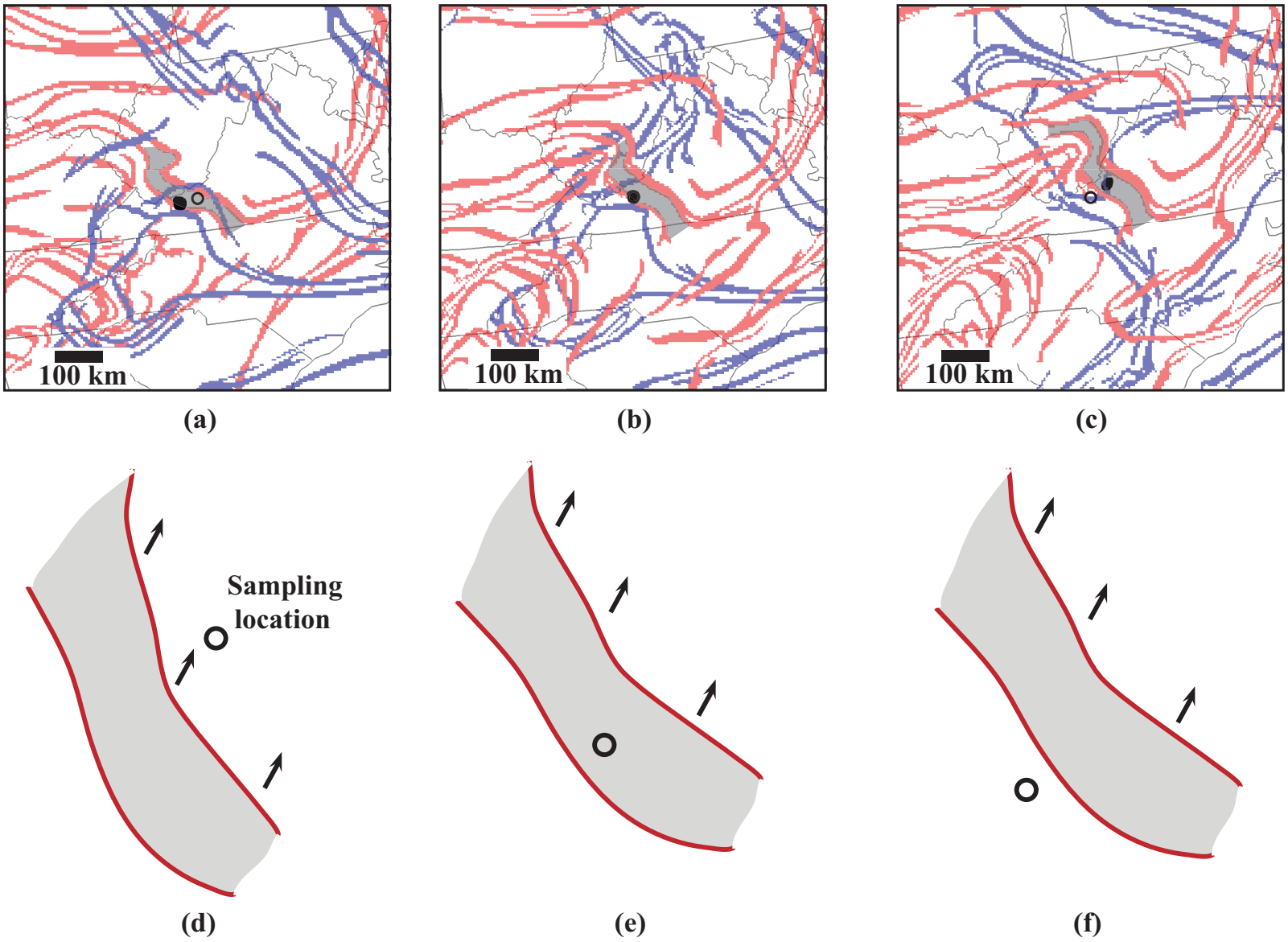

Coherent sets and set-based definition of FTLE

- Consider, e.g., a flow ϕ_t^{t+T} in $(x_1, x_2) \in \mathbb{R}^2$.
- Treat the evolution of set $B \subset \mathbb{R}^2$ as evolution of two random variables X_1 and X_2 defined by probability density function $f(x_1, x_2)$, initially uniform on B, $f = \frac{1}{\mu(B)}\mathcal{X}_B$, with $\mathcal{X}_B$ the characteristic function of B.
- Under the action of the flow ϕ_t^{t+T}, f is mapped to $\mathcal{P}f$ where $\mathcal{P}$ is the associated Perron-Frobenius operator.
- Let $I(f)$ be the covariance of f and $I(Pf)$ the covariance of Pf.

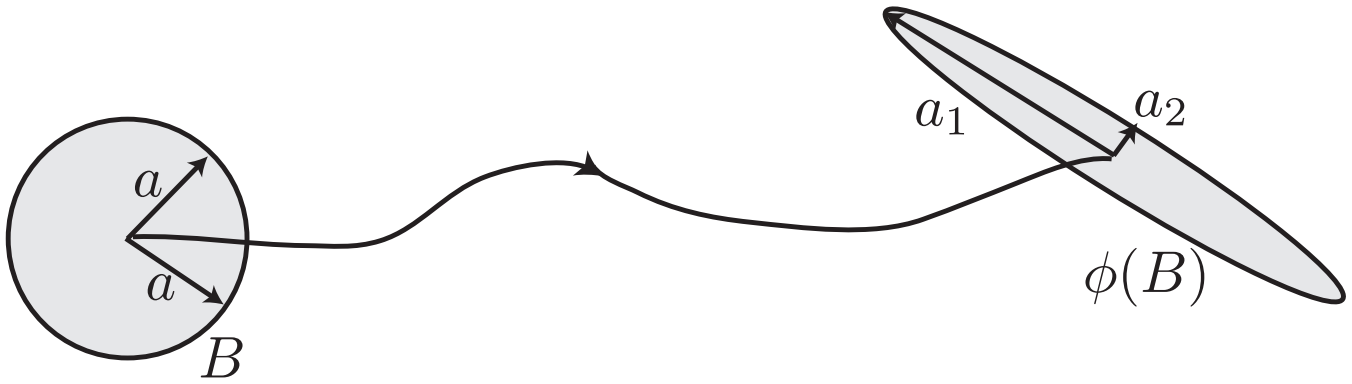

Deformation of a disk under the flow during $[t, t+T]$

Coherent sets and set-based definition of FTLE

- **Definition.** The **covariance-based FTLE** of B is

$$\sigma_I(B,t,T) = \frac{1}{|T|}\log\left(\frac{\sqrt{\lambda_{max}(I(Pf))}}{\sqrt{\lambda_{max}(I(f))}}\right).$$

- Reduces to usual definition of FTLE in the limit that the linearization approximation (i.e., line-stretching method) is valid

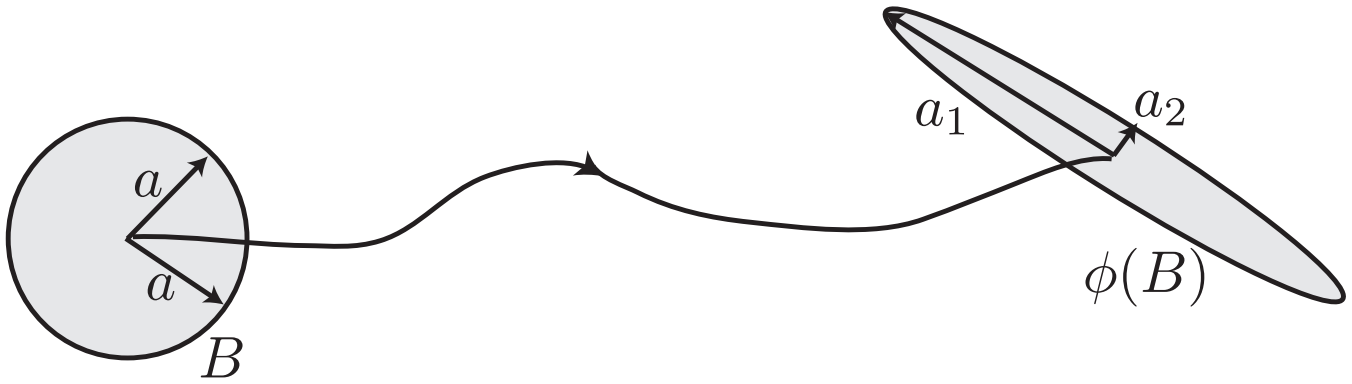

Deformation of a disk under the flow during $[t, t+T]$

Coherent sets and set-based definition of FTLE

- The **coherence** of a set B during $[t, t+T]$ is $\sigma_I(B, t, T)$.
- A set B is **almost-coherent** during $[t, t+T]$ if $\sigma_I(B, t, T) \approx 0$.

- Captures the essential feature of a coherent set: it does not mix or spread significantly in the domain.
- This definition also can identify non-mixing **translating** sets.

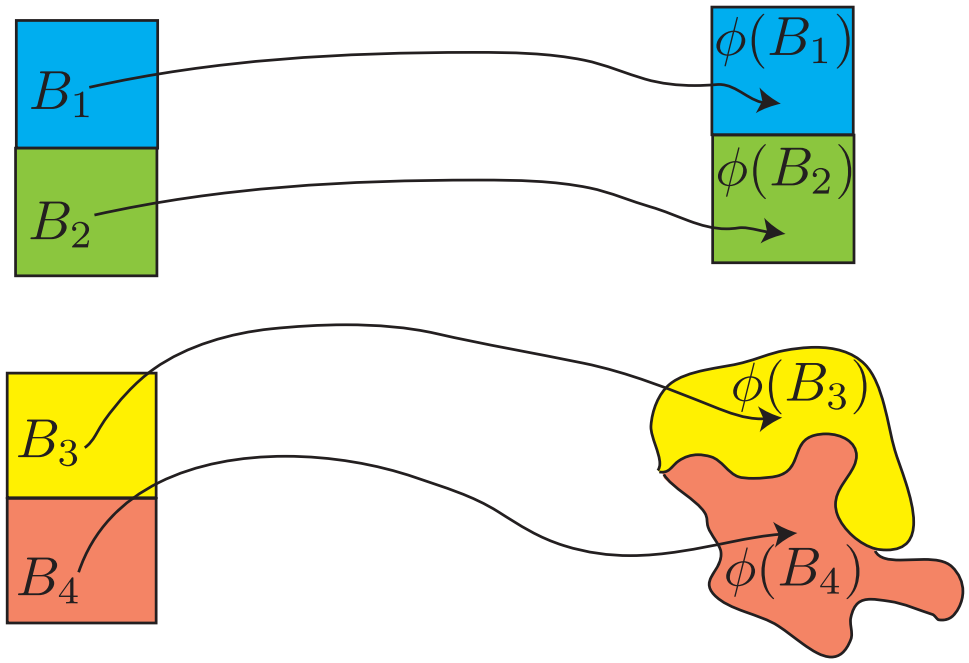

Coherent sets and set-based definition of FTLE

- The **coherence** of a set B during $[t, t+T]$ is $\sigma_I(B, t, T)$.
- A set B is **almost-coherent** during $[t, t+T]$ if $\sigma_I(B, t, T) \approx 0$.

- Captures the essential feature of a coherent set: it does not mix or spread significantly in the domain.
- This definition also can identify non-mixing **translating** sets.

- **Values of $\sigma_I(B, t, T)$ determine the family of sets of various degrees of coherence**.
- Need to set a heuristic threshold on the value of $\sigma_I(B, t, T)$ to determine coherent sets.

- Notice, coherent sets will be separated by ridges of high FTLE, i.e., LCS

Coherent sets in lid-driven cavity flow

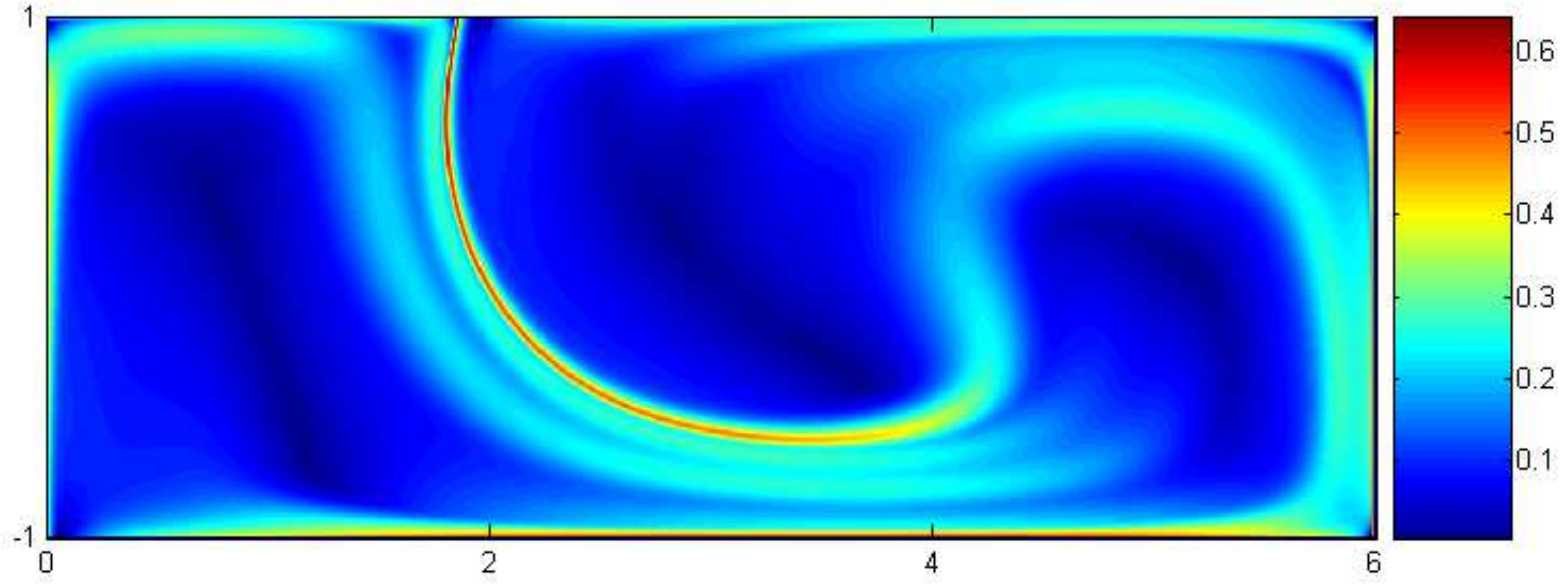

FTLE from line-stretching (conventional) during $[0, \tau_f]$

Coherent sets in lid-driven cavity flow

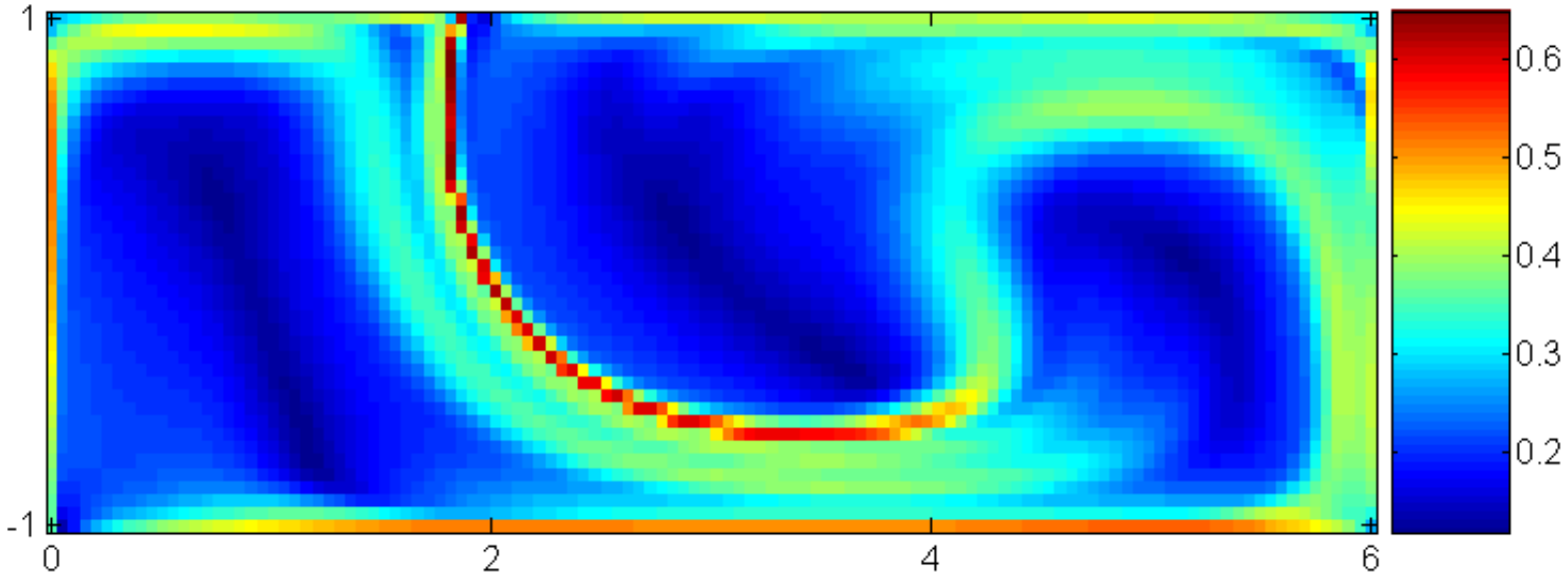

FTLE from covariance-based approach during $[0, \tau_f]$

Coherent sets in lid-driven cavity flow

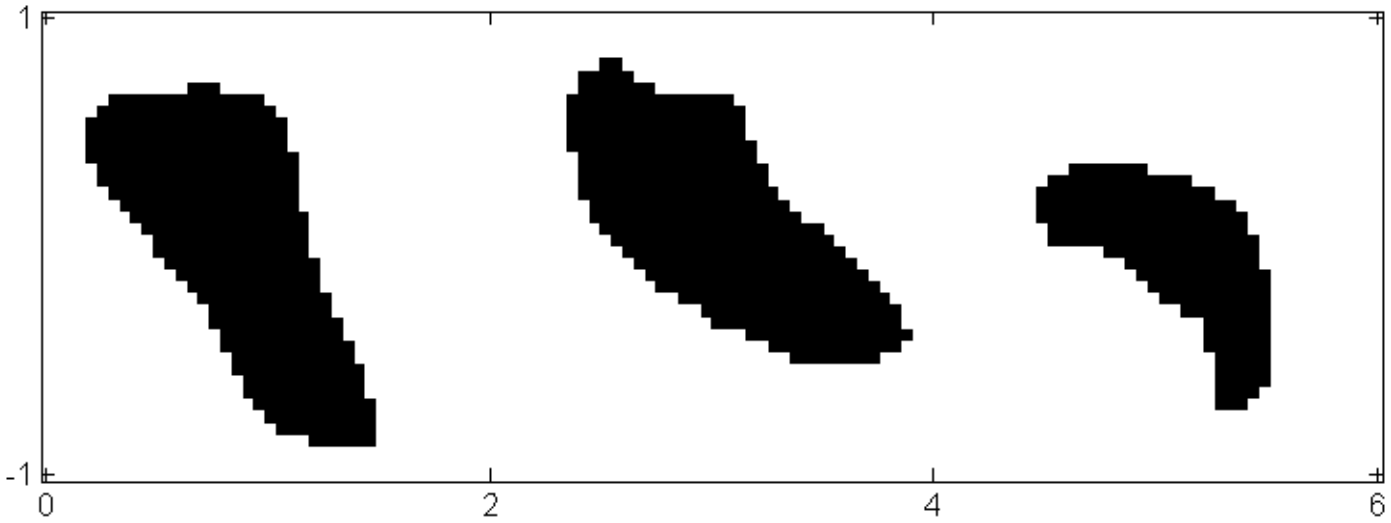

Sets of coherences $\sigma_I(0, \tau_f) < 0.06$

Coherent sets in lid-driven cavity flow

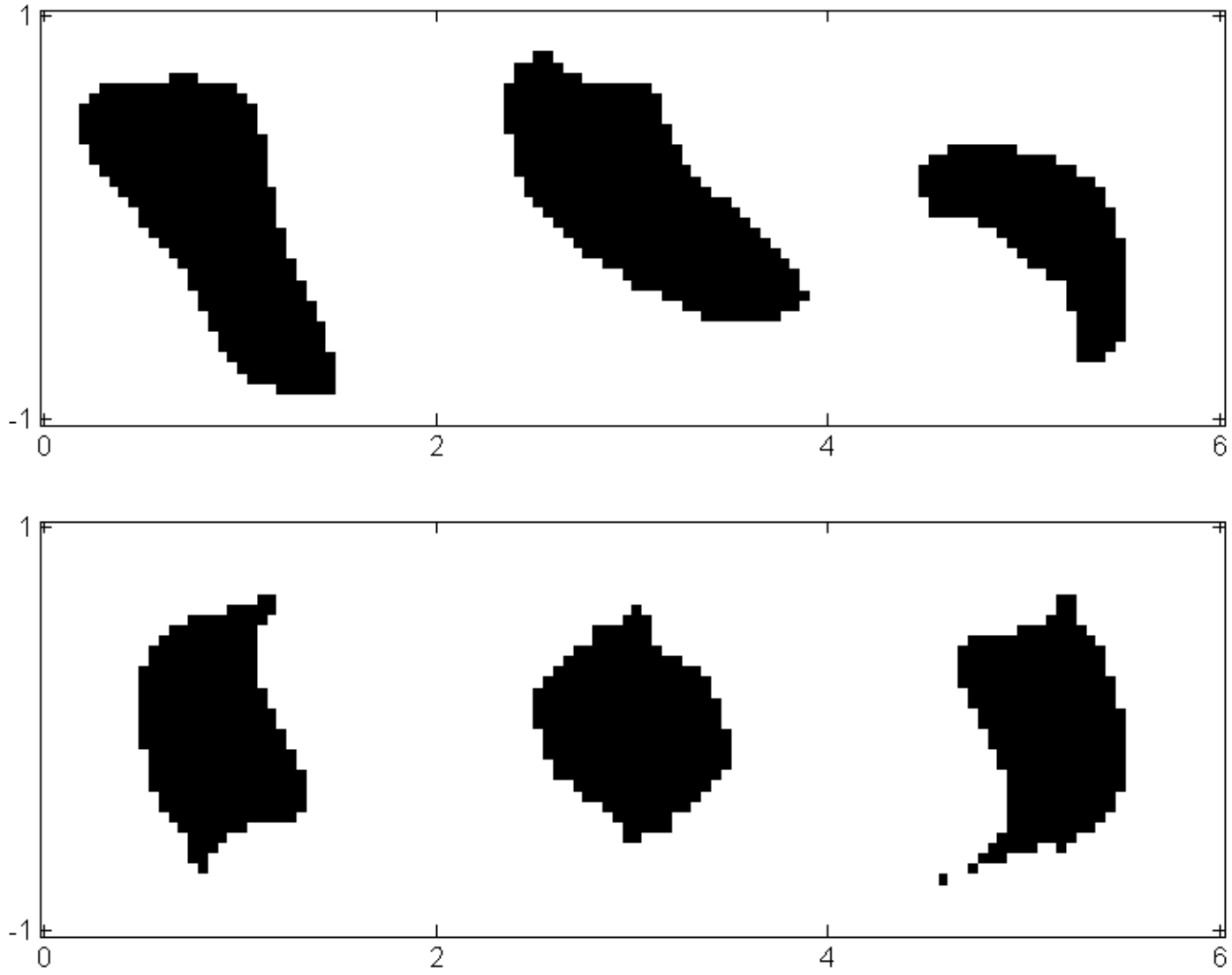

Compare coherent set with AIS from second eigenvector of P

Coherent sets in lid-driven cavity flow

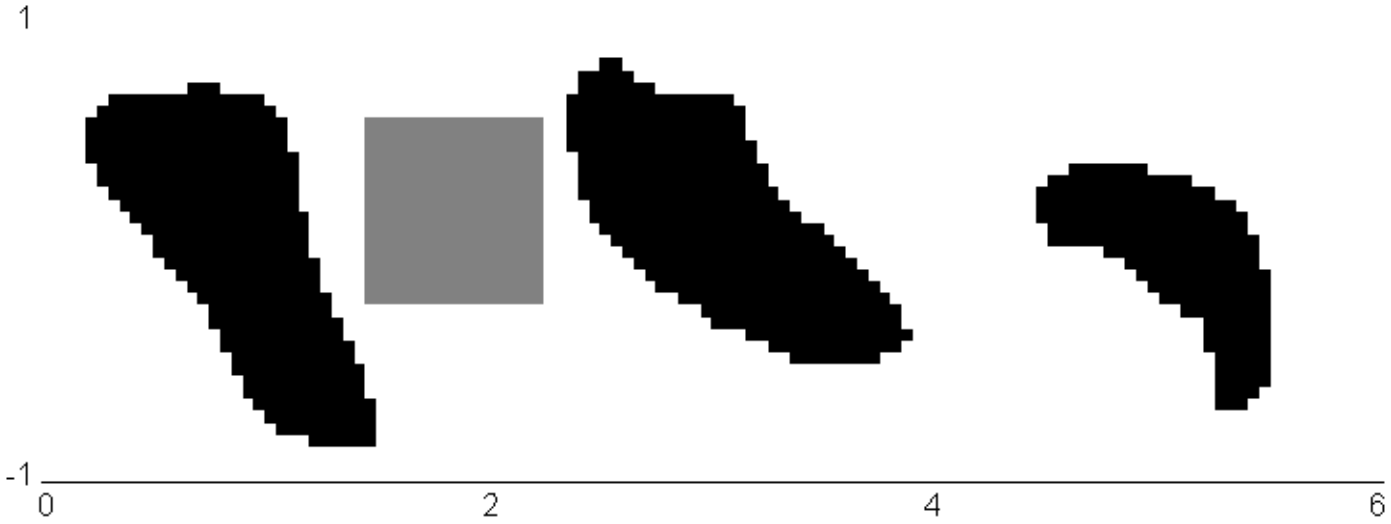

Compare coherent sets with non-coherent set (gray)

Coherent sets in lid-driven cavity flow

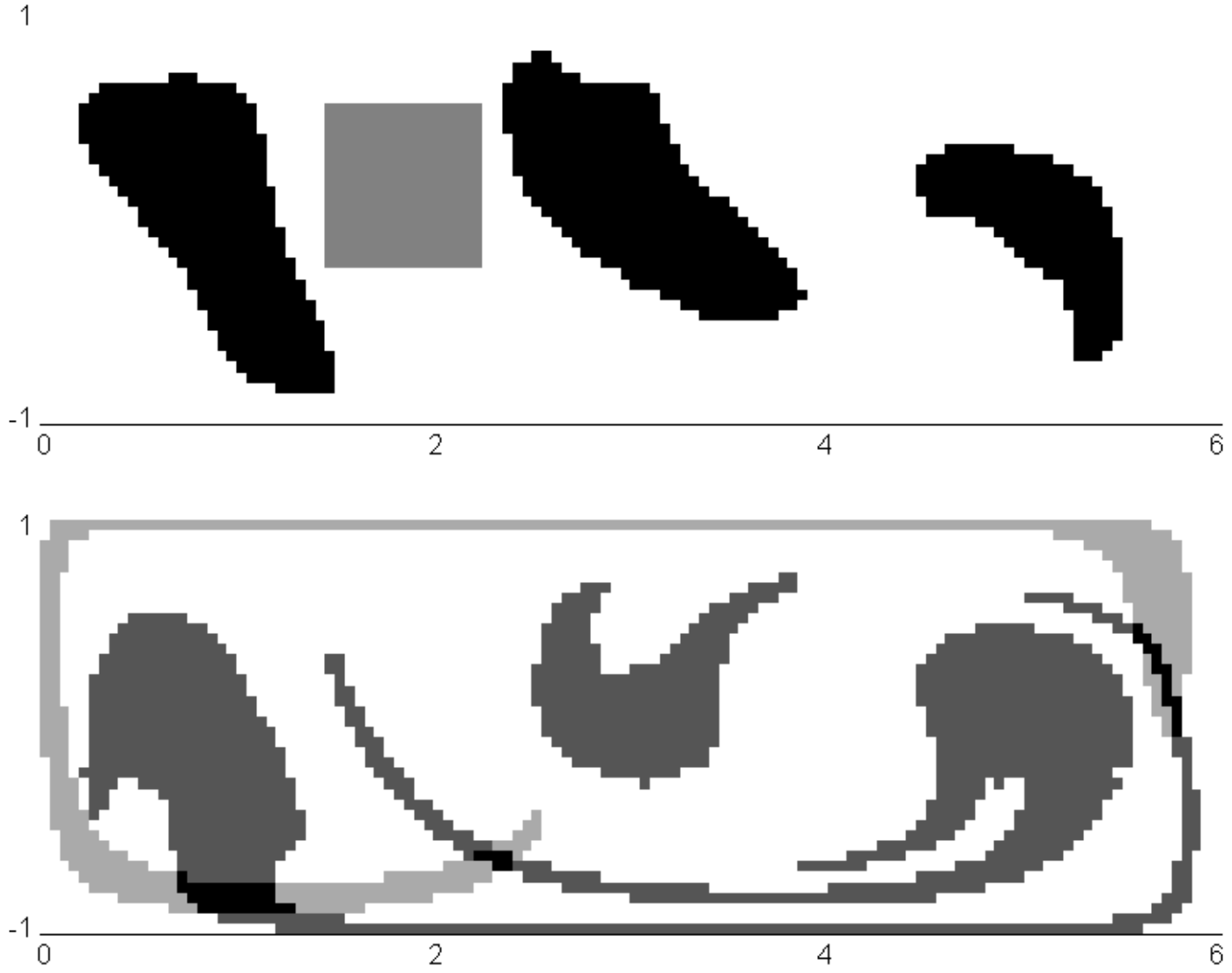

Coherent sets in the atmosphere

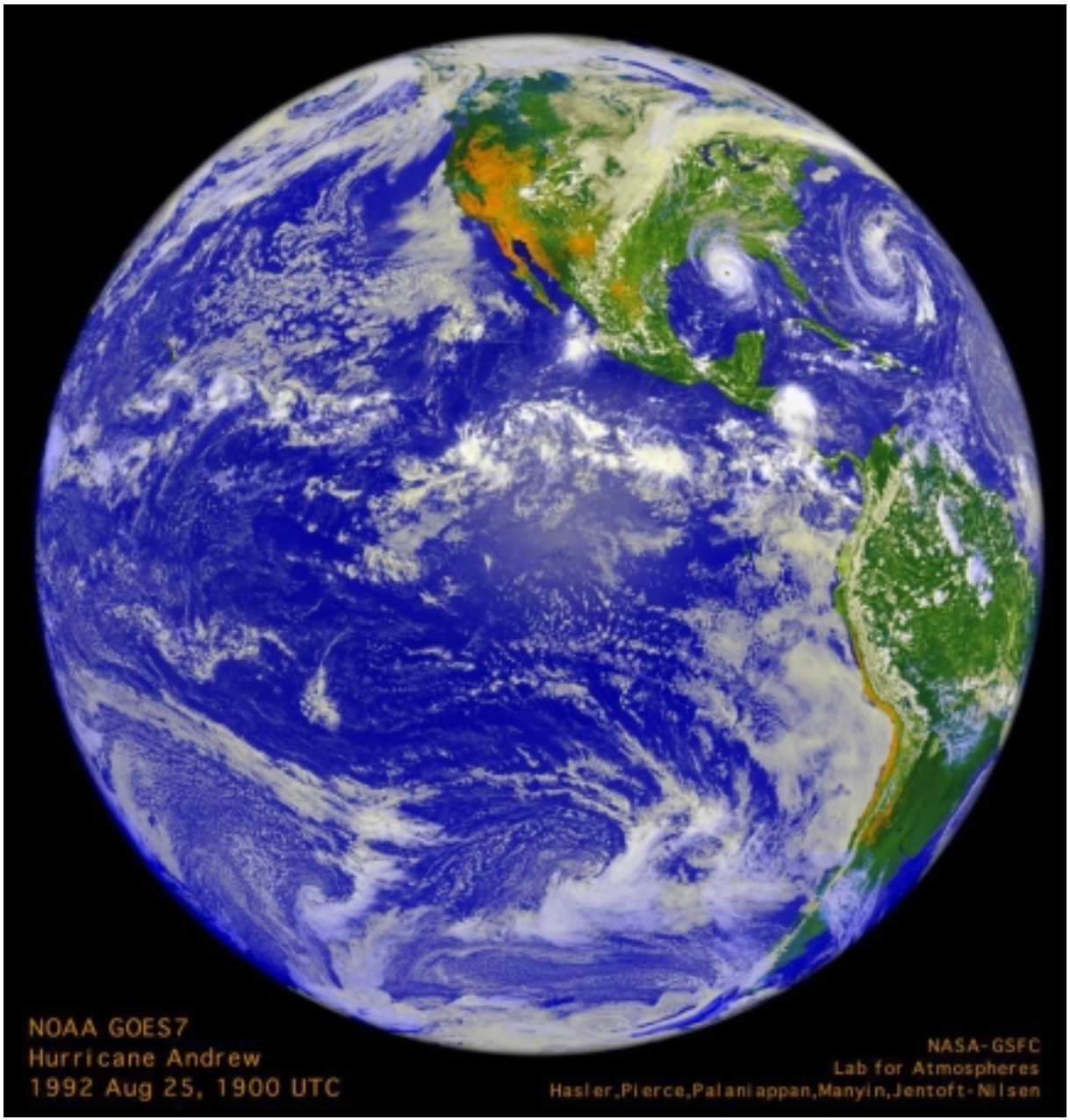

Coherent sets in the atmosphere

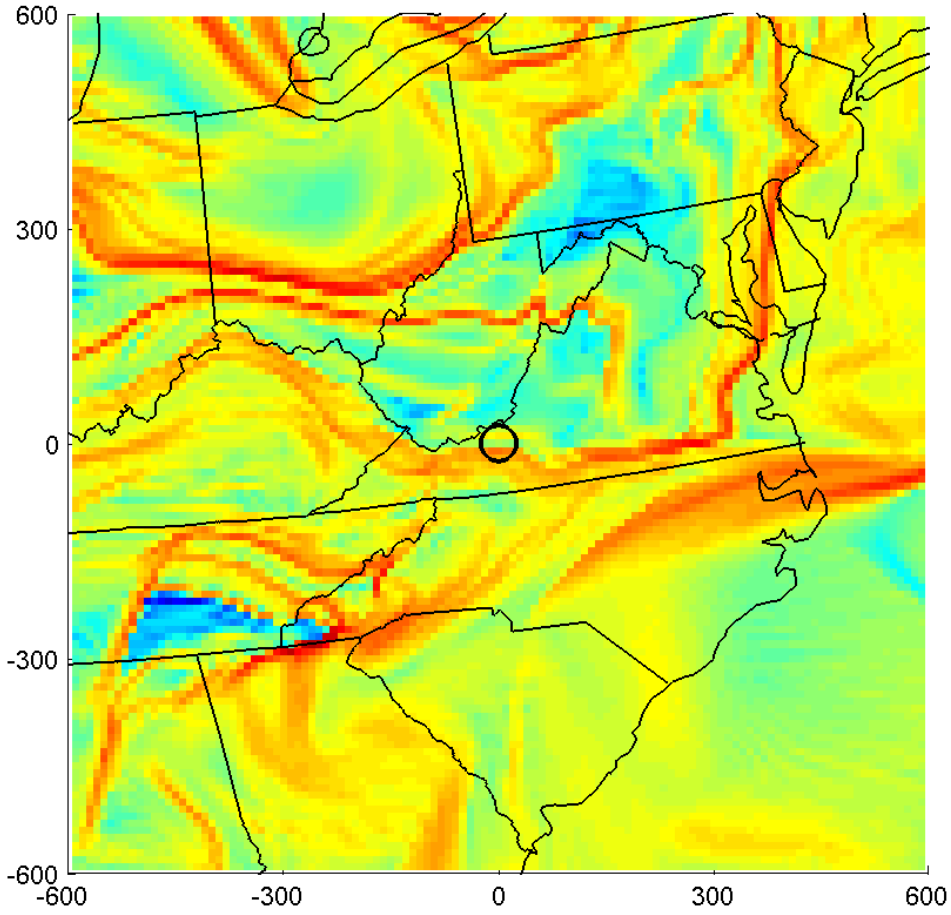

- FTLE from covariance during 24 hours starting 09:00 1 May 2007

Coherent sets in the atmosphere

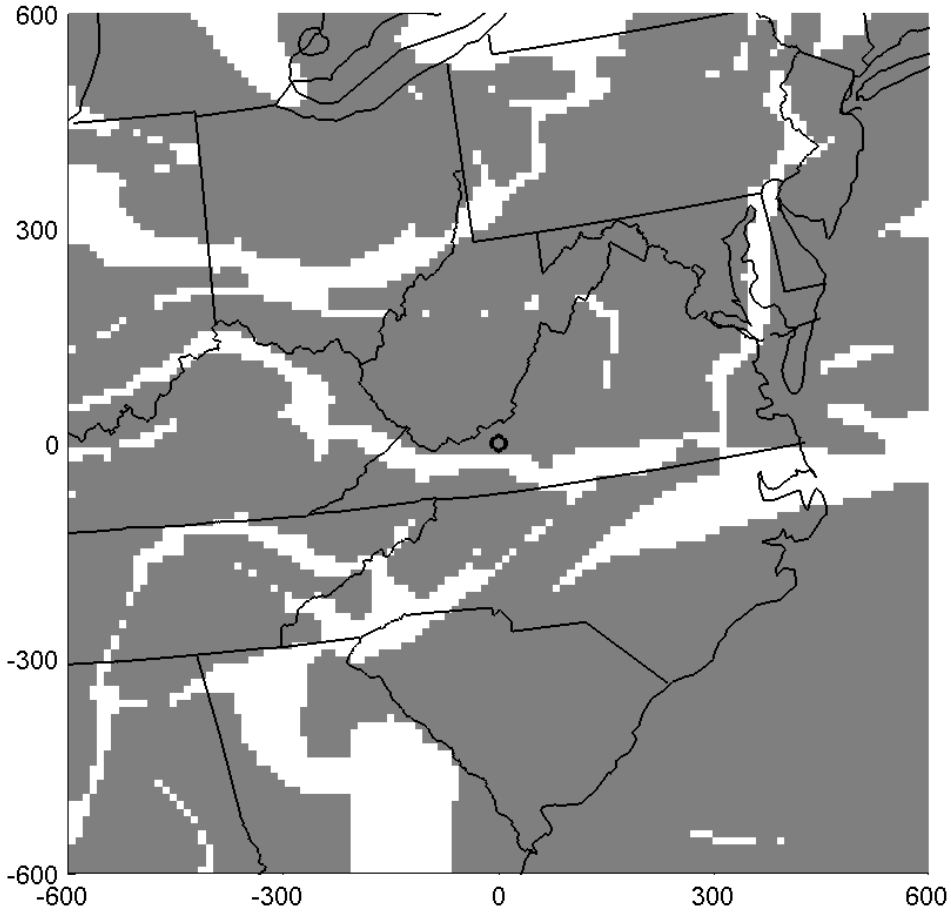

- Coherent sets during 24 hours starting 09:00 1 May 2007

Optimal navigation in an aperiodic setting?

- Selectively 'jumping' between coherent air masses using control
- Moving between mobile subregions of different finite-time itineraries

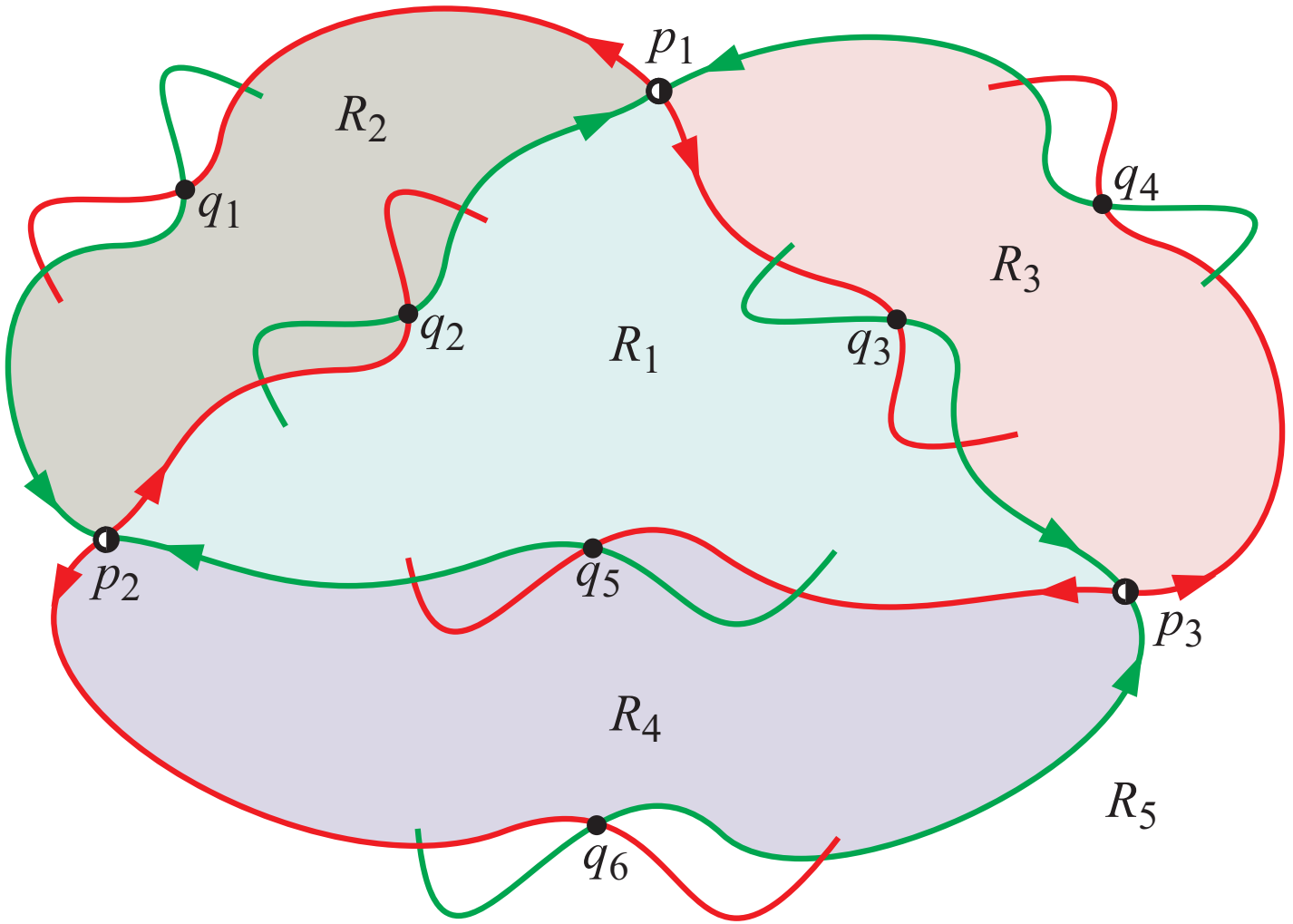

Optimal navigation in an aperiodic setting?

- Selectively 'jumping' between coherent air masses using control
- Moving between mobile subregions of different finite-time itineraries

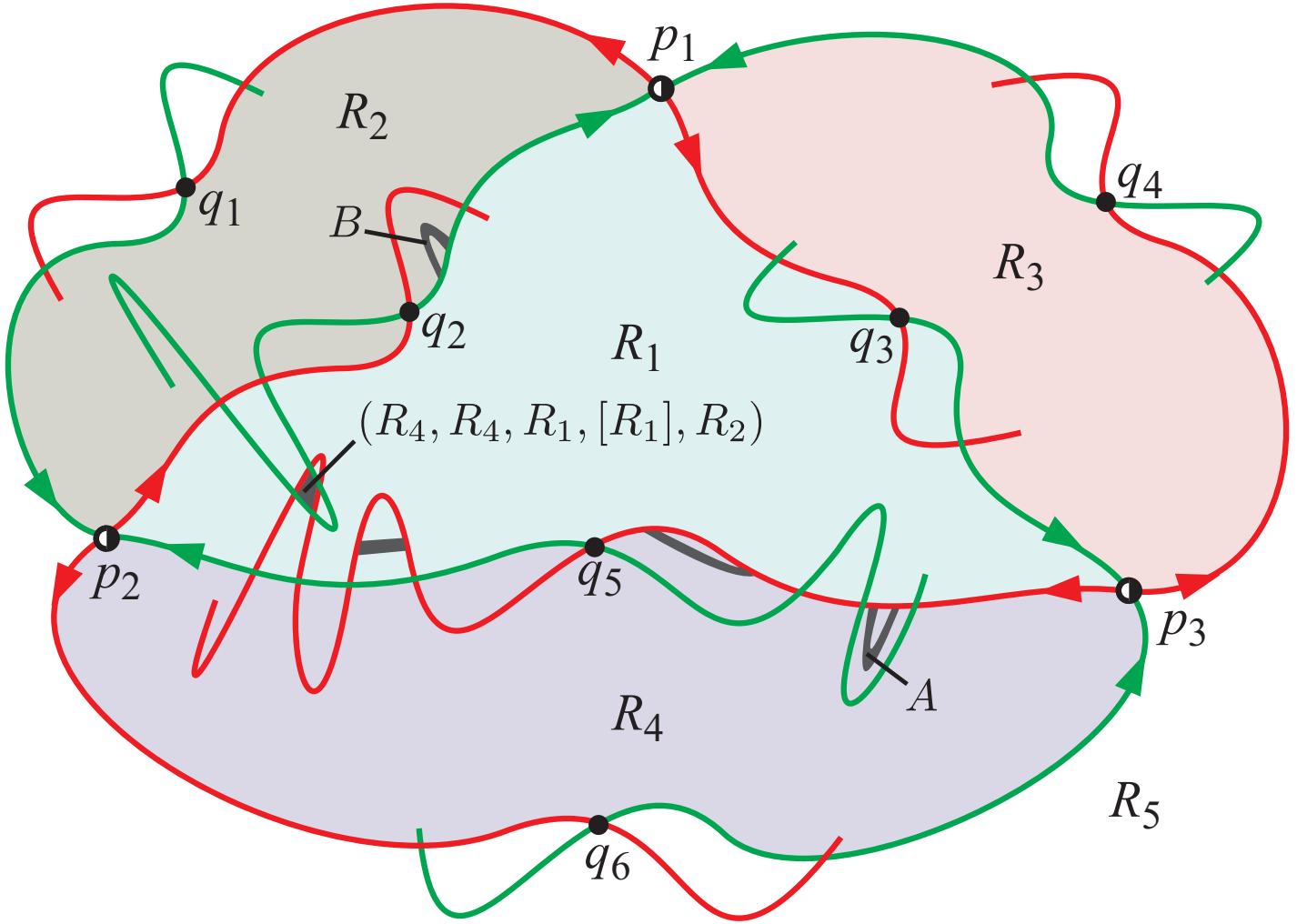

Optimal navigation in an aperiodic setting?

- Selectively 'jumping' between coherent air masses using control
- Moving between mobile subregions of different finite-time itineraries

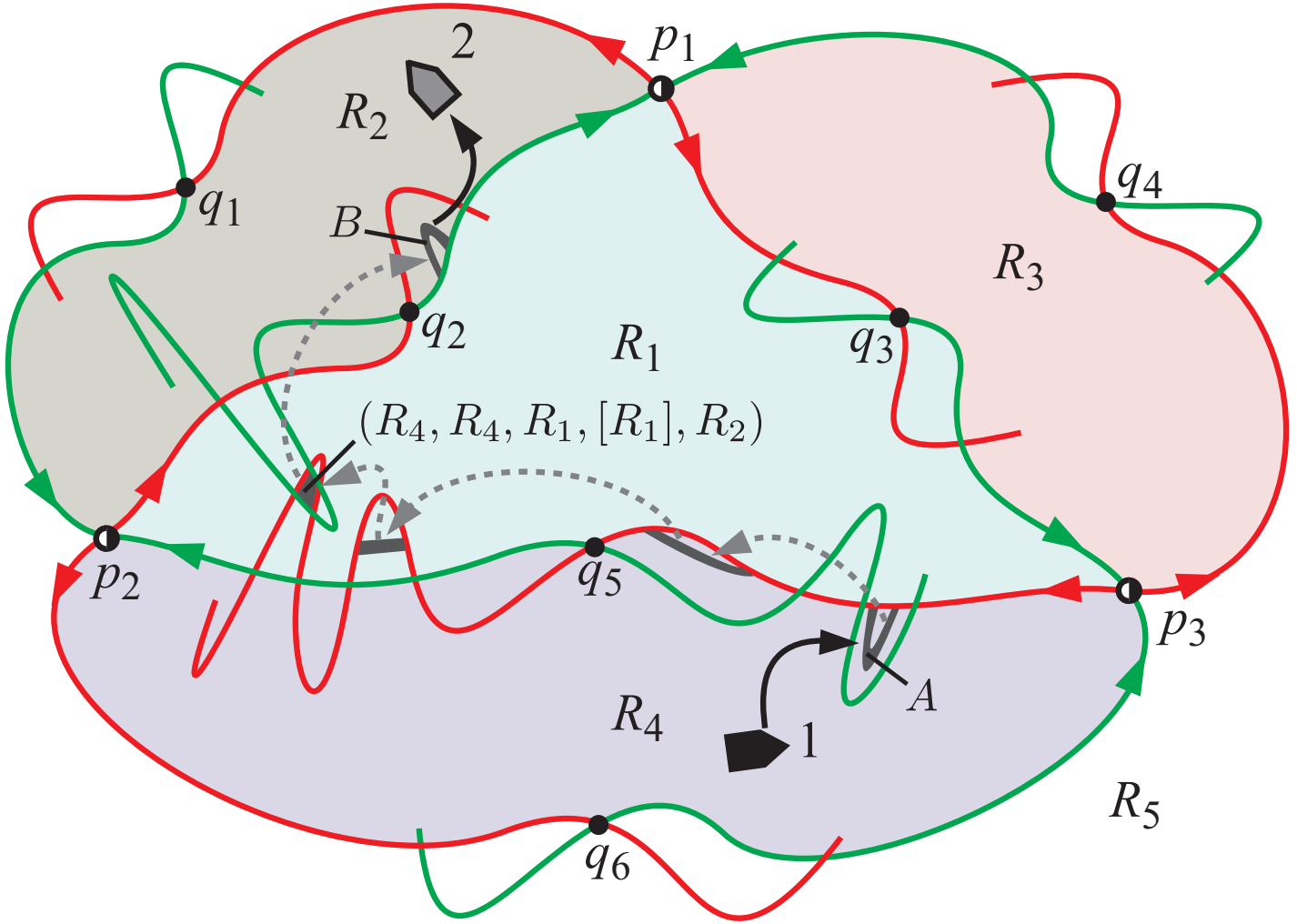

Optimal navigation in an aperiodic setting?

- Selectively 'jumping' between coherent air masses using control
- Moving between mobile subregions of different finite-time itineraries

Final words on chaotic transport

- What are robust descriptions of transport which work in data-driven aperiodic, finite-time settings?
  - Possibilities: finite-time lobe dynamics / symbolic dynamics may work
    — finite-time analogs of homoclinic and heteroclinic tangles
  - Probabilistic, geometric, and topological methods
    — invariant sets, almost-invariant sets, almost-cyclic sets, coherent sets, stable and unstable manifolds, Thurston-Nielsen classification, FTLE, LCS
  - Many links between these notions — e.g., LCS locate analogs of stable and unstable manifolds
    — boundaries between coherent sets are naturally LCS
    — periodic points $\Rightarrow$ almost-cyclic sets
    — their 'stable/unstable invariant manifolds' $\Rightarrow$???

The End

For papers, movies, etc., visit:
www.shaneross.com

Main Papers:

- Stremler, Ross, Grover, Kumar [2011] Topological chaos and periodic braiding of almost-cyclic sets. *Physical Review Letters* 106, 114101.
- Tallapragada, Ross, Schmale [2011] Lagrangian coherent structures are associated with fluctuations in airborne microbial populations. *Chaos* 21, 033122.
- Lekien & Ross [2010] The computation of finite-time Lyapunov exponents on unstructured meshes and for non-Euclidean manifolds. *Chaos* 20, 017505.
- Senatore & Ross [2011] Detection and characterization of transport barriers in complex flows via ridge extraction of the finite time Lyapunov exponent field, *International Journal for Numerical Methods in Engineering* 86, 1163.
- Grover, Ross, Stremler, Kumar [2012] Topological chaos, braiding and breakup of almost-invariant sets. Preprint.
- Tallapragada & Ross [2012] A set oriented definition of the FTLE and coherent sets. Preprint.